Copyright Warning & Restrictions

The copyright law of the United States (Title 17, United States Code) governs the making of photocopies or other reproductions of copyrighted material.

Under certain conditions specified in the law, libraries and archives are authorized to furnish a photocopy or other reproduction. One of these specified conditions is that the photocopy or reproduction is not to be "used for any purpose other than private study, scholarship, or research." If a, user makes a request for, or later uses, a photocopy or reproduction for purposes in excess of "fair use" that user may be liable for copyright infringement,

This institution reserves the right to refuse to accept a copying order if, in its judgment, fulfillment of the order would involve violation of copyright law.

Please Note: The author retains the copyright while the New Jersey Institute of Technology reserves the right to distribute this thesis or dissertation

Printing note: If you do not wish to print this page, then select "Pages from: first page # to: last page #" on the print dialog screen

CHARACTERIZATION OF THIXOTROPIC MATERIALS AND MODIFICATION OF THE WEISSENBERG RHEOGONIOMETER

BY

PAUL JOSEPH OROSZ, JR.

A DISSERTATION

PRESENTED IN PARTIAL FULFILLMENT OF

THE REQUIREMENTS FOR THE DEGREE

OF

DOCTOR OF ENGINEERING SCIENCE IN CHEMICAL ENGINEERING

AT

NEWARK COLLEGE OF ENGINEERING

Newark, New Jersey
1974

APPROVAL OF DISSERTATION

CHARACTERIZATION OF THIXOTROPIC MATERIALS AND MODIFICATION OF THE WEISSENBERG RHEOGONIOMETER

BY

PAUL JOSEPH OROSZ, JR.

FOR

DEPARTMENT OF CHEMICAL ENGINEERING

NEWARK COLLEGE OF ENGINEERING

BY

FACULTY COMMITTEE

APPROVED: _____ CO-CHAIRMAN

_____ CO-CHAIRMAN

_____

_____

_____

NEWARK, NEW JERSEY

OCTOBER, 1974

ABSTRACT

A Weissenberg Rheogoniometer, Model R-18, was modified to give complete rheological curves without resetting the gearbox and generate hysteresis loops for time-dependent, non-Newtonian materials. This modified instrument was used to analyze a number of materials. Standard Newtonian and known time-independent, non-Newtonian materials were studied to insure the accuracy of the instrument. Results indicated that the instrument would reproduce known viscosities of these materials, give consistent results, and not display inherent hysteresis loops with non-thixotropic materials. Materials known and suspected to be thixotropic: silicone grease-oil mixture, montmorillonite clay, and blood were tested. All displayed the characteristic hysteresis loop usually associated with thixotropic materials.

The Huang rheological equation was tested on the thixotropic materials. Having 5 constants which must be evaluated, the final equation with parameters can accurately generate a hysteresis loop for a thixotropic material. It can also generate multiple hysteresis loops using the same 5 constants.

TABLE OF CONTENTS

LIST OF TABLES

LIST OF FIGURES

ACKNOWLEDGEMENTS

The author would like to thank his co-advisors, Drs. Ching-Rong Huang and Jerome J. Salamone, for their guidance, encouragement, and patience shown in various phases of this work.

A great deal of help was extended to the author by the computing centers of the following organizations: Hooker Chemicals and Plastics Corporation, Indiana Institute of Technology, and Newark College of Engineering.

The author would like to also thank the following individuals who aided in the experiment construction, and gave help in working with the computer: Nandor Siskovic, Gary Railsback, and David Chittenden.

Financial aid was provided to the author by the National Science Foundation and ESSO.

The author is especially grateful to his wife, Pamela, for her encouragement and assistance in the preparation of this dissertation.

CHAPTER 1

INTRODUCTION

''Rheology is the science of deformation and flow of matter (37).'' Rheology can also be considered to be the investigation of the transport properties of a material as it flows from one point to another. The characteristic equation is called the rheological equation of state which describes the relationship between the shear stress, τ, the shear rate (rate of shear), $\dot{\gamma}$, and any additional variable that might influence the flow properties, such as temperature. For a particular material of interest, an equation of state has to be determined and the various coefficients in the equation evaluated.

Newtonian Fluids

Consider a fluid contained between two large parallel plates of area, A, separated by small distance, Y. The system is initially at rest. The upper plate is then set in motion in the X-direction at constant velocity, V. When steady-state has been attained, a constant force, F, is required to maintain the motion of the upper plate. Here the force per unit area is

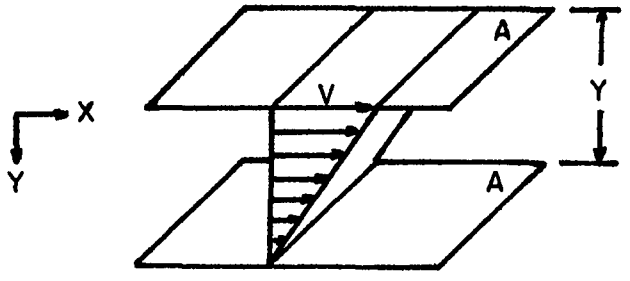

proportional to the velocity increase in the direction, Y. The constant of proportionality, μ, is called the viscosity of the fluid.

$$\frac{F}{A} = \mu \frac{0 - V}{Y - 0} = -\mu \frac{V}{Y} \qquad (1\text{-}1)$$

This equation can be written in a general form. The shear stress (force per unit area) exerted in the direction of flow on a fluid surface perpendicular to the flow direction is designated as, τ. The rate of shear, which is the change in velocity of flow with the distance measured at right angles to the direction of flow, is designated as, $\dot{\gamma}$. Therefore, equation (1-1) can be rewritten as:

$$\tau = -\mu \dot{\gamma} \qquad (1\text{-}2)$$

This equation is an example of a rheological equation of state.

Rheological equations of state can be used to classify viscous fluids. Newtonian fluids are those fluids exhibiting direct proportionality between shear stress and shear rate for laminar flow. The proportionality constant, μ, which is independent of shear rate and time, is called the Newtonian viscosity. This viscosity is affected only by temperature and pressure for a given fluid system. The curve which relates shear stress and rate of shear is called a ''flow curve'' or ''rheogram''. For a Newtonian fluid, the rheogram is a straight

line, through the origin, with a slope equal to the Newtonian viscosity, μ, figure 1-1. Accordingly, a single experimental determination is sufficient to define completely the rheological properties of the fluid. If a greater number of measurements are made at the same temperature and pressure, they serve only to confirm the experimental accuracy of the first one. All gases and liquids of low molecular weight are considered to be Newtonian fluids.

Non-Newtonian Fluids

All fluids for which the flow curve is not linear or does not pass through the origin, are called non-Newtonian fluids. The viscosity of a non-Newtonian fluid is not constant at a given temperature and pressure. Non-Newtonian behavior is commonly observed in the following kinds of systems:

(a) Solution or melts of high-molecular weight polymeric materials which are non-Newtonian except when dilute.

(b) Suspensions of solids in liquids which are non-Newtonian especially at high solid concentrations.

Non-Newtonian behavior is most pronounced at intermediate rates of shear. At very high or very low shear rates, many non-Newtonians approach Newtonian behavior. The completely general case is that of a fluid for which the relationship between shear stress and rate of shear is not linear and may also depend on both the duration of the shear and the extent

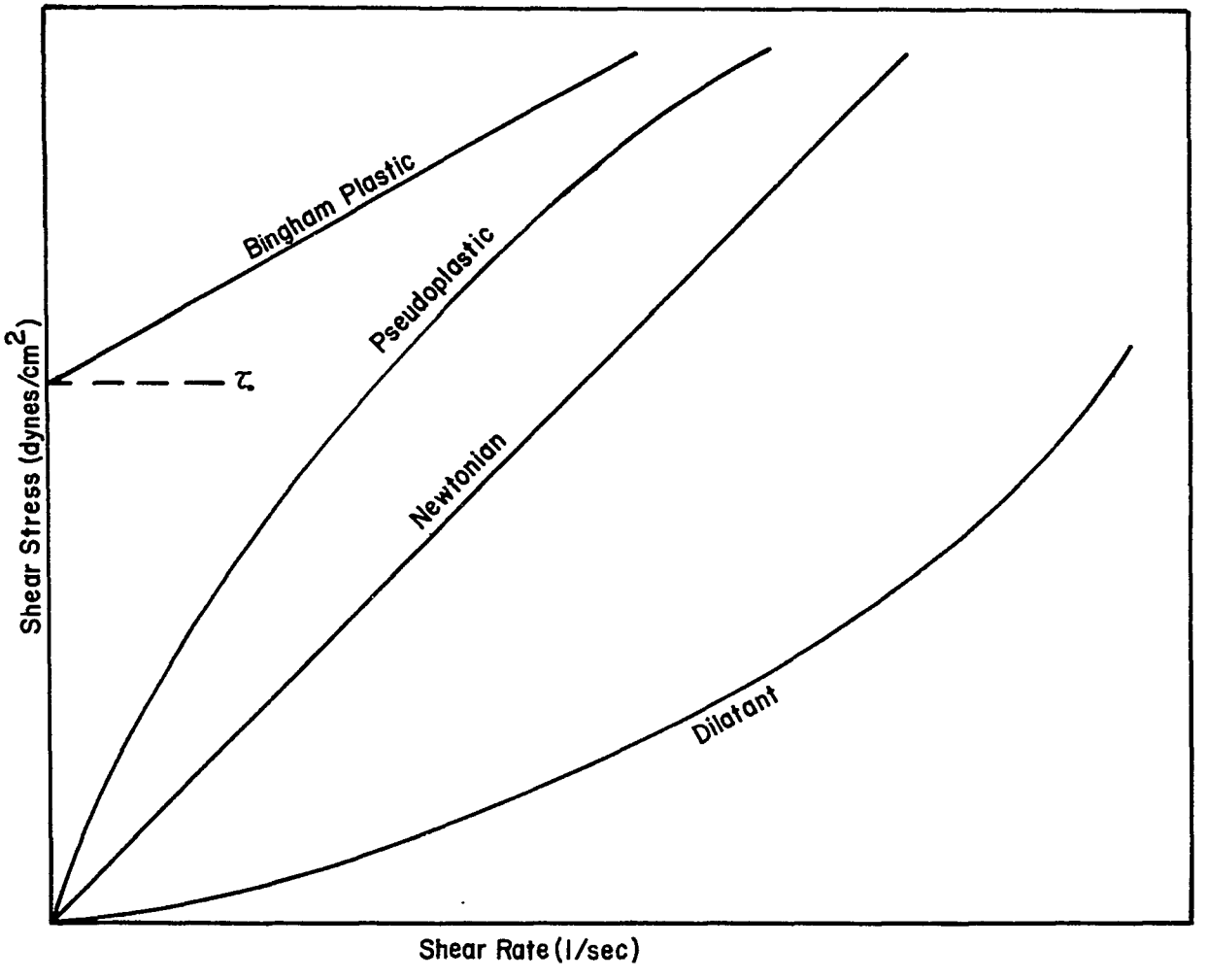

Figure I-1. Time-Independent Flow Curves

of deformation produced. Thus, it is possible to divide non-Newtonian systems into three broad categories.

(a) Time-independent-fluids are those for which the shear stress at any point is some function of the rate of shear at that point. Pseudoplastic, dilatant, and Bingham plastic fluids are considered time-independent, non-Newtonian fluids.

(b) Viscoelastic systems have characteristics of both solids and fluids and exhibit elastic recovery after deformation.

(c) Time-dependent fluids are those for which the shear stress is a function of the rate of shear and the time of shear or its previous shear ''history''. Thixotropic and rheopectic fluids are considered time-dependent, non-Newtonian fluids.

Time-Independent, Non-Newtonian Materials

Bingham plastic. A Bingham-plastic material is characterized by having a flow curve which is a straight line and has an intercept, τ_o, on the shear stress axis, figure 1-1. This yield stress, τ_o, is the shear stress which must be exceeded before the fluid will flow. The equation of the flow curve for stress above, τ_o, is:

$$\tau - \tau_o = -\eta_{pl}\dot{\gamma} \qquad (1\text{-}3)$$

where η_{pl} is the ''coefficient of rigidity'' or ''plastic viscosity'' and represents the slope of the flow curve. The apparent viscosity, which is defined as the shear stress divided

by the rate of shear at that shear stress, is:

$$\eta_a = -\tau/\dot{\gamma} = \eta_{pl} - \tau_o/\dot{\gamma} \qquad (1\text{-}4)$$

The structure of a Bingham-plastic fluid at rest might be compared to a structure of building blocks. The structure is able to withstand a finite force, but once this force is exceeded, the entire structure crumbles. Examples of fluids which have been found to approximate Bingham-plastic behavior include: drilling muds, suspensions of chalk, grains, rock and sewage sludge, oil paints, and toothpaste.

Pseudoplastic fluids. An important classification for non-Newtonian fluids is that of pseudoplasticity. It is characterized by a flow curve which is non-linear and usually does not have a yield value, figure 1-1. Another property of a pseudoplastic fluid is that the apparent viscosity decreases with increase in shear rate. These fluids are usually characterized by the empirical power law:

$$\tau = -k\dot{\gamma}^n \qquad (1\text{-}5)$$

where k is a measure of the consistency of the fluid (the higher the value of k , the more viscous the fluid) and n is a measure of non-Newtonian behavior ($n<1$ for a pseudoplastic). The apparent viscosity corresponds to

$$\eta_a = \frac{k\dot{\gamma}^n}{\dot{\gamma}} = \frac{k}{\dot{\gamma}^{1-n}} \qquad (1\text{-}6)$$

With $n = 1$, the formula reduces to the Newtonian situation. When discussing apparent viscosities, the rate of shear that relates this viscosity and shear stress is usually specified.

Qualitatively, pseudoplasticity might be discussed in the following manner. Assume a pseudoplastic material is initially at rest with molecules or particles randomly interspersed. When a shear is applied, these particles would tend to align. If this alignment-dispersion criteria, were an indication of the fluid viscosity, the randomly dispersed particles would have a higher viscosity than the more aligned particles (large resistance to flow vs. small resistance to flow). The more aligned the particles, the smaller the viscosity as shear rate is increased. This type of phenomena is indicated by the curvature of the flow curve for a pseudoplastic fluid. At very low shear rates, the force is too small to align the particles a Newtonian-type region is present. At very high rates of shear, the particles might be completely aligned, indicating another Newtonian-type region. This straight line-curvature-straight line form of flow curve for pseudoplastic materials is consistent with experimental data. Examples of fluids which exhibit pseudoplastic behavior include: polymeric solutions, cellulose acetate, Napalm, and dilute suspensions of solids.

Dilatant fluids. Dilatant fluids are similar to pseudoplastic fluids except that the apparent viscosity increases with increase in rate of shear, figure 1-1. The power law also applies to dilatant fluids with $n>1$.

One explanation of dilatant fluids states that these fluids when at rest, consist of densely packed particles in which the voids are small and perhaps at a minimum. Sufficient liquid is present only to fill these voids. The motion or shear of such fluids at low rates of shear requires only small shear stresses since the liquid lubricates the passage of one particle past another. At increasing rates of shear, the dense packing of the solid particles is progressively broken up, and since the packing initially involved a minimum of voids, there is now insufficient liquid present to enable the particles to flow smoothly past one another. Therefore, the shear stress increases more than proportionately with shear rate (increase in apparent viscosity with increase in shear rate).

Some examples of dilatant fluids include: starch pastes, potassium silicate in water and gum arabic in water.

Viscoelastic Fluids

A viscoelastic material possesses both solid (elastic) and liquid (viscous) properties. The rheological equation for a viscoelastic fluid is usually of the following form:

$$f_1(D)\,\tau = f_2(D)\,\dot{\gamma} \tag{1-7}$$

$$\sum_{n=0}^{N} \alpha_n D^n \tau = \sum_{m=0}^{M} \beta_m D^m \dot{\gamma} \tag{1-8}$$

where

$$D \doteq \frac{d}{dt} \tag{1-9}$$

$$\dot{\gamma} = \frac{d\gamma}{dt} \tag{1-10}$$

This equation is general and if solved subject to the correct boundary conditions, will give the response of the material to any imposed stress or strain. An important property which is determined from these equations is the time the material will take to return to its original form. This time is called the relaxation time. The flow of polymers is one field in which viscoelasticity is investigated.

Time-Dependent, Non-Newtonian Fluids

Time-dependent, non-Newtonian fluids are those fluids for which the shear stress, at constant shear rate and temperature, varies as a function of the duration of shear.

$$\tau = -\eta_a(\dot{\gamma}, t)\,\dot{\gamma} \tag{1-11}$$

where τ is the shear stress, $\dot{\gamma}$ is the rate of shear, $\eta_a(\dot{\gamma},t)$ is the apparent viscosity and is a function of shear rate and time, and t is the time variable which is actually the history or total time of application of shear rate. Time-dependency excludes irreversible changes in the fluids where there is destruction of the particles.

The time-of-shear dependent, non-Newtonian materials may be divided into two groups, thixotropic or rheopectic. Thixotropy and rheopexy both have the following characteristics (10):

1. They accompany an isothermal structural change brought about by applying a mechanical disturbance to the system.

2. When the mechanical disturbance is removed, the system recovers its original structure.

3. The flow curve of the system shows a hysteresis loop, figure 1-2.

Thixotropy. A thixotropic material behaves similar to a pseudoplastic material except that a time or shear history of the material has to be included in the analysis. For a pseudoplastic fluid, continually increasing the rate of shear (at a constant rate of increase in shear rate) to a predetermined point and then decreasing the rate of shear (constant rate of decrease) in a similar manner to zero will generate a single curve. The ''upcurve'' and ''downcurve'' for a pseudoplastic material will coincide, figure 1-1. For a thixotropic fluid, repeating the above procedure

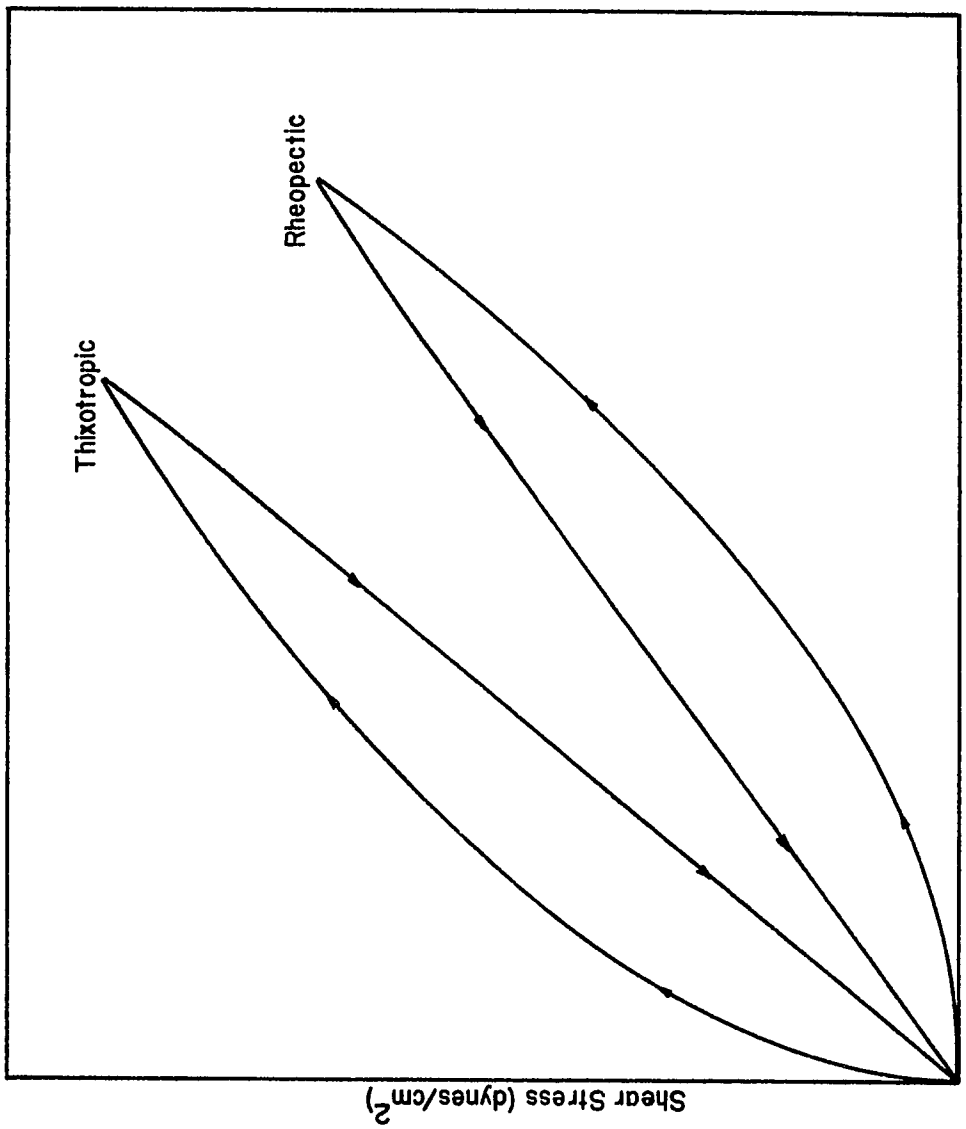

Figure I-2. Time-Dependent Flow Curves

will result in two distinct curves, an upcurve and a downcurve. These curves will form a type of hysteresis loop, figure 1-2.

A thixotropic system exhibits a time-dependent, reversible, and isothermal decrease of viscosity with shear. Thixotropic systems will also exhibit the following phenomena (8):

1. Viscosity changes with time when sheared at a constant rate.

2. The viscosity decreases provided that the shear rate applied increases over that previously experienced by the material.

3. The viscosity increases provided that the shear rate applied decreases below that previously experienced by the material.

4. If an applied shear rate is maintained at a constant value for a sufficient length of time, the viscosity will approach a limiting value, dependent only on the shear rate.

5. In steady viscometric flow, thixotropic systems will exhibit the phenomena of pseudoplasticity.

6. Thixotropic systems may also exhibit a yield stress, i.e., the graph of shear stress or shear rate may not pass through the origin, but instead, the stress may approach a finite as the shear rate approaches zero.

A single hysteresis loop for a thixotropic material was shown in figure 1-2. After completion of this hysteresis loop and returning to the origin, if a second experimental run

could be immediately determined in the exact manner as the first run, the results would not be the same. This can be seen in figure 1-3, where loop #2 was performed after returning to the origin. The shear stress for this loop is lower at similar shear rates and the area of the loop is smaller. This indicates a memory for the material, where the material has retained some of the structural breakdown from the first loop. This is the characteristic time or history for a thixotropic material. If the material had been allowed to rest and recover its original structure, the first loop would have been duplicated. From figure 1-3, each succeeding hysteresis loop would decrease in area until the material reaches an equilibrium relationship with respect to shear rate. The material now behaves similar to a pseudoplastic in that the shear stress is dependent upon shear rate but not on time.

Another characteristic flow curve for a thixotropic material is shown in figure 1-4. Here the upcurve is generated followed by a constant shear rate zone. As time of shearing increases for the region of constant shear rate, the shear stress decreases. This indicates a continual breakdown in structure for the material. Eventually, an equilibrium position is obtained, where continuing to shear the material at a constant rate of shear will no longer decrease the shear stress for the material. This point can be considered an equilibrium point. The material will again behave in a pseudoplastic manner and be time independent.

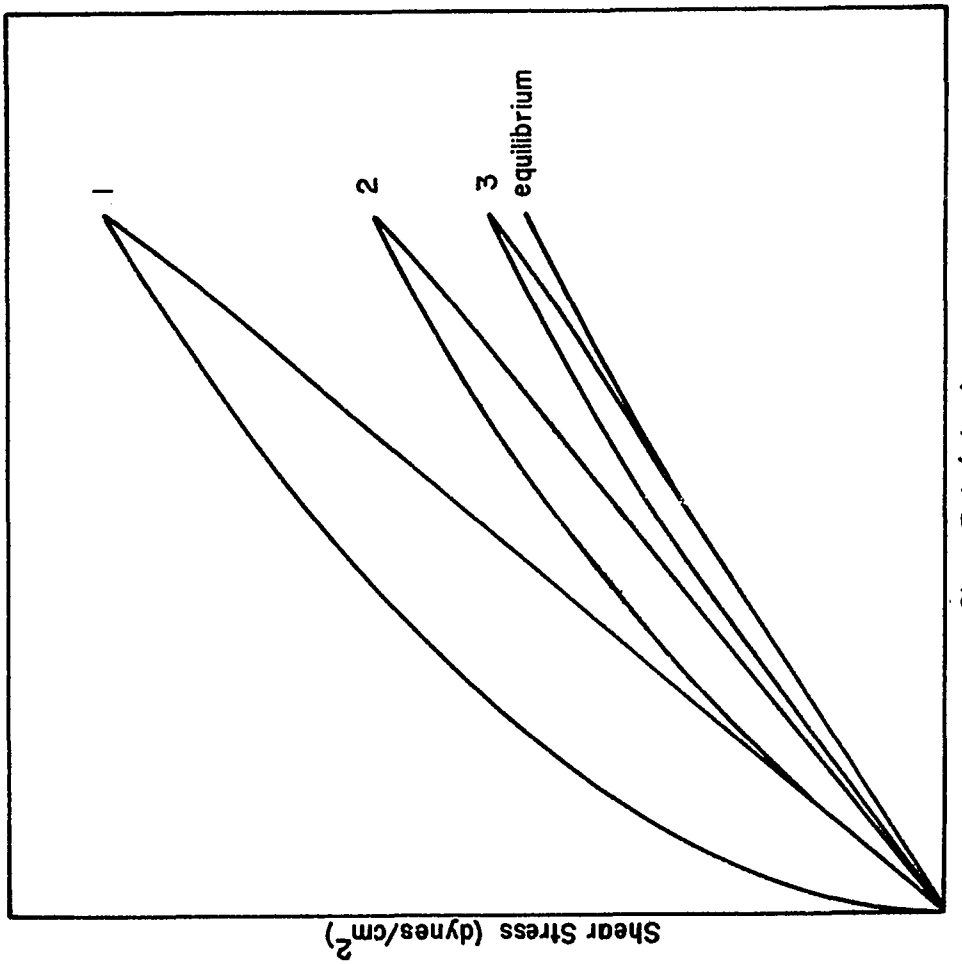

Figure I-3. Multiloop Hysteresis Curves

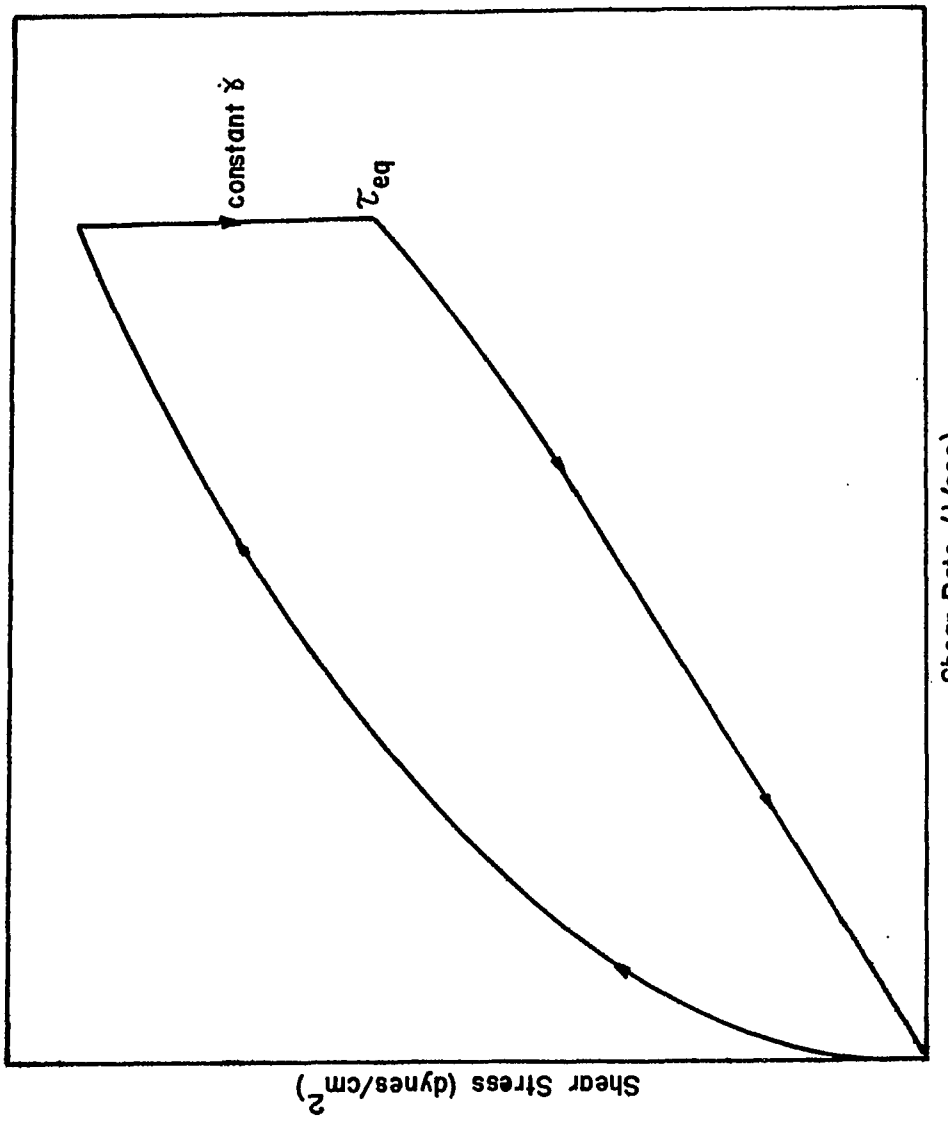

Figure I-4. Hysteresis Loop with Constant Shear Rate

One additional flow curve which can be generated for a thixotropic material is shown in figure 1-5. This curve is another form of the constant rate of shear curve. The material is sheared at constant shear rate and shear stress is plotted versus time of shearing. As the time of shearing increases, the shear decreases. Eventually, a constant shear stress is measured for the particular rate of shear and becomes independent of the time of shearing. Using different shear rates will give different shear stress versus time of shearing curves. In figure 1-5, $\dot{\gamma}_1$, is greater than $\dot{\gamma}_2$ which is greater than $\dot{\gamma}_3$. This indicates that the higher the rate of shear, the greater the shear stress of the material.

The causes for thixotropy are very similar to those for pseudoplasticity, the alignment of asymmetrical particles. When this alignment is not instantaneous with respect to time, the material is considered to be thixotropic. A limiting condition or instantaneous alignments would indicate a pseudoplastic material. Here the time would be too small to measure. Thixotropy is common to paints, ketchup and other foods, some greases, some clay suspensions, and some polymeric solutions.

Rheopexy. A rheopectic material is similar to a thixotropic material, since its flow curve is also a hysteresis loop, figure 1-2. Whereas, a thixotropic material breaks down with the application of a shear, a rheopectic material has structural build up. Rheopectic fluids include gypsum paste in water and ammonium oleate suspension.

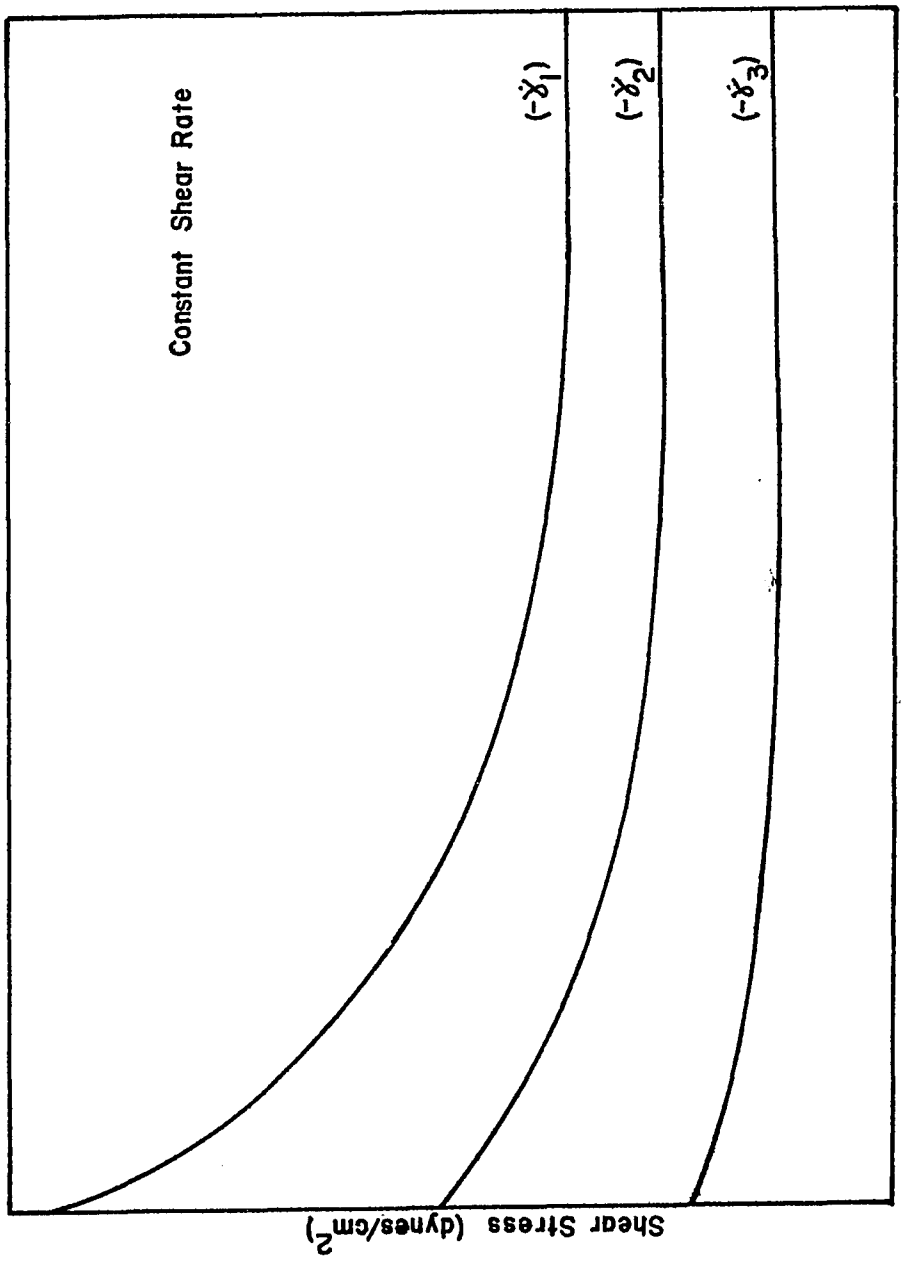

Figure I-5. Torque-Decay Curves

CHAPTER 2

THIXOTROPIC EQUATIONS

Review

Various theoretical and experimental approaches have been attempted to explain or correlate the rheological properties of thixotropic materials. Synopses of some of the more important papers will be given.

Goodeve and Whitfield (12) presented an analogy to reaction kinetics which is applicable to weakly thixotropic systems, i.e. systems in which the structure is only partially built up. They described a thixotropic system as consisting of ''cells'' having solid properties. The total volume of cells per unit volume is denoted by X and the maximum possible value of X is X_m. The rate of increase in variable X or the building up process will be defined as:

$$\frac{dX}{dt} = k''(X_m - X)^a \qquad (2\text{-}1)$$

where a is the order of the reaction and k'' is a proportionality constant for the backward reaction. They assumed the breakdown process to be proportional to the shear rate, $\dot{\gamma}$:

$$-\frac{dX}{dt} = K\dot{\gamma}X \qquad (2\text{-}2)$$

where K is the forward reaction proportionality constant. Finally, Goodeve and Whitfield stated that the apparent viscosity, η_a, is proportional to X:

$$\eta_a - \eta_o = k'X \tag{2-3}$$

where η_o is the apparent viscosity at equilibrium (residual viscosity) and k' is a constant. Combining equations (2-1) and (2-2) at equilibrium gives:

$$X = \frac{k''(X_m - X)^a}{K\dot{\gamma}} = \frac{k''X_m^a}{K\dot{\gamma}} \tag{2-4}$$

since X is small compared to X_m at equilibrium. Substituting into equation (2-3) gives:

$$\eta_a - \eta_o = \frac{k'k''X_m^a}{K}\frac{1}{\dot{\gamma}} = \theta\frac{1}{\dot{\gamma}} \tag{2-5}$$

where θ is called the ''coefficient of thixotropy''. The apparent viscosity, η_a, is defined in the usual manner:

$$\eta_a = K'(\tau/\dot{\gamma}) \tag{2-6}$$

where K' is an instrument constant. Substituting equation (2-5) into equation (2-6) gives:

$$K'\tau = \eta_o\dot{\gamma} + \theta \tag{2-7}$$

This is the form of the normal Bingham-plastic equation where θ is τ_o, the yield stress.

Most of the work on hysteresis loops was done by Green and Weltmann(13, 14, 15, 16, 17, 39, 40, 41). In their work on thixotropy, they employed a rotational viscometer which was capable of generating both up and down curves (hysteresis loop) on a rheogram. They analyzed the extent of thixotropic breakdown by the area of the hysteresis loop bounded by the upcurve and the downcurve. The larger the area of the hysteresis loop, the greater the thixotropic breakdown of the material. Green and Weltmann distinguished between the rate of shear and duration of shear (time) for a thixotropic material.

An equation of thixotropic breakdown with time has been determined experimentally by Weltmann (40). This equation gives the relationship between the rate of decrease in plastic viscosity and the time of application of a constant rate of shear as:

$$B = -\frac{d\eta_{pl}(t)}{dt} \qquad (2\text{-}8)$$

where B is the coefficient of thixotropic breakdown with time and η_{pl} is the plastic viscosity. The plastic viscosity can also be defined as the shear stress in excess of the yield value that will induce a unit rate of shear, or from figure 2-1:

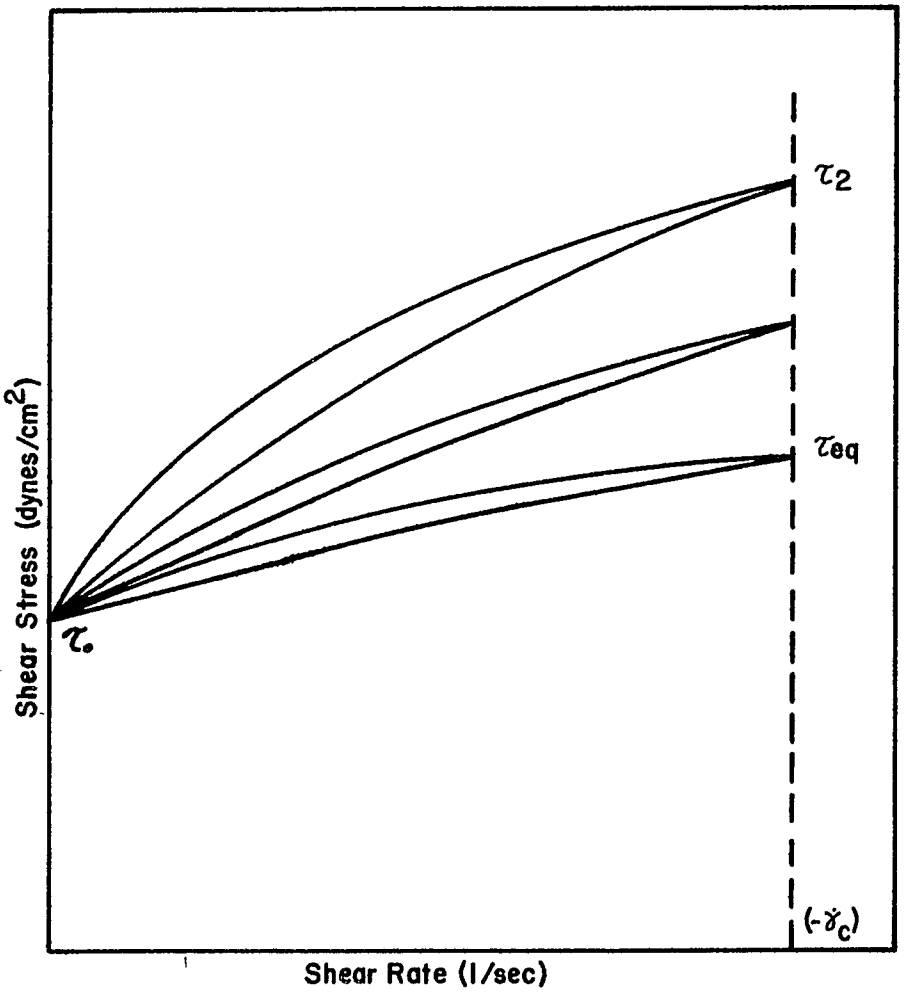

Figure 2-1. Multiloop Hysteresis Curves

$$\eta_{pl} = \frac{\tau_2 - \tau_o}{\dot{\gamma}_c - 0} \qquad (2\text{-}9)$$

The numerical value of B can be determined experimentally from a series of hysteresis loops and by integrating equation (2-8).

$$B = \frac{\eta_2 - \eta_3}{\ln(t_3/t_2)} \qquad (2\text{-}10)$$

Dahlgren (6) studied the thixotropic breakdown with increase of rate of shear based on the experimental work of Green and Weltmann. He found that the plastic viscosity is a function of the shear rate as:

$$d\eta_{pl} = - M(d\dot{\gamma}/\dot{\gamma}) \qquad (2\text{-}11)$$

where M is the coefficient of thixotropic breakdown with shear rate. He then uses equations (2-8) and (2-11) to obtain an equation for the area of a hysteresis loop, by which he was able to fully characterize a thixotropic material. This equation has eight constants that have to be evaluated.

Moore (31) assumed that a thixotropic material being sheared at constant rate has a structure developed as a result of a dynamic equilibrium between two processes, the natural tendency to build up and the destruction process due to shear. He represented the structure as being composed of a large number of separate ''links''.

The linkage is indicated by λ, which is the number of links actually formed divided by the total number of links in the completely built up state. He assumed the linkage or structural parameter changes according to the equation:

$$\frac{d\lambda}{dt} = a(1 - \lambda) - b\lambda\dot{\gamma} \qquad (2\text{-}12)$$

where a and b are constants. When equation (2-12) is integrated for $\dot{\gamma}$ = constant, it gives:

$$\lambda = \lambda_D - (\lambda_D - \lambda_o)\, e^{-(a + b\dot{\gamma})t} \qquad (2\text{-}13)$$

where:

$$\lambda_D = a/(a + b\dot{\gamma})$$

and λ_o is the value of λ at t = 0. He then obtained a rheological equation by assuming that the apparent viscosity is linear with λ :

$$\tau/\dot{\gamma} = \eta_a = \eta_o + c\lambda \qquad (2\text{-}14)$$

where η_o is the viscosity of the completely broken down structure and c is a material constant. This equation does not explain a yield stress noted in some materials.

Hahn, Ree, and Eyring (20, 21, 22) assumed a model for a thixotropic system which contained two kinds of molecules, entangled

and disentangled. The entangled molecule whose flow behavior is non-Newtonian, transforms to the disentangled molecule of Newtonian character as a result of shear stress. The rheological equation which contains Newtonian and non-Newtonian units is:

$$\tau = \frac{\lambda_1 \beta_1}{\alpha_1} + \frac{\lambda_2}{\alpha_2} \sinh^{-1} \beta_2 \dot{\gamma} \qquad (2\text{-}15)$$

where λ_i is the fraction of the area occupied by the i^{th} kind of flow units

$$\alpha_i = \frac{(\lambda \lambda_2 \lambda_3)_i}{2KT}$$

$$\beta_i = 1/(2K' \lambda / \lambda_1) \qquad \text{the relaxation time}$$

$\lambda, \lambda_1, \lambda_2, \lambda_3$ are parameters in Eyring's theory of flow, K is Boltzmann's constant, K' is the specific rate of flow when there is no stress, λ_i is the fraction of the area of the shear surface occupied by the i^{th} kind of flow units, and T is the absolute temperature. Subscripts 1 and 2 refer to Newtonian and non-Newtonian units, respectively. The net rate of transformation from entanglement to disentanglement is:

$$-\frac{d\lambda_2}{dt} = \lambda_2 k_f e^{\frac{\mu c \dot{\gamma}^2}{KT}} - \lambda_1 k_b e^{-\frac{(1-\mu) c \dot{\gamma}^2}{KT}} \qquad (2\text{-}16)$$

where k_f is the specific rate for the forward reaction at zero stress, k_b is the specific rate for the reverse reaction at zero

stress, c is a constant, and μ is a reaction constant. For the upcurve, the shear rate, $\dot{\gamma}$, is changing with time according to the relation:

$$\dot{\gamma} = S\, t \tag{2-17}$$

where S is a constant to be determined by the experimental conditions. Substituting equation (2-17) into equation (2-16) and integrating, gives:

$$\lambda_2 = (\lambda_2)_o e^{-k_f \gamma I} \tag{2-18}$$

where:

$$I = \int_o^y e^{y^2} dy$$

$$y = \frac{t}{\gamma} = t/(KT/\mu c S^2)^{\frac{1}{2}} = \dot{\gamma}/(KT/\mu c)^{\frac{1}{2}} = \frac{\dot{\gamma}}{\gamma S}$$

and $(\lambda_2)_o$ is the fraction of the area occupied by the entangled molecules at t = 0. Substituting equation (2-18) into equation (2-15) yields:

$$\tau = \left\{1 - (\lambda_2)_o e^{-k_f \gamma I}\right\} \frac{\beta_1}{\alpha_1} \dot{\gamma} + \frac{1}{\alpha_2} (\lambda_2)_o e^{-k_f \gamma I} \sinh^{-1} \beta_2 \dot{\gamma} \tag{2-19}$$

Similarly for the downcurve:

$$\tau = \left\{1 - (\lambda_2)_o e^{-k_f \gamma I_m}\right\} \frac{\beta_1}{\alpha_1}\dot{\gamma} + \frac{1}{\alpha_2}(\lambda_2)_o e^{-k_f \gamma I_m} \sinh^{-1} \beta_2 \dot{\gamma} \quad (2\text{-}20)$$

where I_m is the value of I at the apex.

Pinder (33) studied the time-dependent rheology of tetrahydrofuran - hydrogen sulfide gas hydrate slurry at constant shear rates. He felt that because there is an equilibrium value of apparent viscosity, η_a, the time-dependency of viscosity might be approximated by a reversible reaction mechanism:

$$(\eta_a)_1 \underset{k_b}{\overset{k_f}{\rightleftharpoons}} (\eta_a)_2 \quad (2\text{-}21)$$

where subscripts 1 and 2 refer to two extremes of particle orientation, complete randomness and equilibrium order, respectively. For the second order - zero order reversible mechanism, which the author found to give the best fit for his experimental data, the rate can be represented by:

$$-\frac{d(\eta_a)_1}{dt} = k_f(\eta_a)_1^2 - k_b \quad (2\text{-}22)$$

at time t. With the equilibrium condition and the initial condition known, equation (2-22) can be integrated to give:

$$\ln \frac{(\eta_{a_e} + \eta_a)(\eta_{a_o} - \eta_{a_e})}{(\eta_a - \eta_{a_e})(\eta_{a_e} + \eta_{a_o})} = 2\eta_e k_f t \quad (2\text{-}23)$$

where η_{a_e} is the apparent viscosity at equilibrium and η_{a_o} is the

yield value of apparent viscosity.

Chang and Evans (4) expressed the rheological equation of state for thixotropic fluids as:

$$\tau = \eta(\lambda, \dot{\gamma})\dot{\gamma} \tag{2-24}$$

where the viscosity is a function of the shear rate as well as the structural parameter. They expressed the rate equation for structural breakdown as:

$$\frac{d\lambda}{dt} = g_{\dot{\gamma}}(\lambda, \dot{\gamma}) \tag{2-25}$$

which states that the rate at which the structure changes is a function of both the shear rate and the structural parameter. From the defined rheological behavior of thixotropic fluids, the authors postulated that the functional forms of τ and $g_{\dot{\gamma}}$ are subjected to the following restrictions:

$$\eta(\lambda, \dot{\gamma}) > 0 \tag{2-26}$$

$$(\partial\tau/\partial\dot{\gamma})_{\lambda} > 0 \tag{2-27}$$

$$(\partial\tau/\partial\lambda)_{\dot{\gamma}} > 0 \tag{2-28}$$

$$g_{\dot{\gamma}}(\lambda, \dot{\gamma}) = 0 \text{ when } \lambda = \lambda_e(\dot{\gamma}) \tag{2-29}$$

$$g_{\dot{\gamma}}(\lambda, \dot{\gamma}) < 0 \text{ when } \lambda > \lambda_e(\dot{\gamma}) \tag{2-30}$$

$$g_{\dot{\gamma}}(\lambda, \dot{\gamma}) > 0 \text{ when } \lambda < \lambda_e(\dot{\gamma}) \tag{2-31}$$

$$(\partial g / \partial \dot{\gamma})_{\lambda} < 0 \tag{2-32}$$

where the subscript e refers to the equilibrium condition. The authors then used the Moore model to illustrate their model. The constitutive equations can then be written as:

$$\tau = (\eta_o + c\lambda)\dot{\gamma} \tag{2-33}$$

and

$$\frac{d\lambda}{dt} = g_{\dot{\gamma}}(\dot{\gamma}, \lambda) = a - (a + b\dot{\gamma})\lambda \tag{2-34}$$

where η_o, a, b, and c are positive material constants. For the upcurve, they assume that:

$$\dot{\gamma}(t) = \dot{\gamma}_o + At \tag{2-35}$$

which can be substituted into equation (2-34) to give:

$$\frac{d\lambda}{d\dot{\gamma}} + \frac{a + b\dot{\gamma}}{A}\lambda = \frac{a}{A} \tag{2-36}$$

This equation can be solved with the initial conditions: t = 0, $\dot{\gamma} = \dot{\gamma}_o$, and $\lambda = \lambda_o$ to give:

$$\lambda = \left\{ \frac{\lambda_o}{\phi'_o} + \pi^{\frac{1}{2}} \frac{\alpha}{\beta} (\epsilon - \epsilon_o) \right\} \phi' \qquad (2\text{-}37)$$

Substituting this equation into equation (2-33) gives:

$$\tau_{up} = \eta_o \dot{\gamma} + c\dot{\gamma} \left\{ \frac{\lambda_o}{\phi'_o} + \pi^{\frac{1}{2}} \frac{\alpha}{\beta} (\epsilon - \epsilon_o) \right\} \phi' \qquad (2\text{-}38)$$

where $\alpha = a/2A$

$$\beta^2 = b/2A$$

$$\phi' = \phi'\left(\frac{\alpha}{\beta} + \beta\dot{\gamma}\right) = \frac{2}{\pi^{1/2}} \exp\left\{ -\left(\frac{\alpha}{\beta} + \beta\dot{\gamma}\right)^2 \right\}$$

$$\epsilon = \epsilon\left(\frac{\alpha}{\beta} + \beta\dot{\gamma}\right) = \int_o^{\frac{\alpha}{\beta} + \beta\dot{\gamma}} e^{S^2} \, dS$$

which is the Dawson Integral. For the downcurve:

$$\dot{\gamma}(t) = \dot{\gamma}_m - At \qquad (2\text{-}39)$$

and

$$\tau_{down} = \eta_o \dot{\gamma} + c\dot{\gamma} \left\{ \frac{\lambda_m \phi_m' + 2\frac{\alpha}{\beta}(\phi_m - \phi)}{\phi'} \right\} \qquad (2\text{-}40)$$

where:

$$\phi = \phi\left(\frac{\alpha}{\beta} + \beta\dot{\gamma}\right) = \frac{2}{\pi^{1/2}} \int_0^{\frac{\alpha}{\beta}+\beta\dot{\gamma}} e^{-S^2} dS$$

is the error integral.

Seno (34) discussed thixotropic behavior based on the thermodynamics of irreversible processes (18):

$$T\frac{dS}{dt} = \frac{dU}{dt} + v \sum_{\alpha,\beta=1}^{3} \tau_{\alpha\beta}^{eq} \frac{d\,\gamma_{\alpha\beta}}{dt} \qquad (2\text{-}41)$$

where S is the specific entropy, U is the specific internal energy, v is the specific volume, T is the absolute temperature, $\tau_{\alpha\beta}^{eq}$ is the equilibrium stress tensor, and $\gamma_{\alpha\beta}$ is the total strain tensor. The author assumed that the total pressure causes both the flow of the fluids and the destruction of the internal structure as follows:

$$\tau_{\alpha\beta} = \tau_{\alpha\beta}^{def} + \tau_{\alpha\beta}^{des} \qquad (2\text{-}42)$$

He further assumes that the stress tensor for deformation, $\tau_{\alpha\beta}^{def}$, is divided into two parts, the equilibrium stress tensor and the viscous stress tensor:

$$\tau_{\alpha\beta}^{def} = \tau_{\alpha\beta}^{eq} + \tau_{\alpha\beta}^{v} \qquad (2\text{-}43)$$

The stress and strain tensors can be divided into a tangential part and a normal part:

$$\tau_{\alpha\beta} = \tilde{\tau}_{\alpha\beta} + \tau \delta_{\alpha\beta} \tag{2-44}$$

$$\gamma_{\alpha\beta} = \tilde{\gamma}_{\alpha\beta} + \gamma \delta_{\alpha\beta} \tag{2-45}$$

where $\delta_{\alpha\beta}$ is Kronecker's delta. He also states that only the tangential force breaks down the internal structure of the system. Seno defines the apparent viscosity, η_a, as:

$$\tilde{\tau}_{\alpha\beta} = \tilde{\tau}_{\alpha\beta}^{def} + \tilde{\tau}_{\alpha\beta}^{des} = -\eta_a \frac{d\,\tilde{\gamma}_{\alpha\beta}}{dt} \tag{2-46}$$

From this equation, he obtains:

$$\eta_a = \mu + \zeta \frac{(d\xi/dt)}{(d\,\tilde{\gamma}_{\alpha\beta}/dt)} \tag{2-47}$$

where μ is the ordinary viscosity which is not dependent on the shear, ξ is a state variable representing the structural breakdown, and ζ is the rate constant. Equation (2-47) can be obtained from equation (2-46) and the following phenomenological expressions:

$$\tilde{\tau}_{\alpha\beta}^{def} = -\mu \frac{d\,\tilde{\gamma}_{\alpha\beta}}{dt} \tag{2-48}$$

$$\tilde{\tau}_{\alpha\beta}^{des} = -\zeta \frac{d\underline{\xi}}{dt} \qquad (2\text{-}49)$$

Although the author has developed a mechanism for thixotropic breakdown, he states that a full quantitative description has not yet been successful.

Huang Equation

Most of the equations available in the literature are unable to explain the various thixotropic phenomena, i.e., the hysteresis loop, multiple hysteresis loops, and shear stress-time results as a function of constant rate of shear. Some equations are specific and can describe a particular property of thixotropy. Others which are more general and versatile require too many constants to be evaluated, are not quantitative, or have not been rigorously tested. One such relationship, which is general and has only 5 constants, is the Huang (23) equation based on irreversible thermodynamics. In this equation, a molecular arrangement parameter is used to describe the breakdown of a thixotropic material with shear rate. An outline of the derivation will be given and a general equation presented which will be used to analyze the rheological behavior of thixotropic materials.

Huang assumes that a molecular arrangement parameter, β_{ij}, is related to entropy under non-equilibrium conditions by:

$$\rho \frac{D\hat{S}}{Dt} = -\frac{1}{T} \tau^{ij} \frac{d\beta_{ij}}{dt} \qquad (2\text{-}50)$$

where $D\hat{S}/Dt$ is the substantial time derivative of specific entropy, T is the absolute temperature, t is the time, ρ is the density, and τ^{ij} is the stress tensor. In this equation, the entropy varies with the change of molecular arrangement which is induced by the rate of deformation of the fluid.

From irreversible thermodynamics (18), the author then assumes that when the total system is not in equilibrium, there exists within small mass elements a state of local equilibrium. The entropy balance equation for a homogeneous fluid is:

$$\rho \frac{D\hat{S}}{Dt} = -\frac{1}{T} \left\{ q^{i}_{,i} + \tau^{ij} \frac{d\gamma_{ij}}{dt} \right\} \qquad (2\text{-}51)$$

where $q^{i}_{,i}$ is the divergence of the heat flux vector and γ_{ij} is the strain tensor. When the molecular arrangement induced by the deformation rate is taken into consideration, equation (2-51) becomes:

$$\rho \frac{D\hat{S}}{Dt} = -\frac{1}{T} \left\{ q^{i}_{,i} + \tau^{ij} \frac{d\gamma_{ij}}{dt} + \tau^{ij} \frac{d\beta_{ij}}{dt} \right\} \qquad (2\text{-}52)$$

Therefore, the rate of generation of entropy, σ, is:

$$\sigma = -\frac{1}{T}\left\{\frac{1}{T} q^{i} T_{,i} + \tau^{ij}\frac{d\gamma_{ij}}{dt} + \tau^{ij}\frac{d\beta_{ij}}{dt}\right\} \qquad (2\text{-}53)$$

where q^{i} is the heat flux vector and $T_{,i}$ is the temperature gradient vector.

Huang then related the contravariant tensors of first and second order in equation (2-53) to the temperature gradient, the rate of strain, and the rate of molecular arrangement parameter by the following phenomenological equations:

$$q^{i} = -\lambda g^{ik} T_{,k} \qquad (2\text{-}54)$$

$$\tau^{ij} = -\eta_{a}\frac{d\gamma^{ij}}{dt} \qquad (2\text{-}55)$$

$$\tau^{ij} = -\zeta\frac{d\beta^{ij}}{dt} \qquad (2\text{-}56)$$

where λ is the thermal conductivity, g^{ik} is the associated metric tensor, η_{a} is the apparent viscosity, and ζ is the coefficient which relates the rate of molecular arrangement parameter and the shear stress. The apparent viscosity is a function of the second and third principal invariants of the rate of strain tensor.

Substituting these phenomenological equations into equation (2-53), the equation of entropy production becomes:

$$\sigma = -\frac{1}{T}\left\{-\frac{\lambda}{T} g^{ik} T_{,k} T_{,i} - \eta_a \frac{d\gamma^{ij}}{dt}\frac{d\gamma_{ij}}{dt} - \zeta \frac{d\beta^{ij}}{dt}\frac{d\beta_{ij}}{dt}\right\} \quad (2\text{-}57)$$

The last two terms of equation (2-57) correspond to the entropy production due to the shear stress. An overall apparent viscosity, $(\eta_a)_t$, can be defined which will relate the shear stress to the rate of strain by considering both the rate of strain effect and the rate of molecular arrangement effect:

$$\tau^{ij} = -(\eta_a)_t \frac{d\gamma^{ij}}{dt} = -\eta_a \frac{d\gamma^{ij}}{dt} - \zeta \frac{d\beta^{ij}}{dt} \quad (2\text{-}58)$$

When the equation is rewritten in terms of viscosity, it becomes:

$$(\eta_a)_t = \frac{\tau^{ij}}{\dot{\gamma}^{ij}} = \eta_a + \zeta \frac{\dot{\beta}^{ij}}{\dot{\gamma}^{ij}} \quad (2\text{-}59)$$

where $\dot{\beta}^{ij}$ is the rate of molecular arrangement parameter and $\dot{\gamma}^{ij}$ is the rate of strain.

Huang then assumed that the rate of change of the molecular arrangement parameter for a thixotropic, homogeneous fluid is

sensitive to the rate of deformation in the following way:

$$\frac{d\beta^{ij}}{dt} = -C_1 \beta^{ij} |\dot{\gamma}^{ij}|^n \quad \text{for } |\dot{\gamma}^{ij}| > 0 \tag{2-60}$$

$$\frac{d\beta^{ij}}{dt} = C_2(\beta_e^{ij} - \beta^{ij}) \quad \text{for } |\dot{\gamma}^{ij}| = 0 \tag{2-61}$$

where $|\dot{\gamma}^{ij}|$ is the absolute value of the rate of strain, β_e^{ij} is the equilibrium value of the molecular arrangement parameter, C_1 and C_2 are rate constants, and n is the order of the rate equation (n has to be greater than zero). Integrating equation (2-60) between the limits:

$$t = o, \beta^{ij} = \beta_e^{ij}; \; t = t, \beta^{ij} = \beta^{ij} \tag{2-62}$$

giving:

$$\beta^{ij} = \beta_e^{ij} \exp(-C_1 \int_o^t |\dot{\gamma}^{ij}|^n dt) \tag{2-63}$$

As can be seen from equation (2-63), an increase in rate of shear produces a decrease in the molecular arrangement parameter. Substituting equation (2-63) into equation (2-60), gives:

$$\frac{d\beta^{ij}}{dt} = -C_1 |\dot{\gamma}^{ij}|^n \beta_e^{ij} \exp(-C_1 \int_o^t |\dot{\gamma}^{ij}|^n dt) \qquad (2\text{-}64)$$

and then substituting equation (2-64) into equation (2-59), yields an expression of overall apparent viscosity for thixotropic fluids:

$$(\eta_a)_t = \eta_a - \frac{\Sigma\left\{C_1 \beta_e^{ij} e^{-C_1 \int_o^t |\dot{\gamma}^{ij}|^n dt}\right\} |\dot{\gamma}^{ij}|^n}{(\dot{\gamma}^{ij})} \qquad (2\text{-}65)$$

Equation (2-65) gives the overall apparent viscosity as a function of shear rate and duration of shear. It represents an equation for the overall apparent viscosity as a function of different kinds of apparent viscosity, η_a. The simplest form of the equation is:

$$(\eta_a)_t = \mu - C_1 \Sigma \beta_e^{ij} \frac{|\dot{\gamma}^{ij}|^n}{(\dot{\gamma}^{ij})} e^{-C_1 \int_o^t |\dot{\gamma}^{ij}|^n dt} \qquad (2\text{-}66)$$

where μ is a constant for η_a. Substituting equation (2-66) into equation (2-59) gives:

$$\tau^{ij} - \tau_o^{ij} = -\left\{\mu - C_1 \Sigma \beta_e^{ij} \frac{|\dot{\gamma}^{ij}|^n}{(\dot{\gamma}^{ij})} e^{-C_1 \int_o^t |\dot{\gamma}^{ij}|^n dt}\right\} \dot{\gamma}^{ij} \qquad (2\text{-}67)$$

where τ_o is the yield stress of the fluid.

Rewriting equation (2-67) in non-tensor units and rearranging terms:

$$\tau = \tau_o - \mu\dot{\gamma} + C_1 \xi \beta_e |\dot{\gamma}|^n e^{-C_1 \int_o^t |\dot{\gamma}|^n dt} \qquad (2\text{-}68)$$

Since μ is a positive constant and $\dot{\gamma}$ was defined as a negative quantity by equation (2-55), the term $(-\mu\dot{\gamma})$ is a positive quantity. Because C_1, ξ, and β_e are positive constants and the equation uses the absolute value of the shear rate, $\dot{\gamma}$, the third term in equation (2-68) is also positive. The manipulation and use of this equation is described in Appendix C.

CHAPTER 3

EXPERIMENTAL EQUIPMENT

Introduction

There are a variety of viscometers available which will measure shear stress as a function of rate of shear or shear rate as a function of shear stress. They include capillary tube, falling ball, concentric cylinder, and cone-and-plate. When studying time-dependent, non-Newtonian rheology, a viscometer of the rotational type is used, i.e., a concentric cylinder or a cone-and-plate viscometer. A rotational viscometer is used for thixotropic materials because the viscosity changes as a function of time, in addition to changing as a function of shear rate. With the capillary tube or falling-ball viscometers the tube diameter or ball density have to be varied to introduce a change in shear rate. This means a discontinuity in the time function during the course of an experiment. With a rotational viscometer, a change in RPM, using the same sample, will change the rate of shear applied to the sample. This variation in shear rate can be performed continuously, either through mechanical means or through the use of an automatic control mechanism.

Coaxial-cylinder viscometers. The most common commercial viscometer is the coaxial cylinder type, figure 3-1. This viscometer consists of an inner cylinder or bob, of radius, R_b, suspended in the sample fluid in a cylinder or cup, of radius,

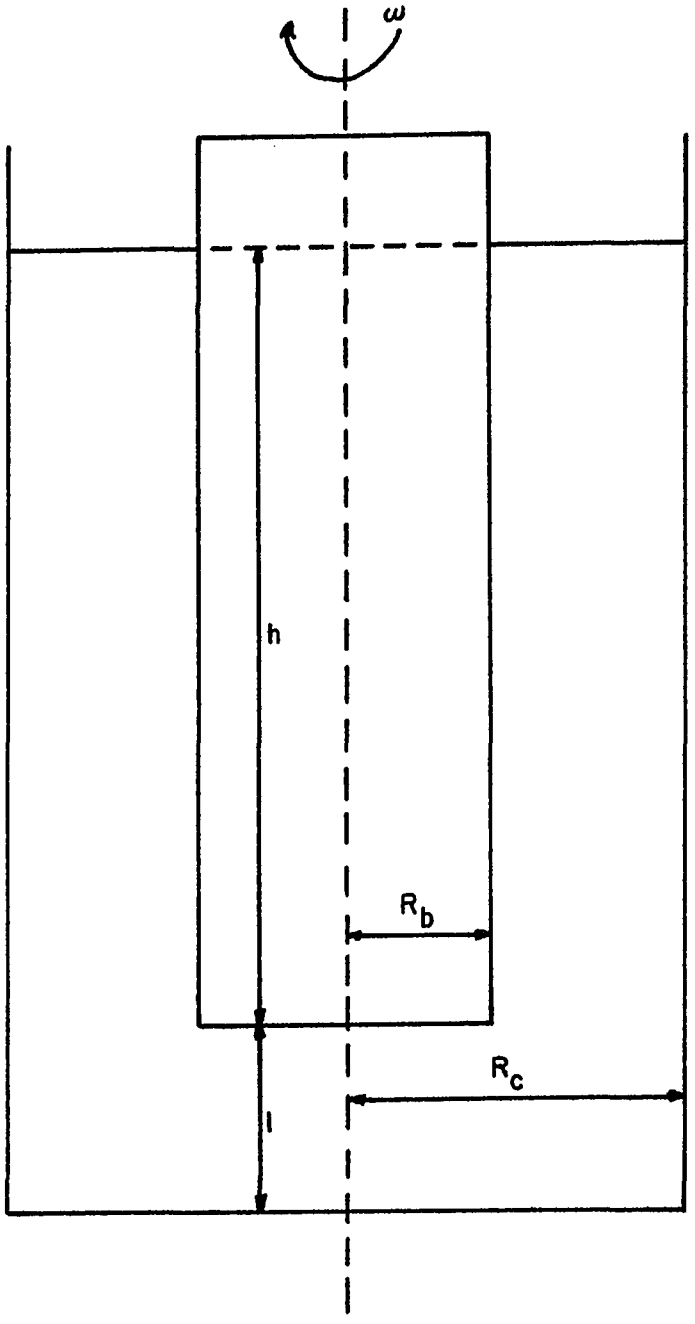

Figure 3-1. Coaxial Cylinder Viscometer

R_c. The liquid covers the inner cylinder to a height, h. The bottom of the bob is separated from the bottom of the cup by a distance, l. The inner cylinder rotates with an angular velocity, ω, though the cup rather than the bob could equally well be rotating.

When the cup is rotated, the liquid is sheared in the annular space, and attains a steady state for a given annular velocity. The torque acting on every molecular layer of the liquid is the same. The torque on a molecular layer located at a distance, r, from the common axis is given by M. The total torque is given by:

$$M = 2\pi r^2 h \tau \tag{3-1}$$

where τ is the shear stress acting on the molecular layer under consideration and h is the height of the bob immersed in the liquid. Under a shear stress, τ, successive molecular layers shear with respect to the neighboring layer. The rate of shear, $\dot{\gamma}$, is given by:

$$\dot{\gamma} = \frac{dv}{dr} = r\left(\frac{d\omega}{dr}\right) \tag{3-2}$$

where v is the linear velocity and ω is the angular velocity. Generally, $\dot{\gamma}$ is a function of τ, i.e.,

$$\dot{\gamma} = F(\tau) = r \frac{d\omega}{dr} \qquad (3\text{-}3)$$

From equation (3-1), $dr/r = - d\tau/2\tau$; substituting into equation (3-3) gives:

$$\omega = \int_o^{\omega} d\omega = - \frac{1}{2} \int_{\tau_b}^{\tau} F(\tau) \frac{d\tau}{\tau} \qquad (3\text{-}4)$$

where $\tau_b = M/2\pi R_b^2 h$ is the shear stress on the surface of the bob and $\tau = M/2\pi r^2 h$ is the stress on the representative molecular layer a distance, r, from the axis of the bob.

For Newtonian fluids, the relation, $F(\tau) = \tau/\eta$ (η is the viscosity, which is independent of τ or $\dot{\gamma}$), is introduced into equation (3-4) and by integrating the latter from τ_b to τ_c ;

$$\omega = \frac{\tau}{4\pi\eta h} \left\{ \frac{1}{R_b^2} - \frac{1}{R_c^2} \right\} \qquad (3\text{-}5)$$

where $\omega = \frac{2\pi n}{60}$ and n being RPM. From equations (3-1) and (3-5),

$$\eta = \tau_b \Big/ \left[\frac{4\pi n}{60 \left\{ 1 - (R_b^2/R_c^2) \right\}} \right] \qquad (3\text{-}6)$$

Cone-and-plate viscometers. The conventional coaxial cylinder suffers the disadvantages of shear rate variations across the measuring annulus, end effects, limited range of operation, and filling, cleaning, and centering difficulties. The cone-and-plate configuration provides an almost constant shear condition without introducing construction complexity.

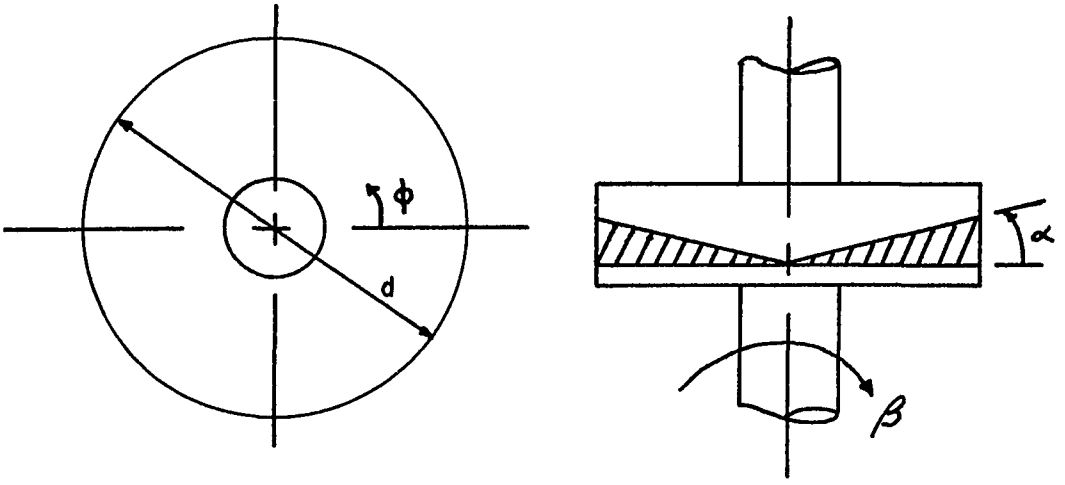

Cone-and-Plate Configuration

FIGURE 3-2

This type of instrument shown diagrammatically in figure 3-2, consists of a rotating flat plate and a cone with a very obtuse angle. The apex of the cone just touches the plate surface and the fluid fills the narrow gap formed by the cone and plate.

The linear velocity at any radius, r, is β_r and the gap width at this radius, r, is r tan α. The rate of shear at any radius, r, is then given by:

$$\dot{\gamma}(r) = \beta r/r \tan\alpha = \beta/\tan\alpha = \beta/\alpha \qquad (3\text{-}7)$$

Because of the small angle of the cone and small gap width, the rate of shear is assumed constant and independent of radius.

$$\dot{\gamma} = \beta/\alpha \qquad (3\text{-}8)$$

$$\dot{\gamma} = 180\beta/\pi\alpha \qquad \text{sec}^{-1} \qquad (3\text{-}9)$$

$$\dot{\gamma} = 360/\alpha\, t \qquad (3\text{-}10)$$

where β is the angular rotation of the platen (radians/sec)

α is angle of cone (degrees)

$t = 2\pi/\beta$ (sec/rev)

The torque, T, measured on the top platen of radius, R, (cm) is given by:

$$T = \int_0^{2\pi}\int_0^R \tau r^2 dr\, d\phi \qquad (3\text{-}11)$$

$$T = 2\pi\int_0^R \tau r^2 dr$$

$$T = 2\pi\tau R^3/3 \qquad (3\text{-}12)$$

$$\tau = 3T/2\pi R^3 \qquad \text{dyne/cm}^2 \qquad (3\text{-}13)$$

where ϕ is the angle in the plane of angular motion.

Equations (3-8) and (3-13) are simplified expressions for the rate of shear and shear stress, respectively. They depend on the following assumptions (25):

(1) Angle α is small, such that $\tan \alpha = \alpha$.

(2) Velocity is linear with respect to α.

(3) Velocity is linear with respect to r.

(4) Flow is tangential.

(5) Edge effects are negligible.

Assumption (3) and (4) are good approximations if α is less than four degrees and speed is moderate. Assumption (5) of the edge effects introduces no significant error because the height of the gap at the cone periphery is small. The error in τ and $\dot{\gamma}$ due to assumptions (1) and (2) varies depending on the angle α and the rheological property of the fluid. The employment of the assumption that the velocity is linear with respect to α may lead to significant error in the calculation of the shear rate.

Weissenberg Rheogoniometer

The availability of a Weissenberg Rheogonimeter* dictated the particular cone-and-plate instrument that was to be used in

---

* Sangamo Controls Limited, North Bersted, Bognor Regis, Sussex, England.

the experimental analysis of thixotropic materials. This instrument is an extremely versatile and accurate rheological tool. The Weissenberg Rheogoniometer comes in four models with the fourth model being the combined form of the other three models. As seen in the block diagram, figure 3-3, the Rheogoniometer consists of essentially three parts: (a) drive unit, (b) measuring section, and (c) control and readout section. The differences in the various models are in the measuring section.

The drive unit consists of a 1 h.p., 1800 RPM synchronous motor which is the input to a 60 step gearbox which provides reduction ratios from $1:10^{-5.9}$ to 1:1 in steps of $10^{0.1}$. When the drive unit is coupled to the measuring section, in which there is a further reduction of 4:1, the lower platen is driven at speeds from $5.68 \cdot 10^{-4}$ RPM to 450 RPM. Gear changing is effected by unlocking and rotating the gear box end plates to the desired new gear. A similar drive unit may be used to drive the variable sine wave generator of the measuring section.

The first model (Model A) of the different versions of the Rheogoniometer is called the Rheo-Viscometer and is basic to all other models. A two way drive box, translates the continuous rotational drive from a horizontal axis to a vertical axis through a gear reduction connected to a worm and wheel and rotates the lower platen containing the sample. The viscous drag is transmitted through the sample to the upper platen which is attached to the

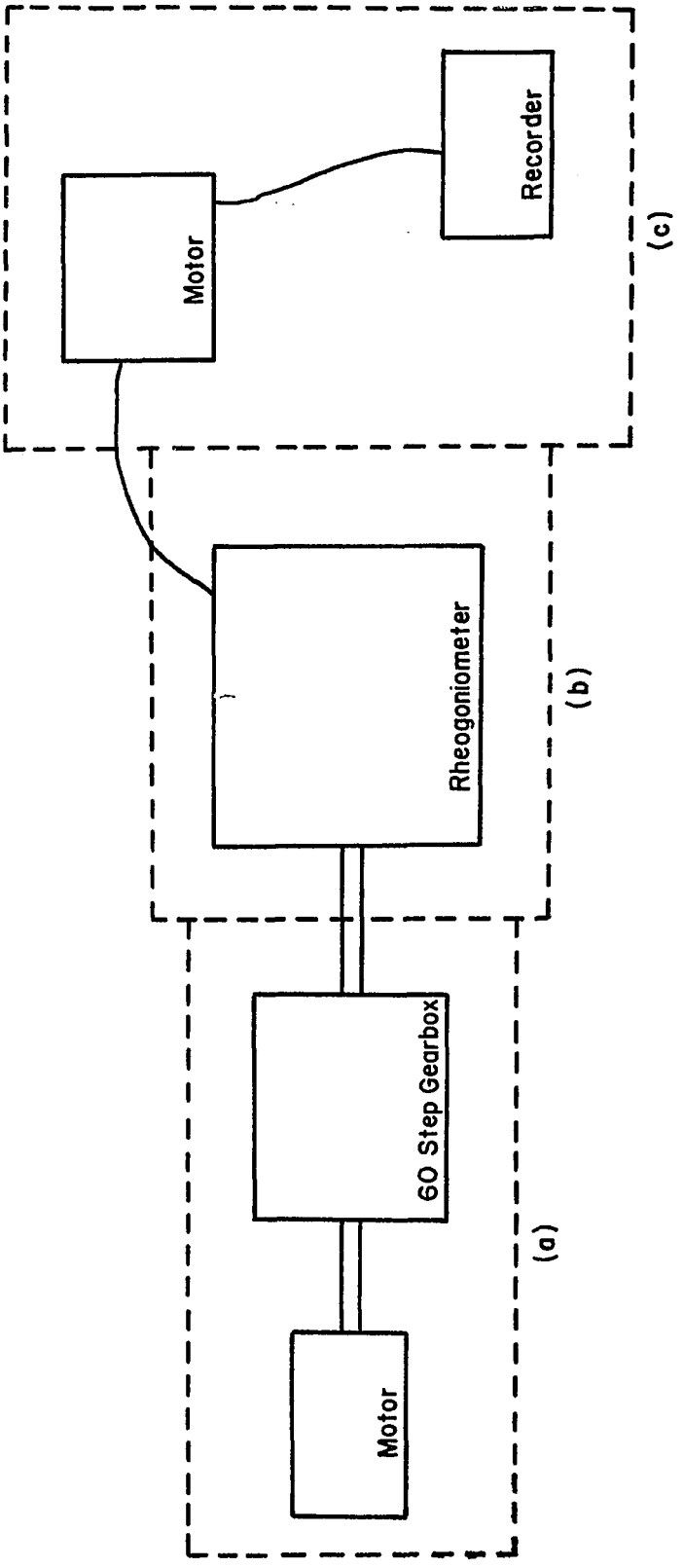

Figure 3-3. Standard Weissenberg Rheogoniometer

rotor of an air bearing, torsion head. This allows a small almost frictionless circular movement of the upper platen against a calibrated torsion bar. The small movement of the torsion bar is detected by a linear displacement inductive transducer. In the Rheogoniometer cone-plate system, the cone is normally truncated to avoid errors which would result through friction and wear. During shearing, the gap between the upper and lower platens is held constant and may be measured by means of another transducer. An electromagnetic clutch-brake device placed between the main drive unit and the two-way drive box enables instantaneous application or termination of shear. This allows studies of peak stress and relaxation to be made.

The overall range of the instrument is:

Viscosity: $1 \cdot 10^{-3}$ to $5 \cdot 10^{7}$ poise

Rate of shear: $8.42 \cdot 10^{-3}$ to $1.07 \cdot 10^{4}$ $sec.^{-1}$

Shear Stress: $1.91 \cdot 10^{-2}$ to $1.22 \cdot 10^{7}$ $dynes/cm^{2}$

These ranges available to the instrument result from various combinations of torsion bars, platen diameters, cone angles, and gear box settings. The minimum or maximum conditions cannot be obtained with any single set of accessories or settings. For example, in the low viscosity and low shear rate range a small torsion bar, large diameter platen, large cone angle, and large gear box setting (small RPM) would be used to perform the experiment.

Model B of the Rheogoniometer is called a NF-Rheo-Visco-Elastometer. This model provides the same facilities as the Rheo-Viscometer plus a provision for measuring the normal force (normal to the direction of shear) which is exhibited by many materials when subjected to steady shear. The normal force tends to force down the lower platen which in Model B is free to move in a vertical direction. The downward movement of the platen is restrained by the restoring force of a leaf spring. The platen gap change is detected by an inductive transducer and controller within predetermined limits either manually or by a servo system which restores the lower platen to the desired position. The ranges available when using the servo gap adjustment system are:

Normal force: $2.04 \cdot 10^{6}$ to $1.08 \cdot 10^{2}$ dynes/cm^2

Modulus of Elasticity: 10^{-8} to 10^{14} dynes/cm^2

These ranges again depend upon the spring constant, torsion bar, platen diameter, and gear box setting.

Model C of the Rheogoniometer is called the OS Rheo-Visco-Elastometer. This model also provides the same facilities as the Rheo-Viscometer plus an oscillatory facility which enables sinusoidal oscillation of the lower platen to take place. There is no normal force measuring system with this model. In addition to the continuous shear drive unit, a second drive unit is necessary to drive the variable sine wave generator which operates through the two way drive box and the worm and wheel. A linear displacement

inductive transducer is used to detect the amplitude of the oscillation of the lower platen (applied strain) whereas the torsion head transducer detects the movement of the upper platen (tangential stress). The amplitude ratio of the applied strain and the resultant stress, and phase angle difference between the two, enables the moduli of viscosity and elasticity to be determined. The oscillatory ranges include:

Platen Frequency: $3.16 \cdot 10^{-4}$ to 60 cps.

Platen Amplitude: ±2 to 30 milliradians

These ranges depend on the gear box setting used.

Model D of the Rheogoniometer is called the Weissenberg Rheogoniometer. This model is provided with all the facilities of the other three models and is considered the complete instrument.

The third part of the instrument is the control and readout section. A control panel incorporates three rotary switches. They operate: (a) the drive unit for platen oscillation, (b) the drive unit giving continuous forward or reverse rotation, and (c) the electromagnetic clutch-brake unit. A transducer change over switch enables the signal from either the gap setting transducer or the torsion head transducer to be displayed on the same transducer meter panel. Signals from transducers fitted to the measuring section are fed to panel mounted transducer meters operating on a carrier frequency of 1000 cycles per second.

Each transducer meter is calibrated to read linear displacement directly in microns with ranges of 5 to 2000 microns full-scale deflection. Facilities are also provided on the front panel of the transducer meter for feeding the signals into a recorder or an oscilloscope.

The different models are usually provided with a 5.0 cm, 2° cone and a 5.0 cm platen. Also standard is a 10^8 dyne-cm per radian calibrated strip torsion bar. Additional torsion bars, platen diameters, and cone angles are available to bring the versatility within the wide ranges previously specified. Some additional accessories are required for temperature control and recording.

Sample temperature control can be accomplished by using a high temperature electric oven which surrounds the platens and sample. The oven can be controlled to give sample temperatures from room temperature to +400°C. For lower temperature ranges of below room temperature to above, a temperature control chamber is provided through which a temperature controlled fluid may be circulated. A thermocouple is screwed into the upper platen and the measured temperature is displayed on a thermocouple meter.

Single or twin channel strip chart pen recorders or an ultra-violet recorder can be used to record tangential stress, normal stress, or oscillation measurements. Suitable filters may be used in conjunction with the above recorders to minimize noise

which under some test conditions might affect the results. Noise can result from the natural frequency of vibration of the torsion head, transducer meters, building vibrations, and motor vibrations.

Experimental Procedures

The model of the Rheogoniometer that was used to study the rheological properties of thixotropic materials was Model A, the Rheo-Viscometer. This model is capable of giving tangential shear stress measurements as a function of time at various constant shear rates. The prescribed experimental outline is the same, regardless of what type of material is being studied - Newtonian or non-Newtonian.

A platen diameter, torsion bar, and cone angle is chosen which will give readings of torque in the region of interest. The instruction manual supplies tables and charts which aid in choosing the correct set of accessories. The various accessories are installed on the body of the instrument, calibrated and checked for alignment, squareness, eccentricity, freedom of movement and position. A gap setting, specified for the particular cone being used, is next set on the instrument meter. This gap setting will then be automatically set when samples are placed on the instrument using the calibrated transducer meter. The shear rate of interest is then determined by back calculating the corresponding RPM for the particular accessories on the instrument. This RPM is then correlated to the particular gear box setting through the use of a table supplied in the instruction manual.

A sample of the material to be studied is then placed on the lower platen of the instrument. By turning the lead screw, the upper platen (cone) is lowered into position and the correct gap between the two plates is set with the aid of the gap setting transducer meter. Excess sample will squeeze out from between the two platens and will be wiped or cut from the edges to assure a uniform surface of platen, sample, and platen. A meter setting on the torsion head transducer meter has to be estimated for the particular accessories being used and the viscosity of the sample. Usually, a higher setting is used initially to insure a reading less than full scale deflection. Particular care must be taken in the choice of which torsion bar will be used with a particular shear rate (RPM) and sample viscosity being used. If a highly viscous material is to be studied at a high shear rate, a small torsion bar can be very easily damaged due to excessive torque transferred through the sample. On the other hand, the use of a large torsion bar with small shear rates and a low viscosity material can produce a situation where a negligible reading will result on the torsion bar transducer. A balance of variables is essential in the performance of a run with a particular sample. The correct set of variables can reasonably be estimated with the aid of the charts in the instruction manual and experience.

Once the sample is in place, the gap set, the RPM chosen, and the meter ranges determined, a run can be made. The forward-reverse switch for the rotation motor is engaged. The off-brake-

drive switch for the electromagnetic clutch is then engaged. This will impart a rotational motion on the lower platen which in turn imparts a shear on the sample. The shear on the sample is transmitted to the upper platen which results in a reading on the torsion bar transducer meter. If the reading on the torsion bar transducer meter occupies a reasonable fraction of full scale deflection, the correct meter range has been chosen. If the reading goes off scale, a less sensitive range must be chosen or if the reading is too low, a more sensitive range must be chosen. When working with Newtonian or time-independent, non-Newtonian materials, if the run has to be repeated because of incorrect initial gueses with respect to settings, the same sample can be used. Also if a complete flow curve is to be generated, i.e., shear stress or shear rate, the same sample can be used for all the measurements. The only variable will be changing the shear rate by changing the gear box setting.

Usually the rheological properties of a material are to be determined as a function of temperature or at a known constant temperature. To do this the ambient temperature would have to be very constant or a temperature control chamber and circulation unit will have to be attached to the instrument. The temperature of a run can be monitored through a thermocouple which is placed on the upper platen. Manual or automatic temperature corrections can then be instituted to keep the temperature of the sample constant. Also any increase in temperature of the sample due to

prolonged shearing can be measured to determine what effect temperature fluctuation might have on the accuracy of the results.

Visually recording output readings from the torsion bar, transducter meter can be inconvenient. A recorder-filter arrangement can be hooked up to automatically record the output from the transducer meter. A typical recording for a Newtonian or time-independent, non-Newtonian material would look like figure 3-4. The initial overshoot on the torque axis is due to inertia and might not be noticed with some materials. The reading quickly levels off to give a constant torque reading for a particular RPM. Depending on the particular filter being used or using no filter, a noisy curve similar to figure 3-5 is obtained. It is important to note that the two curves are not the same in magnitude even if all variables and the exact same sample is used, with only the filter or lack of filter being different. This is due to the filter being made up of resistors, inductors, and capacitors and since the output signal is in the form of a voltage reading, the voltage is decreased with increase in internal resistance of the filter circuit. This does not create a problem in the final recorded output since each transducer meter is equipped with a set calibration reading corresponding to a full scale deflection for the particular meter range being used. The recorder is simply calibrated for full scale deflection by taking this set calibration setting off of the meter, running it through the filter being used

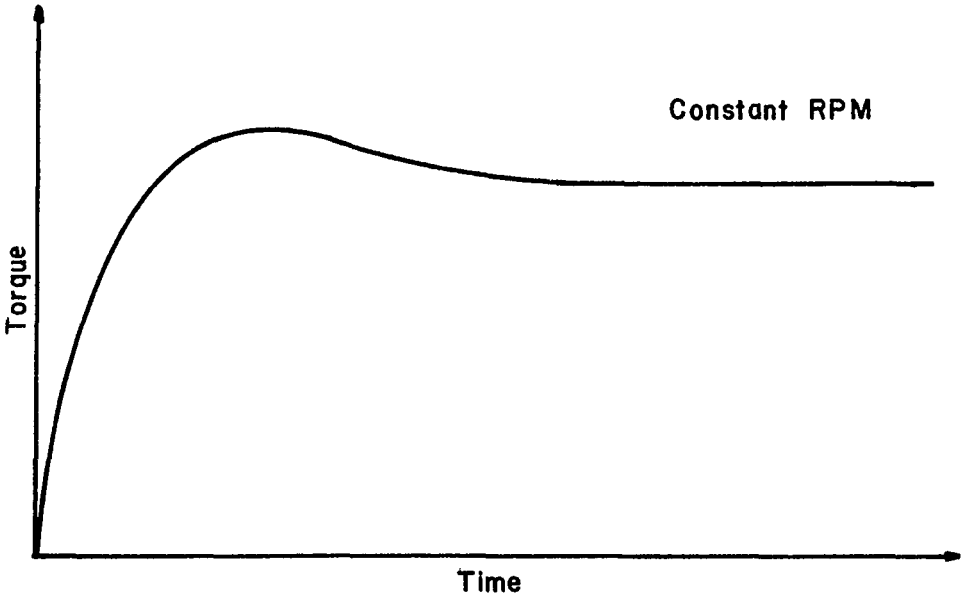

Figure 3-4. Transducer Meter Output - Filtered

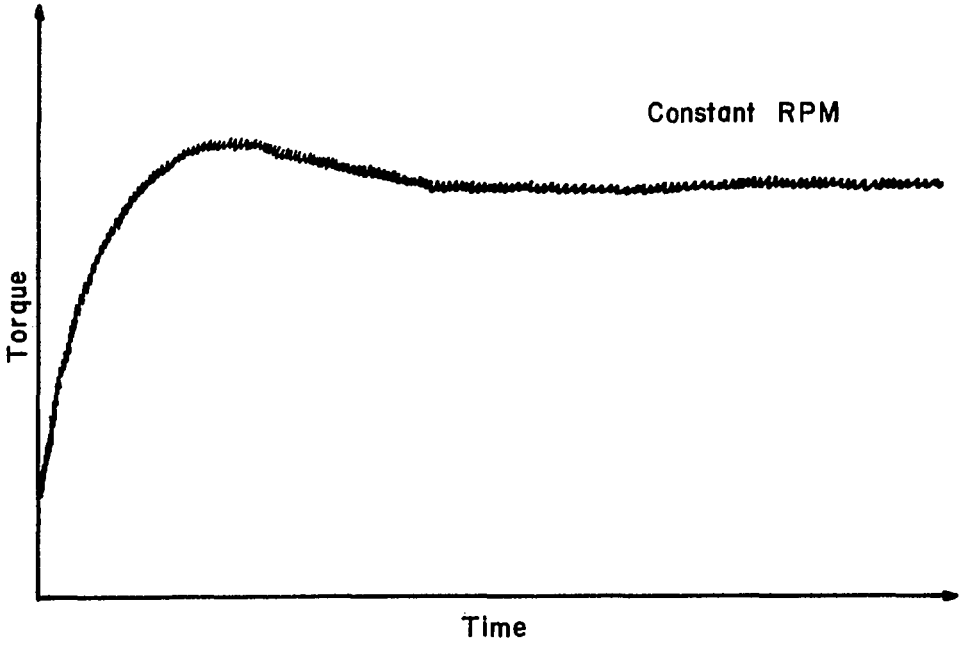

Figure 3-5. Transducer Meter Output - Unfiltered

and setting a corresponding point on the recorder equal to the full scale deflection. The filter which comes with the instrument and designed to cut off all frequencies down to 1/2 cycles per second is shown in figure 3-6.

As described above, the experimental procedure for the Rheogoniometer, is one of pointwise measurements. For time-independent, non-Newtonian materials, the method is adequate though somewhat cumbersome, since each point from the recorded output must be transposed to a flow curve of torque versus RPM. For time-dependent, non-Newtonian materials, this method of generating a flow curve or rheogram is inadequate since the material in question is dependent on its flow history in addition to the rate of shear. After each measurement, the material has time to recover part of its original structure before a new gear box setting can be made and another point measured. Since thixotropic materials are characterized by a rheogram in the form of a hysteresis loop, certain modification to the instrument are necessary in order to generate a representative curve.

Modified Rheogoniometer

The major change in the Rheogoniometer is with respect to shear rate or RPM. Instead of a pointwise change in the shear rate, a continuously variable change is necessary. As can be seen from the block diagram, figure 3-7, a continuously variable speed drive is inserted between the synchronous motor and the 60-step

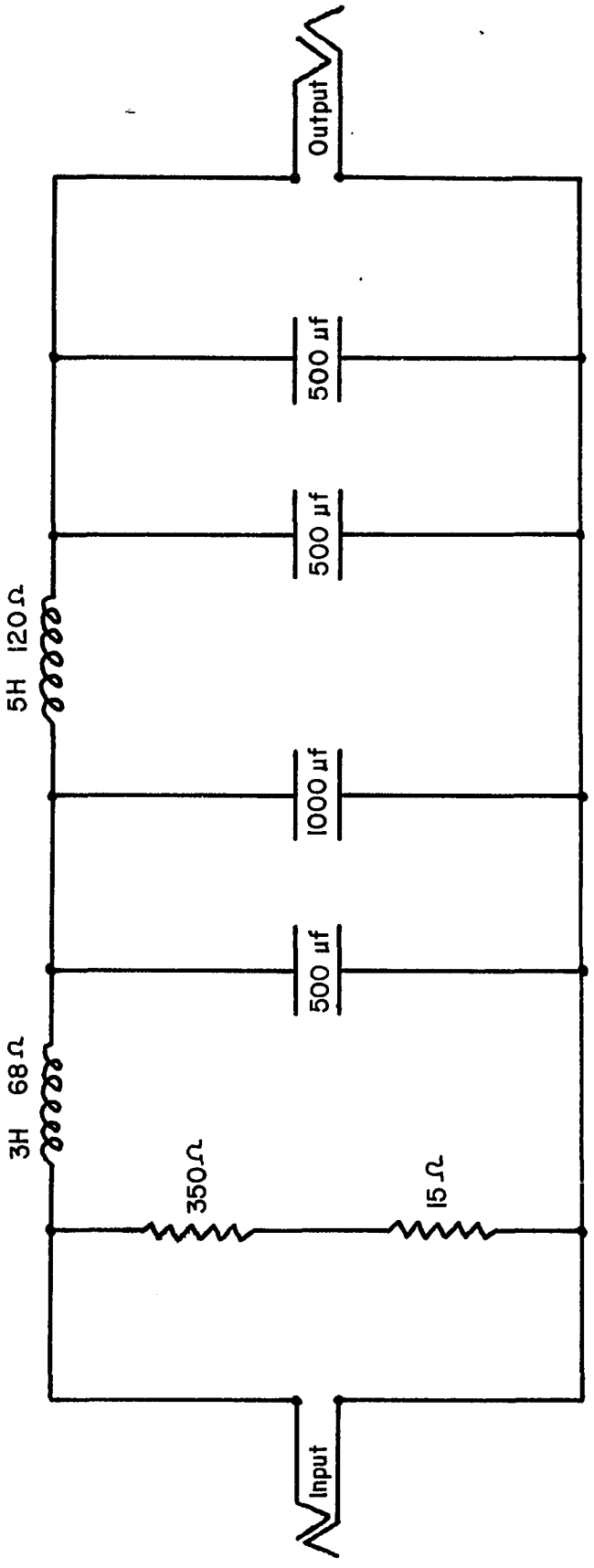

Figure 3-6. Low Frequency Filter Unit

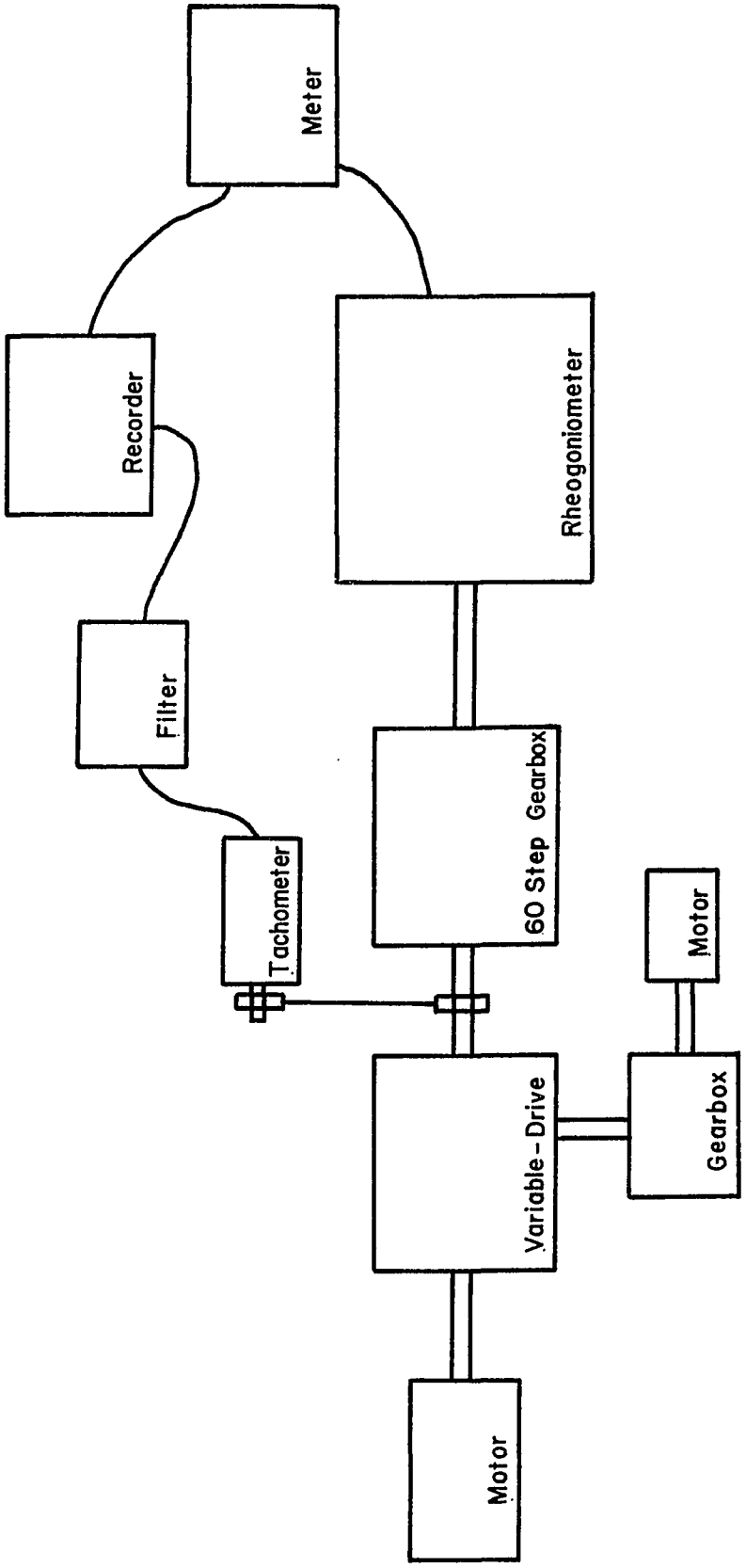

Figure 3-7. Modified Weissenberg Rheogoniometer

gearbox. The particular drive unit is a Graham* transmission fitted with a linear cam, which provides a constant change in RPM. The control arm of the variable-speed transmission rotates the linear cam arrangement which positions a ring along three roller-pinion gears. The input to the transmission is a constant 1800 RPM, whereas the output from the transmission is a function of the position of the control arm. Each turn of the control arm changes the output speed of the transmission by some constant increment. The output speed can cary infinitely from 0 to 525 RPM.

The control arm to the transmission is driven by another gearbox and reversible-constant RPM motor arrangement. The gearbox makes available a change in the rate of change in output RPM of the transmission. For thixotropic materials, a time for completion of the upcurve of the hysteresis loop is estimated and set on the small gearbox, i.e., change the rate at which the control arm turns in RPM'S. This will control the time it takes for the variable-speed transmission to go from 0 to maximum RPM. By reversing the direction of rotation of the small motor which controls the transmission, the downcurve for the hysteresis loop is generated. The arrangement is presently set up to work with manual switches where an operator has to control the starting, reversing, and stopping of the control arm motor. Through the use of microswitches, an automated system can be set up which will reverse and stop the control arm motor at predetermined positions, without operator intervention.

---

* Graham Transmission, Inc., Menomonee, Wis. 53051

The output from the variable-speed transmission is the input to the 60-step gearbox supplied with the Rheogoniometer. Depending on what RPM is required on the instrument, the facility to vary the maximum RPM to the lower platen remains. The only difference is that the absolute maximum RPM to the lower platen has been reduced from 450 RPM to 130 RPM due to gearing in the transmission. Otherwise the use of the 60-step gearbox is basically the same. For example, if the plate is to turn at a maximum of 13 RPM which corresponds to 52 RPM at the outlet from the gearbox (4 to 1 reduction going from horizontal to vertical within instrument), a ten to one reduction in RPM is necessary since the input to the gearbox from the variable-speed transmission will be about 525 RPM maximum.

Since the variable-speed transmission is infinitely variable, some method is necessary to determine what RPM the platen is rotating at corresponding to the particular reading of the transducer meter or recorder at any instant. A 45 volt per 1000 RPM, Servo-Tek[*] tachometer-generator is connected to the drive unit to give a signal in the form of a voltage which might be read on a meter or recorded directly. The position of the tachometer would have to be downstream of the variable-drive transmission. The two most suitable positions would be on either side of the 60-step gearbox. Because of the reduction in RPM due to the 60-step gearbox, it is most advantageous to position the

---

[*] Servo-Tek Products Company, Inc., Hawthorne, New Jersey 07506

tachometer between the variable-drive transmission and the 60-step gearbox. In this manner, the output signal would always be of the same order of magnitude and errors due to very, low RPM which is possible on the output from the gearbox would be eliminated. The recorded reading could easily be corrected for the gearbox ratio set on the 60-step gearbox. Noise inherent in the tachometer-generator was also eliminated through the use of a filter.

A Moseley[☆]-Autograph X-Y recorder, with a time scale, was used to record the results. The output from the torsion head transducer was hooked up to the Y-axis of the recorder, whereas the output from the tachometer-generator was connected to the X-axis of the recorder. The torque measurements were calibrated in the technique previously described using a set calibration output signal for full scale deflection from the transducer meter. This allowed the correct choice of recorder range to expand the scale and increase the accuracy of the results. For the X-axis, the output from the tachometer-generator through a filter had to be calibrated in RPM vs. voltage. To do this, the variable-speed transmission was temporarily removed from the system and the output from the 60-step gearbox measured with the tachometer-generator. Since the output RPM is known for each gearbox setting, the voltage measured for that particular RPM could be recorded. A calibration curve similar to figure G-3 could then be drawn and used to convert voltage to RPM when the transmission was put back into the system.

☆ Hewlett-Packard, Pasedena, California

This modification to the Rheogoniometer made possible the direct generation of a flow curve for the particular material being studied. The technique was essential in the study of thixotropic materials since no human time error was made to the results and a complete hysteresis loop or series of hysteresis loops could be drawn using the same sample. For Newtonian or time-independent, non-Newtonian materials this technique of direct reading of a flow curve simplified their rheological investigation. The manner in which the rheogoniometer has been modified also permits the performance of a run without the variable-speed transmission (torque vs. time at constant RPM) by predetermining a position on the transmission and not running the control arm of the transmission. This can be considered a direct-drive similar to the original drive unit of the instrument.

Making A Run

The procedure for making a run with the modified Rheogoniometer is similar to making a run with the commercial version. After a sample is placed on the instrument, gap setting closed, and meters or recorders set to the correct ranges, a gearbox setting is chosen on the 60-step gearbox to provide the maximum shear rate that is required. A time to complete an upcurve and downcurve on the rheogram is estimated and the corresponding setting on the control arm of the variable-drive transmission determined. The motor on the drive unit is started and transmission set to a position of zero RPM. The electromagnetic clutch is engaged, thus having the drive train to the lower platen

complete. By initiating the motor on the control arm of the transmission the RPM to the lower platen begins to increase steadily at a predetermined rate. When the RPM reaches its maximum, the motor to the control arm of the transmission is immediately reversed. This causes the RPM to the lower platen to steadily decrease at the same predetermined rate. One complete flow curve for the sample on the instrument is drawn in this manner. Successive flow curves could be drawn (a characteristic approach when studying thixotropy) by again reversing the control-arm motor to the transmission when the lower platen RPM returned to zero.

Experimental Shear Stress-Shear Rate Equations

The shear rate being applied to the sample on the instrument can be determined with the help of the voltage-RPM discussion in Appendix G and equations 3-9 and 3-10. The rate of shear from equations 3-9 and 3-10 for a cone-and-plate viscometer is:

$$(-\dot{\gamma}) = \frac{180\beta}{\pi\alpha} = \frac{360}{\alpha t} \qquad (3\text{-}14)$$

where $(-\dot{\gamma})$ is the shear rate in sec^{-1}, α is the angle of the cone in degrees, β is the angular rotation of platen in radians/sec, and t is a term used instead of angular rotation in sec/rev;

$$t = \frac{2\pi}{\beta} \tag{3-15}$$

Equation (3-14) can be modified in terms of platen RPM, to give:

$$t = 60/(RPM)_{pl} \tag{3-16}$$

where $(RPM)_{pl}$ is the angular rotation of lower platen in rev/min. Therefore, substituting equation 3-16 into equation 3-14, gives:

$$(-\dot{\gamma}) = \frac{360}{\alpha\left\{\frac{60}{(RPM)_{pl}}\right\}} = \frac{6(RPM)_{pl}}{\alpha} \tag{3-17}$$

Due to the internal gear reduction of the Rheogoniometer, the angular rotation of the shaft at the input to the instrument is:

$$(RPM)_{pl} = \frac{(RPM)_{shaft}}{4} \tag{3-18}$$

The input to the instrument, given by $(RPM)_{shaft}$, is also the output of the drive unit or 60-step gearbox. Knowing the internal gearing inside of the 60-step gearbox gives the input RPM which is the tachometer RPM and also the output RPM from the variable-speed transmission.

$$(RPM)_{shaft} = (RPM)_{tach}/GBR \tag{3-19}$$

where $(RPM)_{tach}$ is the angular rotation of the tachometer-generator shaft and the quantity being measured and GBR is gearbox ratio of the 60-step gearbox.

Substituting equation 3-19 into equation 3-18 and equation 3-18 into equation 3-17 gives:

$$(-\dot{\gamma}) = \frac{6(RPM)_{tach}}{4\alpha GBR} \qquad (3\text{-}20)$$

From equation G-1 the rev/min of the tachometer can be expressed as a function of the recorded voltage of the tachometer-generator:

$$(RPM)_{tach} = 172.1\ (Volts)_{tach} \qquad (G\text{-}1)$$

The recorded voltage from the shear rate axis of the Moseley X-Y recorder can be converted into a reading from the recorder by:

$$(Volts)_{tach} = (Recorder\ Range)(divisions) \qquad (3\text{-}21)$$

where Recorder Range is the setting of the shear rate axis of the recorder in volts/div, and division is the linear dimension of the shear rate axis of the recorder in inches. Substituting equation G-1 and 3-21 into equation 3-20 gives:

$$(-\dot{\gamma}) = \frac{3(RPM)_{tach}}{2\alpha(GBR)} = \frac{3}{2\alpha(GBR)}(172.1(Volts)_{tach}) \qquad (3\text{-}22)$$

$$(-\dot{\gamma}) = \frac{258.15(\text{Recorder Range})(\text{divisions})}{\alpha\ (\text{GBR})} \qquad (3\text{-}23)$$

Equation (3-23) can then be used to calculate the shear rate being applied to a sample on the rheogoniometer in sec^{-1}. For any single run or sets of runs, variables: α, GBR, and Recorder Range are set once or specified once. Equation (3-23) will then reduce to

$$(-\dot{\gamma}) = f(\text{divisions}) \qquad (3\text{-}24)$$

This means reading the shear rate-axis at a number of positions for a curve drawn by the recorder will transform the coordinates into correct values of shear rate as applied to the sample on the instrument.

As the lower platen of the rheogoniometer turns, it shears the sample which is sandwiched between the lower platen and upper cone. Some of the sample moves with the lower platen (assuming no slippage), whereas other parts of the sample resist this tendency to move. Some sample remains stationary or relatively stationary (again no slippage) with respect to the upper cone. Through the application of shear and its resistance to flow, a torque is applied to the upper cone of the instrument. The upper cone is free to rotate and relatively frictionless in movement due to

the air bearing arrangement. It is fixed to the lower half of a torsion bar which is fixed at the upper half. The rotation of the lower platen imparts a rotation on the sample, which then rotates the upper cone which is prevented from rotating by the torsion bar, but not completely. The torsion bar is calibrated to resist this shearing action. The slight twisting or torque registered by the torsion bar is measured by means of a lever arm fixed to lower half of torsion bar and transducer.

The torque applied to the torsion bar is:

$$T = \Delta_T k_T \tag{3-25}$$

where T is torque in dyne-cm, k_T is calibrated torsion bar constant in dyne-cm/micron movement of transducer, and Δ_T is movement of torsion head transducer in microns. From equation (3-13) the shear stress as applied to the sample and torsion bar is:

$$\tau = \frac{3T}{2\pi R^3} \tag{3-26}$$

where τ is the shear stress in dyne/cm^2, and R is the radius of cone and platen in cm. Rewriting equation (3-26) in terms of platen diameter gives:

$$\tau = \frac{12T}{\pi d^3} \tag{3-27}$$

Substituting equation (3-25) into equation (3-26):

$$\tau = \frac{12\ \Delta_T k_T}{\pi d^3} \qquad (3\text{-}28)$$

The movement of the torsion head transducer, Δ_T, is measured by means of a transducer meter. There are a number of scale settings on the transducer meter, all of which can be read in microns. For example, if the meter switch is set at 50, full-scale deflection (FSD) of the meter in either direction will be equivalent to 50 microns. A set calibration function on the meter is used to insure correct positioning of the needle of the meter at the full scale reading, by means of a test signal. The output from the transducer meter is fed through an electronic filter to a recorder. By means of a zero adjustment on the recorder, this full scale test signal can be equated to a calibrated distance on the recorder. For example, the test signal may give a reading on the recorder of 4 divisions at full scale reading. This indicates that 4 divisions of the recorder is equivalent to 50 microns or whatever happens to the transducer meter setting. If the meter were set to 500 microns, the full scale reading on the recorder which might still be indicated by 4 inches, would be equivalent to 500 microns. A relationship can then be written for a reading of the recorder which will indicate the meter reading:

$$\frac{\text{Transducer Meter Reading}}{\text{Transducer Meter Setting}} = \frac{\text{Recorder Reading}}{\text{Maximum Recorder Reading}} \quad (3\text{-}29)$$

The Transducer Meter Reading is equivalent to Δ_T, the movement of the torsion head transducer and the maximum recorder reading is a value which corresponds to full scale deflection of the transducer meter (in recorder division). Therefore, equation (3-29) can be rewritten as:

$$\frac{\Delta_T}{M.S.} = \frac{div}{FSD} \quad (3\text{-}30)$$

where div is the reading of the shear stress-axis of the recorder in divisions or inches, and M.S. is the transducer meter setting in microns. Transposing equation (3-30) for Δ_T:

$$\Delta_T = \frac{(div)(M.S.)}{(FSD)} \quad (3\text{-}31)$$

and substituting into equations (3-28) gives:

$$\tau = \frac{12(k_T)(M.S.)(div)}{\pi (d)^3(FSD)} \quad (3\text{-}32)$$

The shear stress applied to the sample can then be calculated by means of equation (3-32) in dynes/cm^2. For a particular torsion bar constant (k_T), platen diameter (d), meter setting (MS), and recorder setting for full scale deflection of transducer

meter (FSD), equation (3-32) can be reduced to

$$\tau = f(\text{div}) \tag{3-33}$$

because the variables in equation (3-32) are constant for a single run. To use equation (3-33), read the shear stress axis at a number of positions for the curve drawn by the recorder. These coordinates can then be transformed into the correct values of shear stress for the sample being studied.

In all the experiments, shear rate was recorded on the X-axis and shear stress on the Y-axis, similar to that commonly found in the literature. Equations (3-33) and (3-32) are then rewritten to:

$$(-\dot{\gamma}) = \frac{258.15\ (\text{X-Range})(\text{X-div})}{(\alpha)(\text{GBR})} \tag{3-34}$$

and

$$\tau = \frac{12\ (k_T)(\text{MS})(\text{Y-div})}{\pi\ (\text{d})^3(\text{FSD})} \tag{3-35}$$

An example of the use of equations (3-34 and (3-35) and a computer program which calculates shear stress and shear rate from these equations are given in Appendix B.

CHAPTER 4

EXPERIMENTAL RESULTS

Testing Modified Rheogoniometer

Various tests had to be made with the modified instrument to determine the quality of the experimental results. To perform these tests, Newtonian samples of known viscosity were run. These samples included Brookfield* Viscosity Standards (calibrated to ±1% error) and General Electric** Silicone Fluids (lots reproduced to within 5% of specified value). Tests were made to determine the accuracy of experimental findings when compared to manufacturers specified values, versatility which would indicate the range of shear rates and viscosities which could be measured with the instrument, reproducibility of one run with succeeding runs, and inherent hysteresis loops which would indicate results which actually were not present. This last test was vital since some commercial instruments have been found to produce hysteresis loops with Newtonian fluids due to inertial, mechanical, and electrical deficiencies.

Various samples, ranging in viscosity from about 10 centipoises to 100,000 cp, were tested on the instrument. Actual flow curves are given in figures 4-1 through 4-6. The results

---

* Brookfield Engineering Labs., Stoughton, Mass. 02072

** General Electric Company, Silicone Products Dept.,Waterford,N.Y.

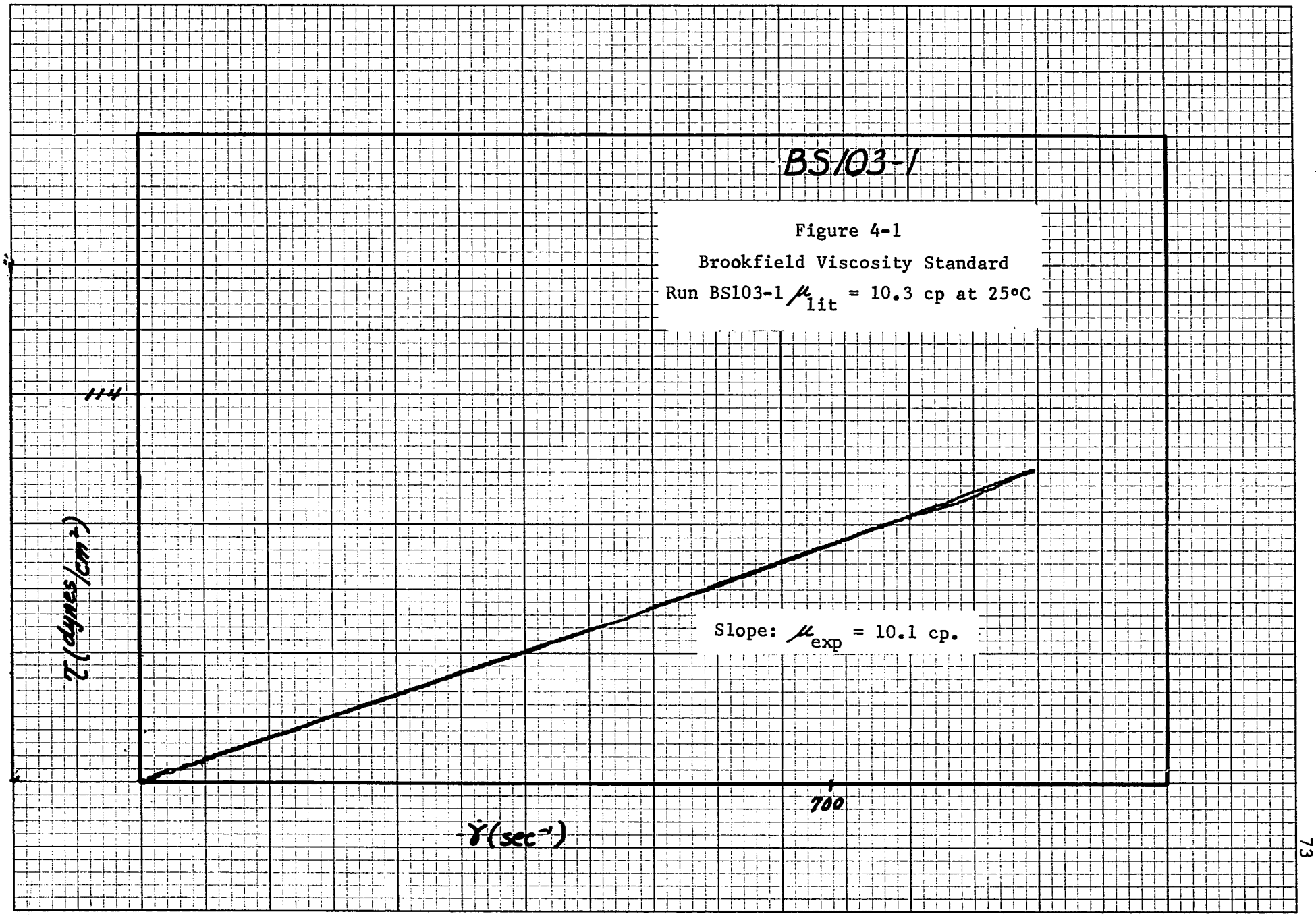

Figure 4-1

Brookfield Viscosity Standard

Run BS103-1 μ_{lit} = 10.3 cp at 25°C

Slope: μ_{exp} = 10.1 cp.

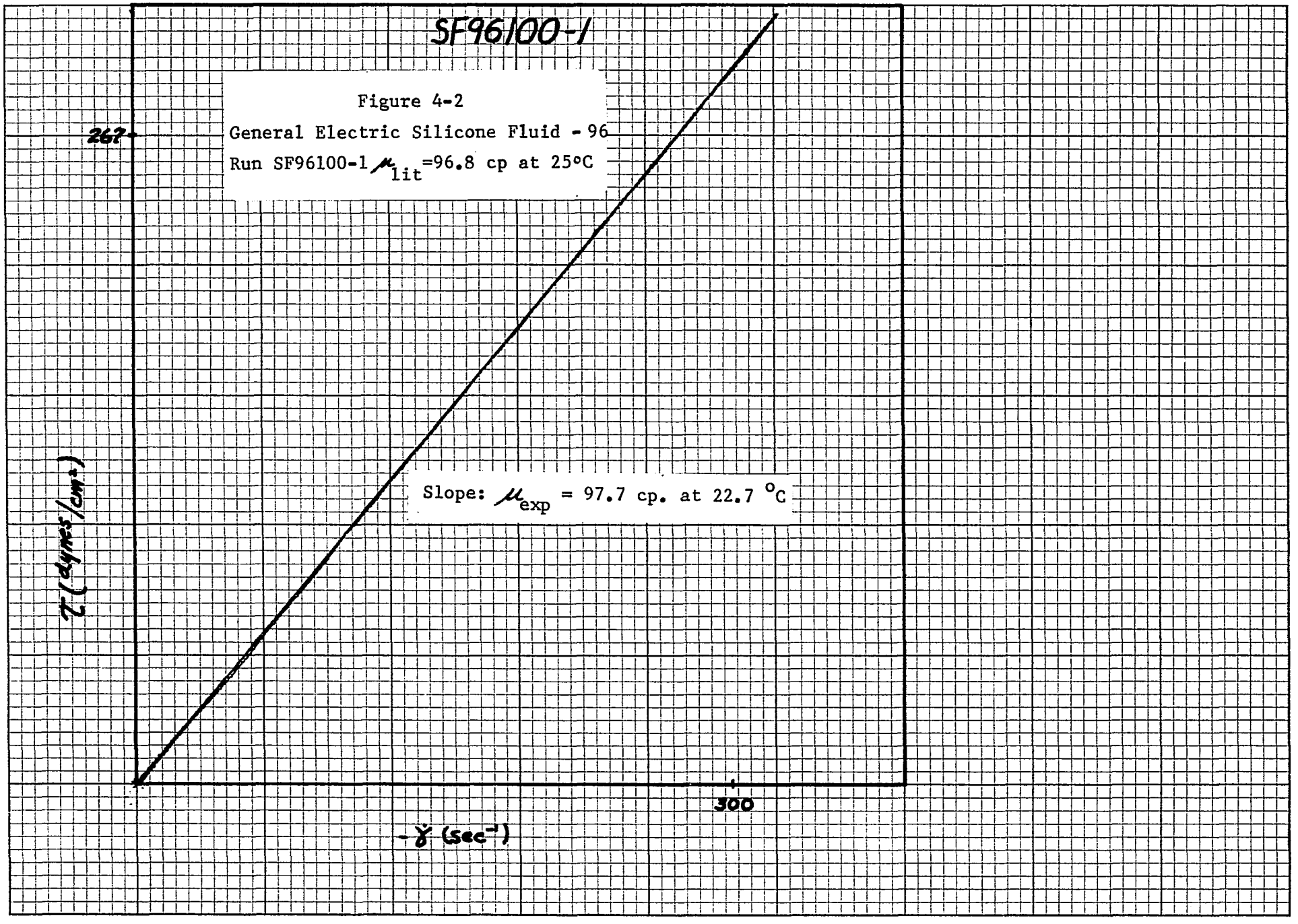
SF96100-1
Figure 4-2
General Electric Silicone Fluid - 96
Run SF96100-1 μ_{lit}=96.8 cp at 25°C
267
Slope: μ_{exp} = 97.7 cp. at 22.7 °C
300
τ (dynes/cm²)
-$\dot{\gamma}$ (sec⁻¹)

6/17/70

SF96500-1

Figure 4-3

General Electric Silicone Fluid - 96

Run SF96500-1 μ_{lit}=486.5 cp at 25°C

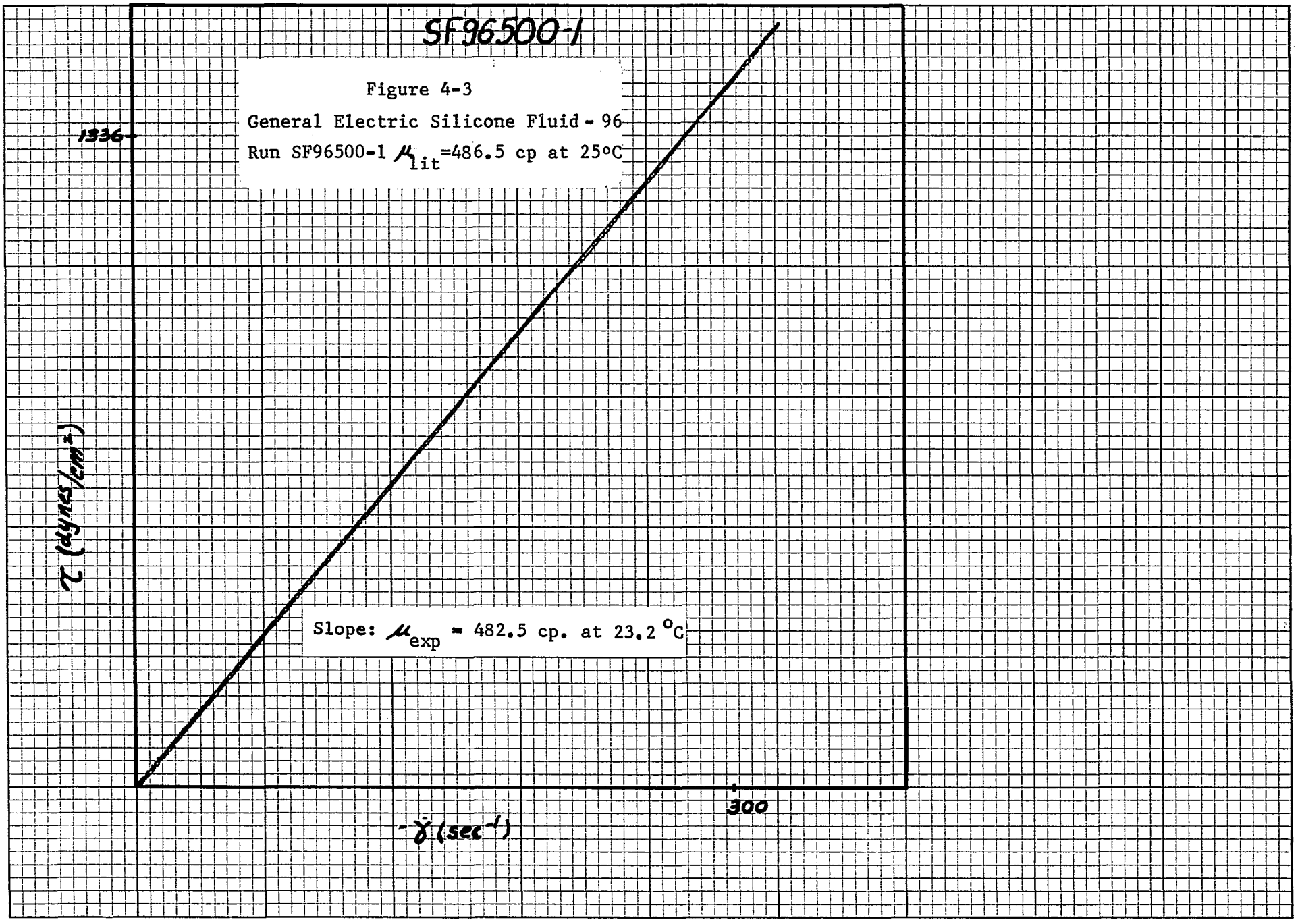

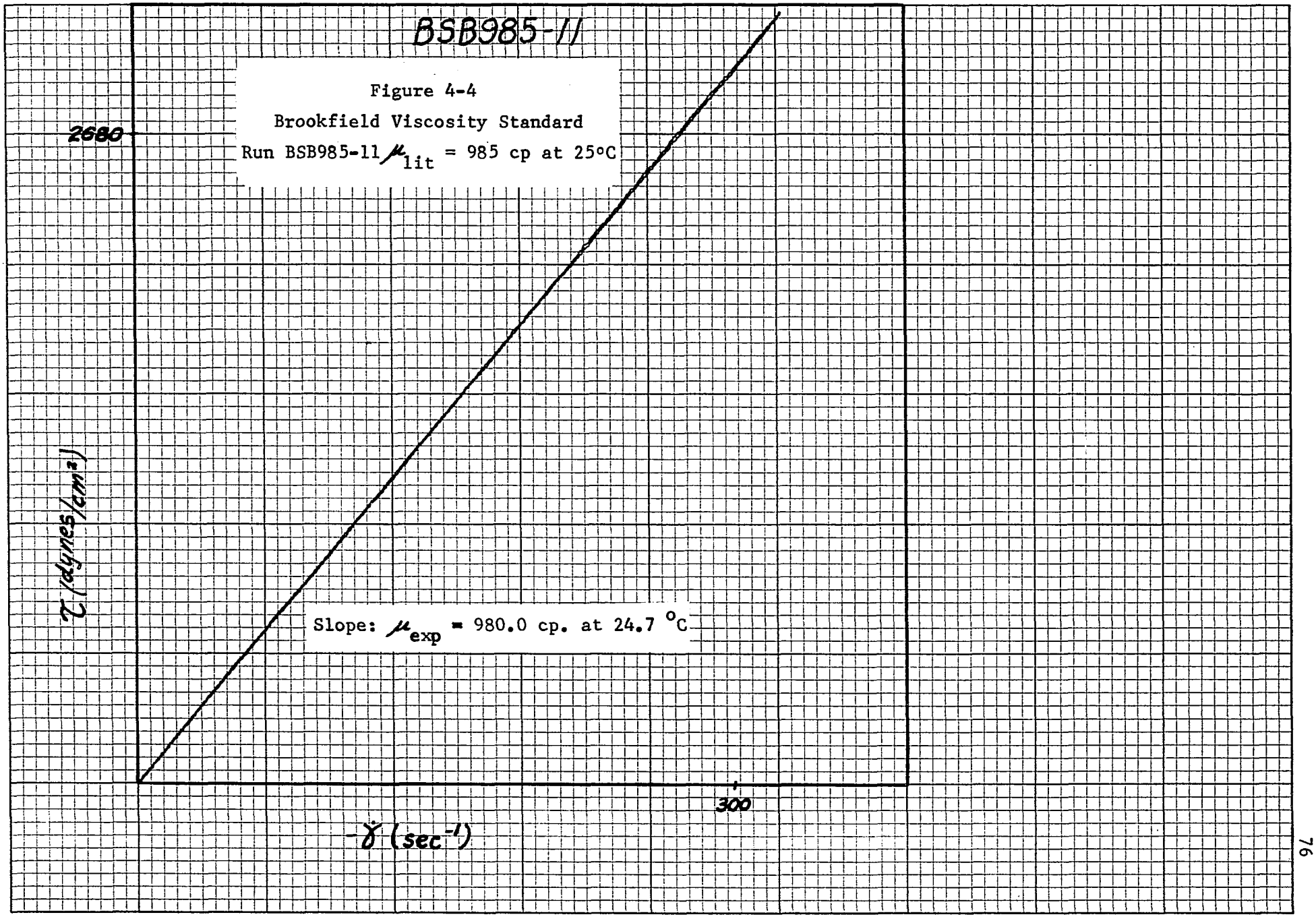

Figure 4-4

Brookfield Viscosity Standard

Run BSB985-11 μ_{lit} = 985 cp at 25°C

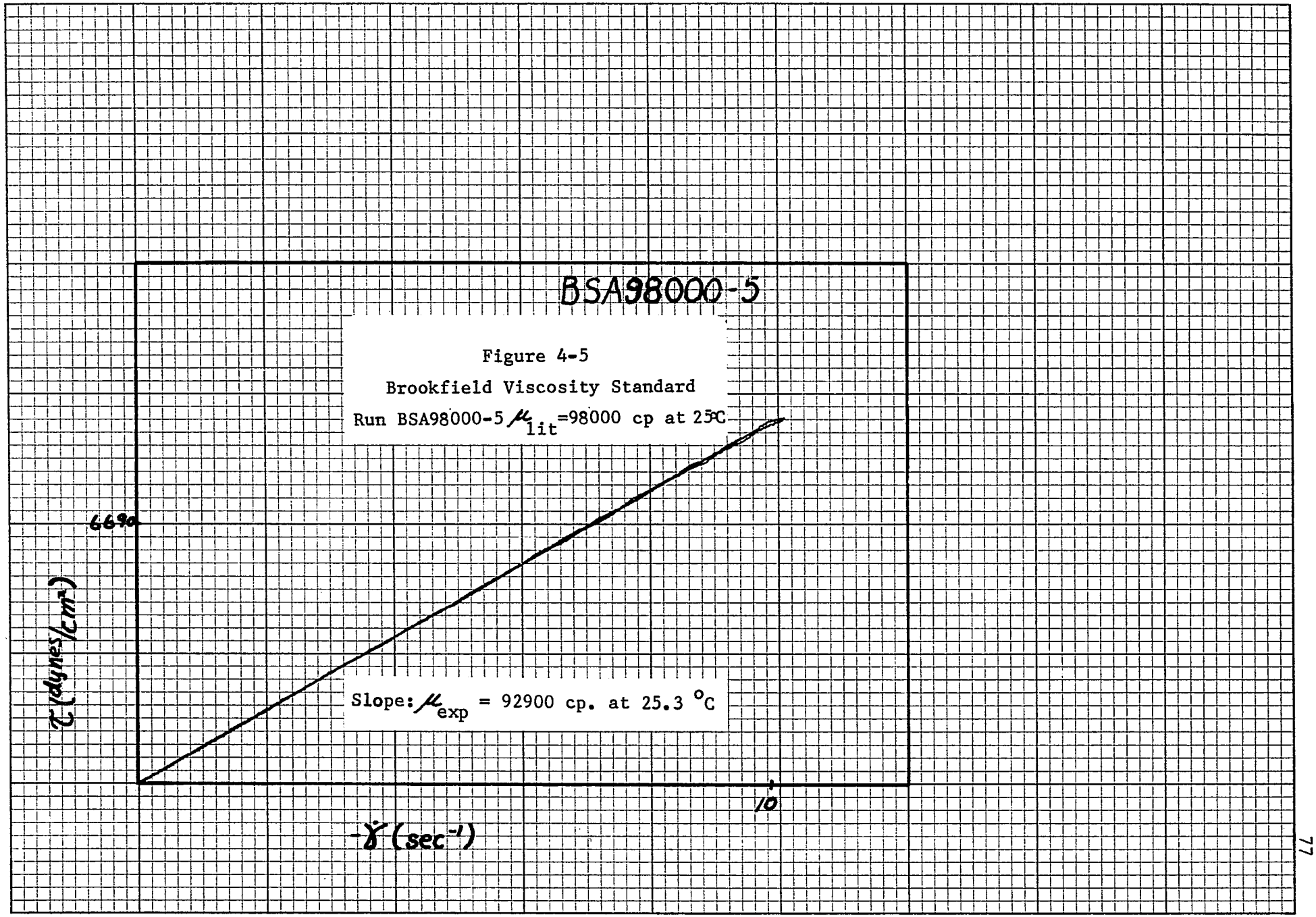

Figure 4-5

Brookfield Viscosity Standard

Run BSA98000-5 μ_{lit}=98000 cp at 25°C

Slope: μ_{exp} = 92900 cp. at 25.3 °C

are tabulated in table 4-1 where experimental and literature values of viscosity are presented. Except for the most viscous materials, the results are excellent. An explanation as to the divergence of the experimental results from the reported values might be due to the variables employed in making the measurements. Because of the highly viscous nature of the materials, lower shear rates (gearbox settings) might have improved the results. Also, by increasing the torsion bar size (torsion bar constant), an increase in shear rate would be indicated for the same transducer meter setting. Changing the diameter (smaller) and the angle (smaller) of the cone could have improved the results for the same RPM (though higher shear rate). During a run, it was noticed that if the input RPM was too high, the material would overcome the surface tension holding the sample between the platens and squeeze out. This was particularly evident with the 98,000 centipoise Brookfield Viscosity Standard. It might be worth mentioning that the General Electric Silicone Fluids were manufactured to within only 5 per cent of specified value. This might account for a large part of the discrepancy between experimental and published results. This could also increase the error on some of the other G.E. Silicone Fluids. Since the 5000 fluid is closer to the 1000 Brookfield Standard than the 100,000 Brookfield Standard by an order of magnitude and from visually studying the experimental determination and performance, the results determined experimentally are probably close to actual values. Not considering this last point, the results found by this instrument are extremely accurate except at

TABLE 4-1

RESULTS FOR STANDARD NEWTONIAN FLUIDS

Cone Diameter: 5 cm.
Cone Angle: 2°
Number of loops performed: 1

Torsion Bar Number: 8
Torsion Bar Constant: 876 dyne-cm/micron

Run Number	Date	Gearbox Setting	Transducer Meter Setting (microns)	Recorder Full Scale Deflection (inches)	Temp (°C)	Viscosity (cp) Lit	Viscosity (cp) Exp	Percent Error
BS103-1*#	4/22/70	0.0	50	4	----	10.3	10.1	-1.94
SF96100-1	6/17/70	0.0	20	10	22.7	96.8	97.7	+0.93
SF96500-1	6/17/70	0.0	200	20	23.2	486.5	482.5	-0.82
BSB985-11	6/11/70	0.0	200	10	24.7	985	980	-0.51
BSA98000-5	6/12/70	1.5	500	4	25.3	98000	92900	-5.2
SIL5000-1	6/11/70	0.0	500	4	25.2	4875	4550[a]	-0.96
SIL5000-2	6/11/70	0.5	200	4	25.6	4875	4610[a]	+0.35
SIL5000-3	6/11/70	1.0	200	20	25.5	4875	4580[a]	-0.30
SIL5000-4	6/11/70	1.5	20	4	25.4	4875	4660[a]	+1.43
SIL5000-5	6/11/70	2.0	20	20	25.4	4875	4570[a]	-0.52
BSB985-33[b]	7/10/70	0.0	200	10	24.9	985	981	-0.41
BSB985-23	6/19/70	0.0	200	10	24.6	985	993	+0.81
BSB985-24	6/19/70	0.0	200	10	24.6	985	990	+0.51
BSB985-25	6/19/70	0.0	200	10	24.8	985	987	+0.20
BSB985-26	6/19/70	0.0	200	10	25.0	985	984	-0.10
BSB985-27	6/19/70	0.0	200	10	25.1	985	981	-0.41

*With damper fluid on torsion bar lever arm
#Torsion bar no. 7; torsion bar constant 99.4 dyne-cm/micron
[a]Percent error based on average experimental viscosity of 4594 cp., not literature value
[b]There were three (3) loops drawn for this run

end conditions for a particular range of variables (instrument accessories) and well within experimental error on all ranges. For a particular set of accessories, #8 torsion bar, and 5 cm diameter platen (2° cone), a range of viscosities from 100 to 5000 centipoises can accurately be measured. By changing the torsion bar to a smaller one, a sample down to 10 centipoises and possibly 1 centipoise can be tested. By increasing the torsion bar to the no. 9 size and decreasing the diameter and angle of the cone, more viscous materials can be accurately measured.

Another characteristic of the instrument indicating its range and versatility can be seen in figures 4-6 through 4-10 and table 4-1. This series of 5 rheological flow curves was made using the same 5000 centistoke silicone fluid for all curves. The same accessories were used for each run with only the input RPM and torsion head transducer meter and recorder setting being varied. This gave the effect of changing the shear rate range being applied to the sample. The difference between the initial and final curves was an approximately 100 fold change in shear rate. Another way of indicating this change would be to take figure 4-10 and show what part of figure 4-6 it represents. This is shown by a tiny square near the origin. Actually because of the large change, it would be easier to visualize by indicating what part of figure 4-8 is represented by figure 4-10 and then showing what part of figure 4-6 is represented by figure 4-8. This is shown by the dashed lines on the respective curves.

6/11/70

SIL 5000-1

Figure 4-6
Silicone Oil
Run SIL 5000-1

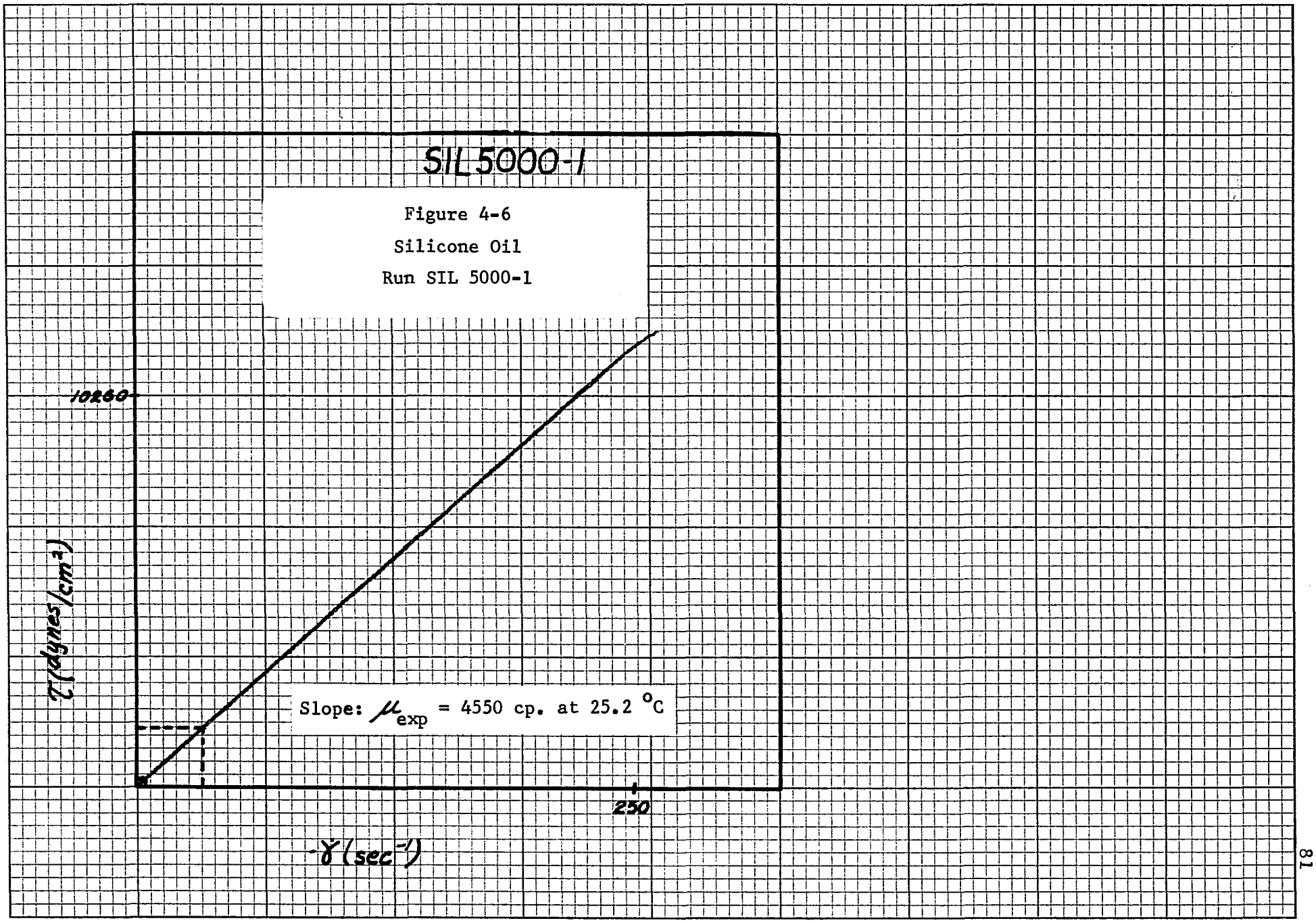

6/11/75

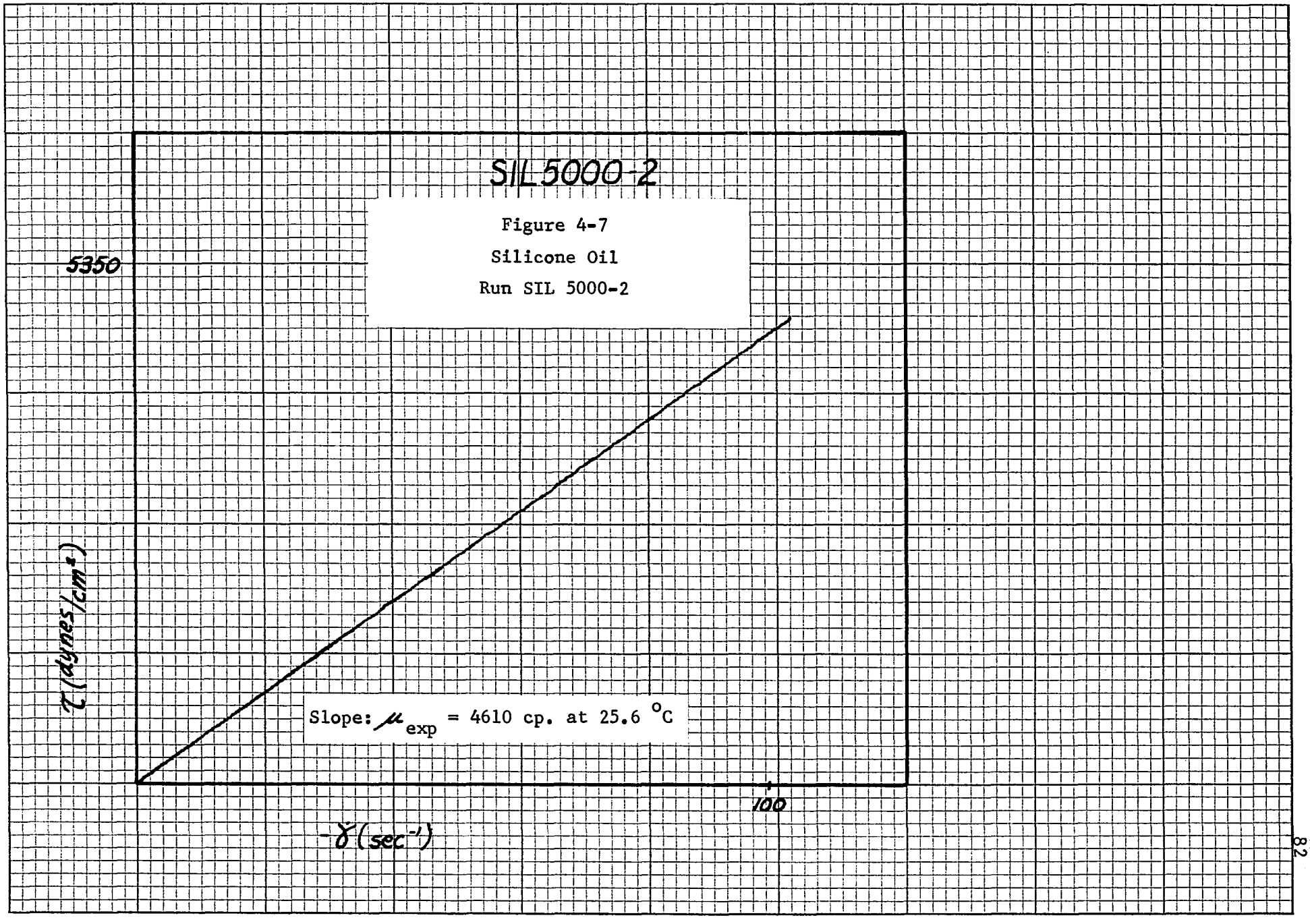

Figure 4-7
Silicone Oil
Run SIL 5000-2

SIL 5000-3

Figure 4-8
Silicone Oil
Run SIL 5000-3

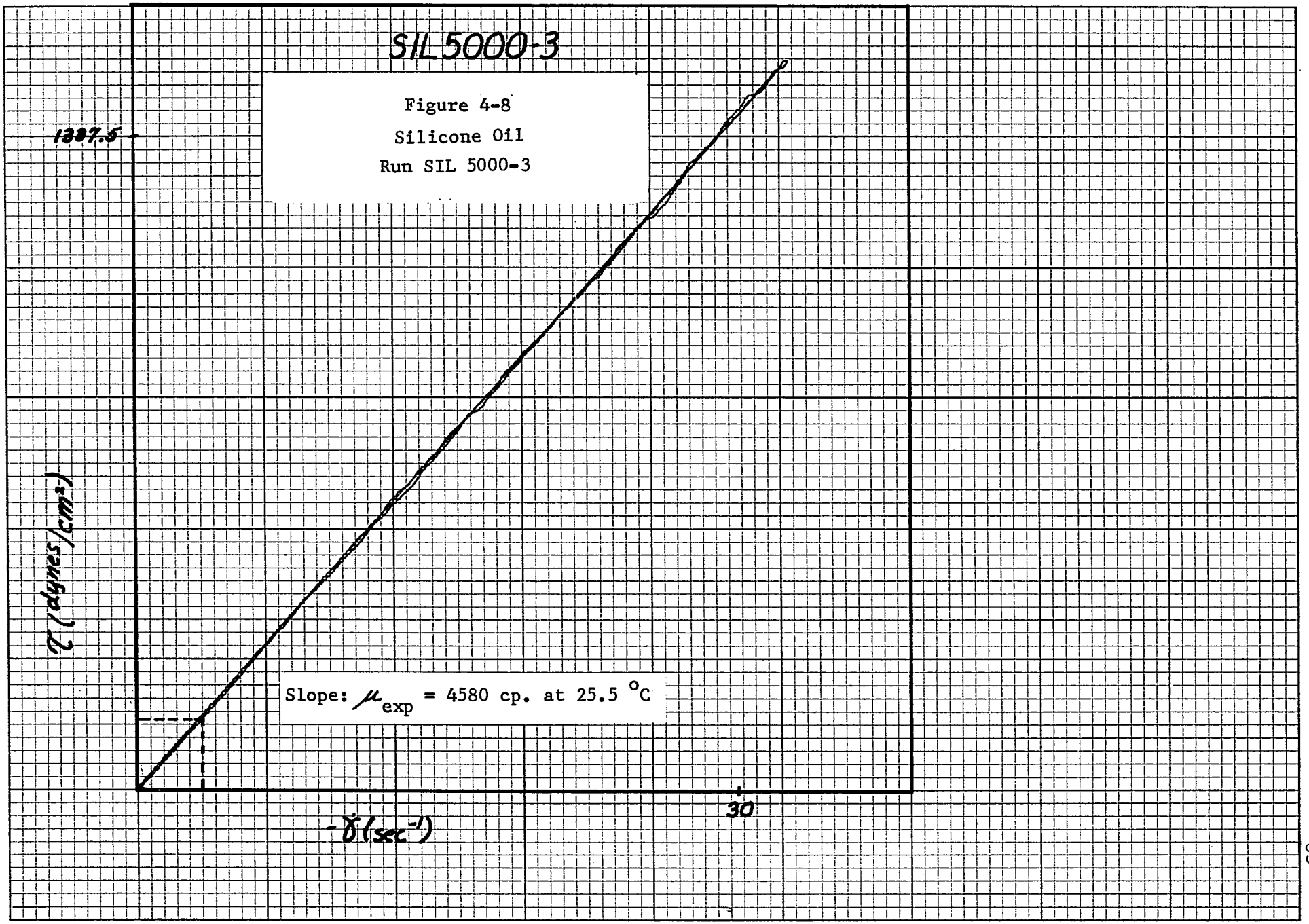

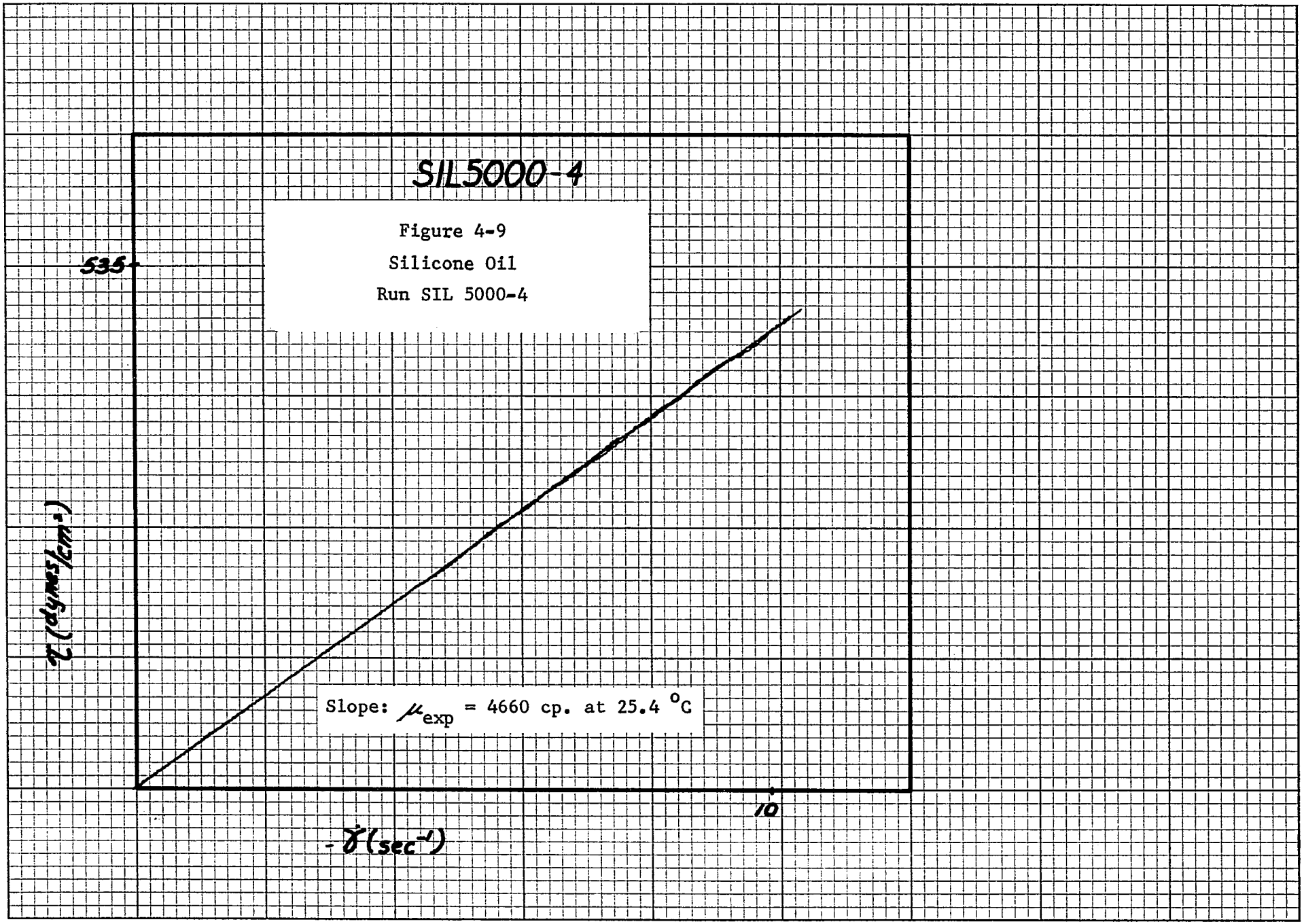

Figure 4-9
Silicone Oil
Run SIL 5000-4

Slope: μ_{exp} = 4660 cp. at 25.4 °C

SIL5000-5

Figure 4-10
Silicone Oil
Run SIL 5000-5

133.75

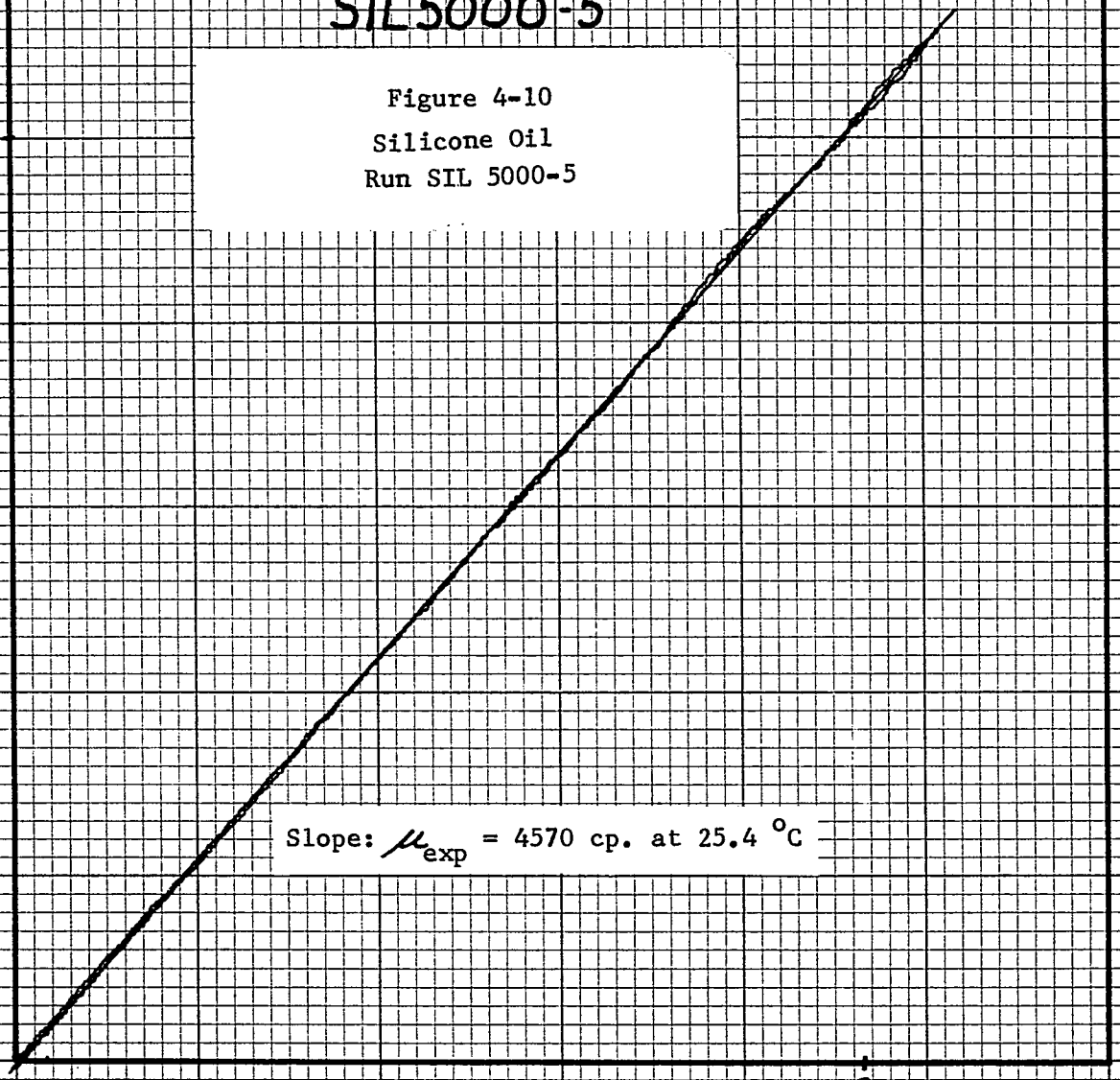

Therefore, by changing the input RPM (shear rate) to the instrument, a small portion of a flow curve can be magnified many times. The accuracy of expanding the curves in this manner can be seen in table 4-1 where the results of the various curves are within 0.62% of the average of all the curves. This may not be extremely important when working with Newtonian materials. However, when working with non-Newtonian materials, a certain shear rate range may be of paramount interest and by simple manipulation, the curve can be magnified many times to give a more accurate picture of the results. Some materials behave differently in different areas of interest. If a study of the flow properties of the material were made at high rates of shear, certain results of interest might go undetected. For example, developing a flow curve with high shear rates may indicate that this material behaves as a Newtonian. Had the flow curve been developed at a much lower shear rate, some non-Newtonian characteristics would have been detected. Consider a pseudoplastic material which behaves according to the power law, equation (1-5). A property of pseudoplastic materials is that their flow curves have a Newtonian region (low shear rate), non-Newtonian region (intermediate shear rate), and a final Newtonian region (high shear rate). If the material had been subjected to a high shear rate (the value would depend on the particular material), the non-Newtonian region might have been camouflaged or just slightly detected since the majority of the flow curve would have been in the second Newtonian region.

Therefore, a complete analysis would require additional variations in rate of shear, easily and accurately accomplished with this instrument.

The 985 centipoise Brookfield Viscosity Standard was used to test the reproducibility of the instrument. One experiment, shown in figure 4-11 and table 4-1, was performed by repeating runs one after another on the same curve. Figure 4-11 has three complete up and down curves shown by a single straight line. The purpose of a test of this type was to determine any variation in the instrument during the performance of a run. Deviations from this single straight line would indicate: errors and inconsistencies in the electrical and mechanical equipment, operator or human weaknesses, temperature variations, set point and starting point drifts, and design imperfections. The results were excellent, no deviations from the line and less than 1/2% error from specified value. This test was performed by taking a sample and varying the shear rate up to a predetermined maximum, then immediately reducing the shear rate back to zero. When the shear rate had returned to zero, the curve (up and down) was immediately repeated. A third curve was also performed in the same manner. Another result of the test was the complete return to zero of both axes of the recorder, indicating no electrical buildup in the filters.

A variation of this test was then performed in approximately the same manner except for one change. After completion of an up

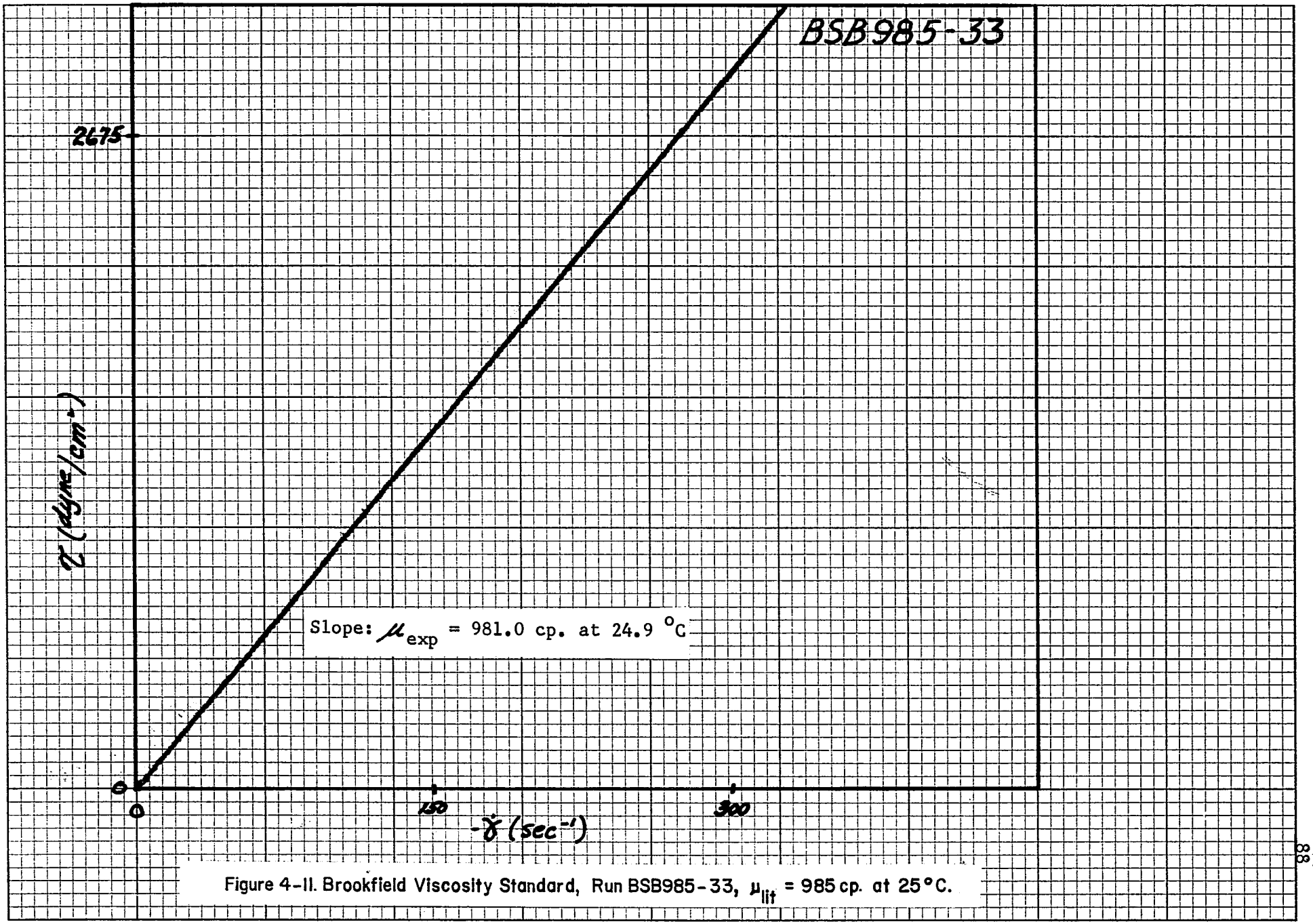

Figure 4-11. Brookfield Viscosity Standard, Run BSB985-33, μ_{lit} = 985 cp. at 25°C.

and down curve, the run was halted and recorder position moved and the zero reset. The curve was then repeated and another position on recorder changed. Five curves were drawn in this manner as can be seen in figure 4-12 and table 4-1. Again single straight lines were obtained with an error of less than 1/2% from the specified value. This indicates no errors due to changes in recorder setting and negligible error due to temperature since the time the sample was on the instrument and undergoing shear was over 3 hours with only a 0.5°C increase in temperature. Also between runs BSB985-25 and BSB985-26 almost 1 hour rest period was taken, again with no change in the results.

One additional result was indicated by the many experimental determinations with Newtonian materials, figures 4-1 through 4-12. No inherent hysteresis loop was found in the performance of these tests. This is of critical importance when studying thixotropic materials since these materials give hysteresis loops as the resulting rheological flow curve. If the known Newtonian materials gave results that contained hysteresis loops, the results for unknown materials could not be accurately verified to be thixotropic. Inherent looping for Newtonian materials would indicate temperature fluctuations contributing to vary the results or electrical and mechanical errors, possibly in the form of builtup capacitance in filters or sloppy stopping and starting in the RPM drive unit. Non-linearity in the variable speed transmission could give non-Newtonian properties to Newtonian materials. The results indicated

6/19/70

BSB985-23,24,25,26,27

Figure 4-12

Brookfield Viscosity Standard
Run BSB985-23,24,25,26,27
μ_{lit} = 985 cp at 25°C

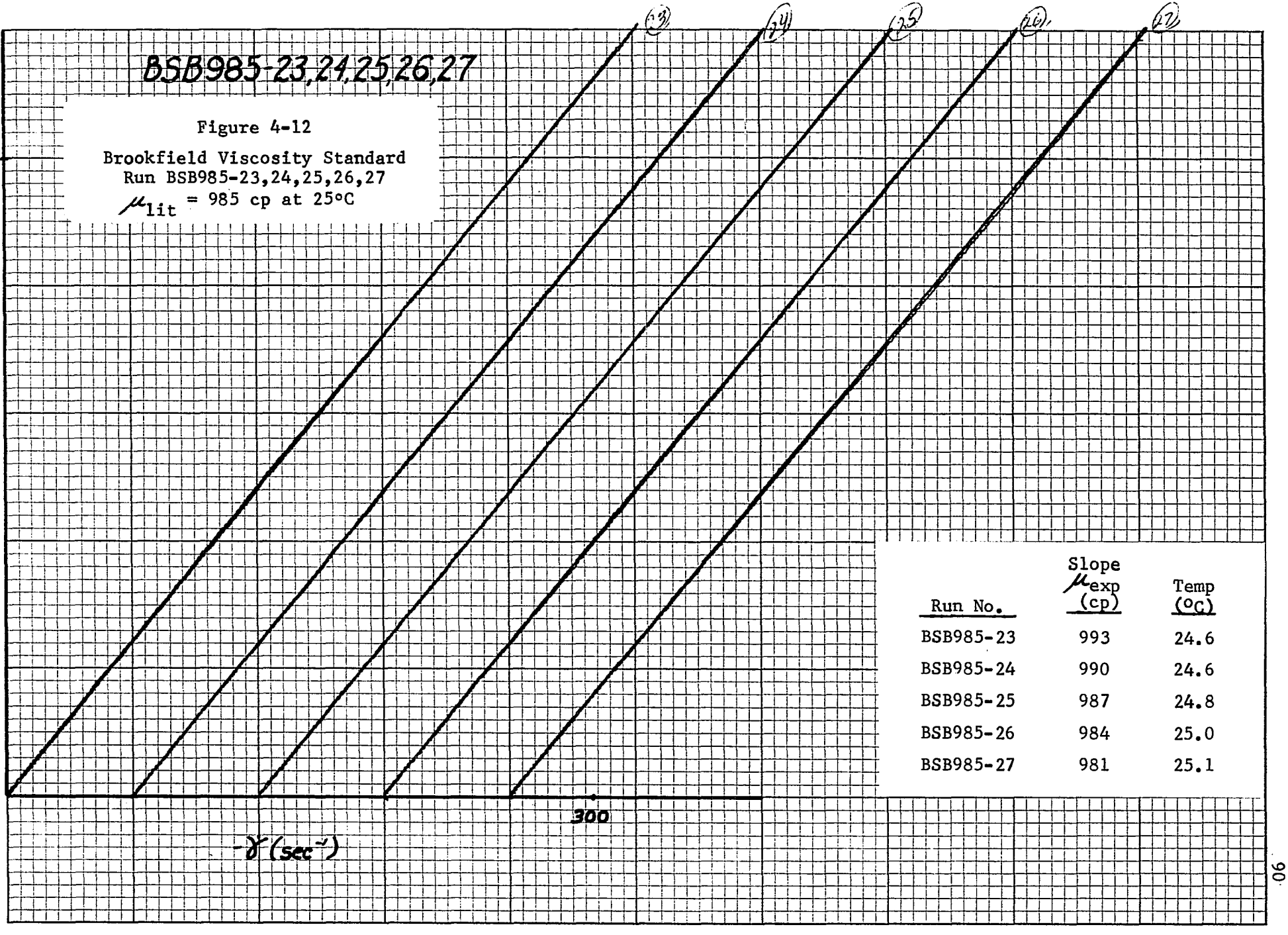

Run No.	Slope μ_{exp} (cp)	Temp (°C)
BSB985-23	993	24.6
BSB985-24	990	24.6
BSB985-25	987	24.8
BSB985-26	984	25.0
BSB985-27	981	25.1

no errors of this type to be present.

Different Types of Materials

A few time-independent, non-Newtonian materials were tested to determine whether the instrument would generate characterstic rheograms for these materials. The quality of the resulting curves would give an indication of the type of results obtained with unknown, thixotropic materials. It was important that a pseudoplastic flow curve be a single curved line in going from zero RPM to maximum and back to zero.

Figure 4-13 shows a flow curve for 0.25% Carbopol* 934. Increasing the shear rate (upcurve) resulted in a decrease in apparent viscosity as a function of shear rate. Decreasing the rate of shear (down curve) shows a decrease in shear stress with a return to zero along the same path as the upcurve. Equally important is the fact that the up and down curves produced a single curved line, characteristic of pseudoplastic materials.

The data from figure 4-13 were replotted on log-log coordinates in figure 4-14. Carbopol is a known pseudoplastic material which behaves according to the power of law:

$$\tau = -k\dot{\gamma}^{n} \qquad (4\text{-}1)$$

---

* B. F. Goodrich Company, Cleveland, Ohio 44115

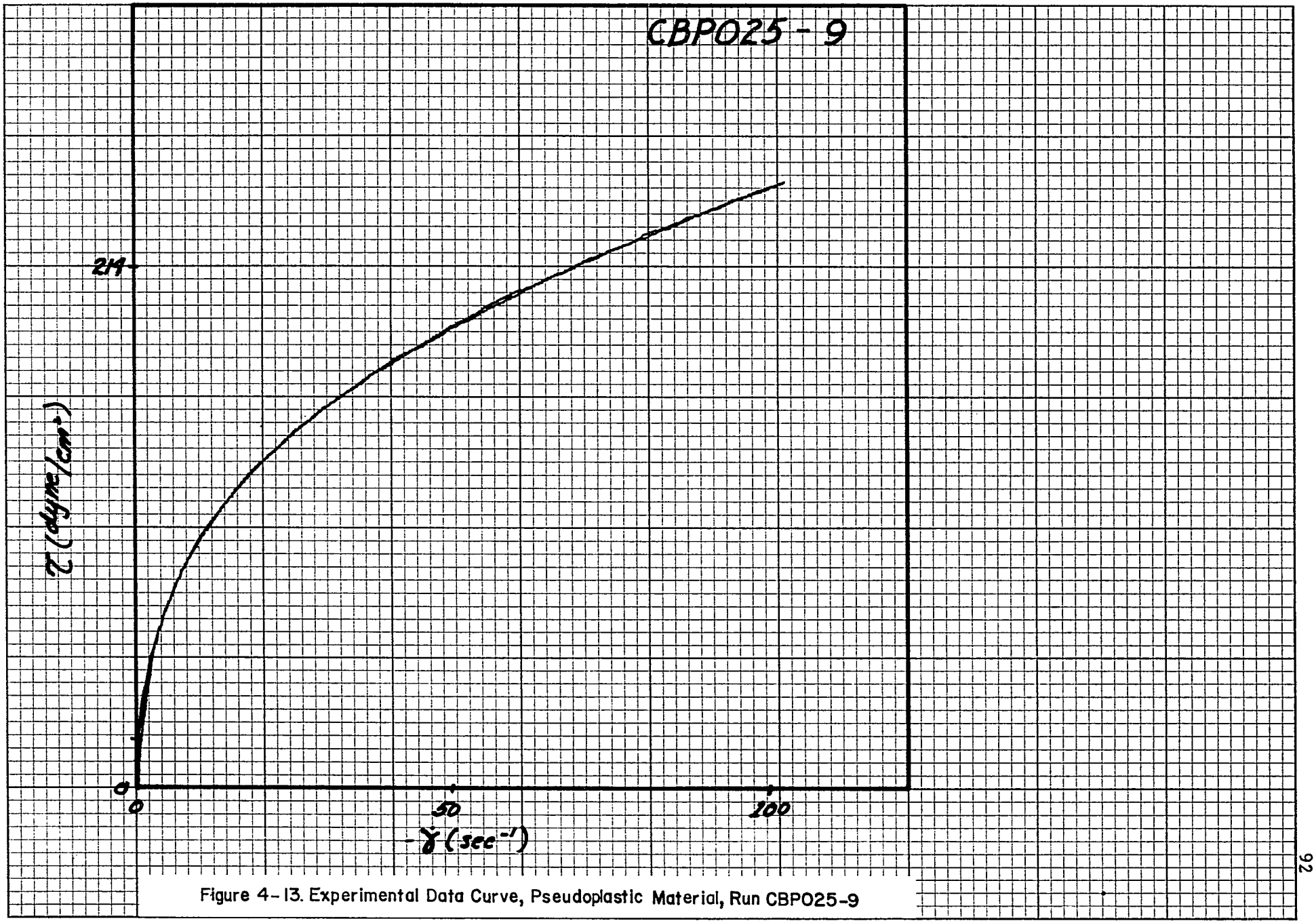

Figure 4-13. Experimental Data Curve, Pseudoplastic Material, Run CBP025-9

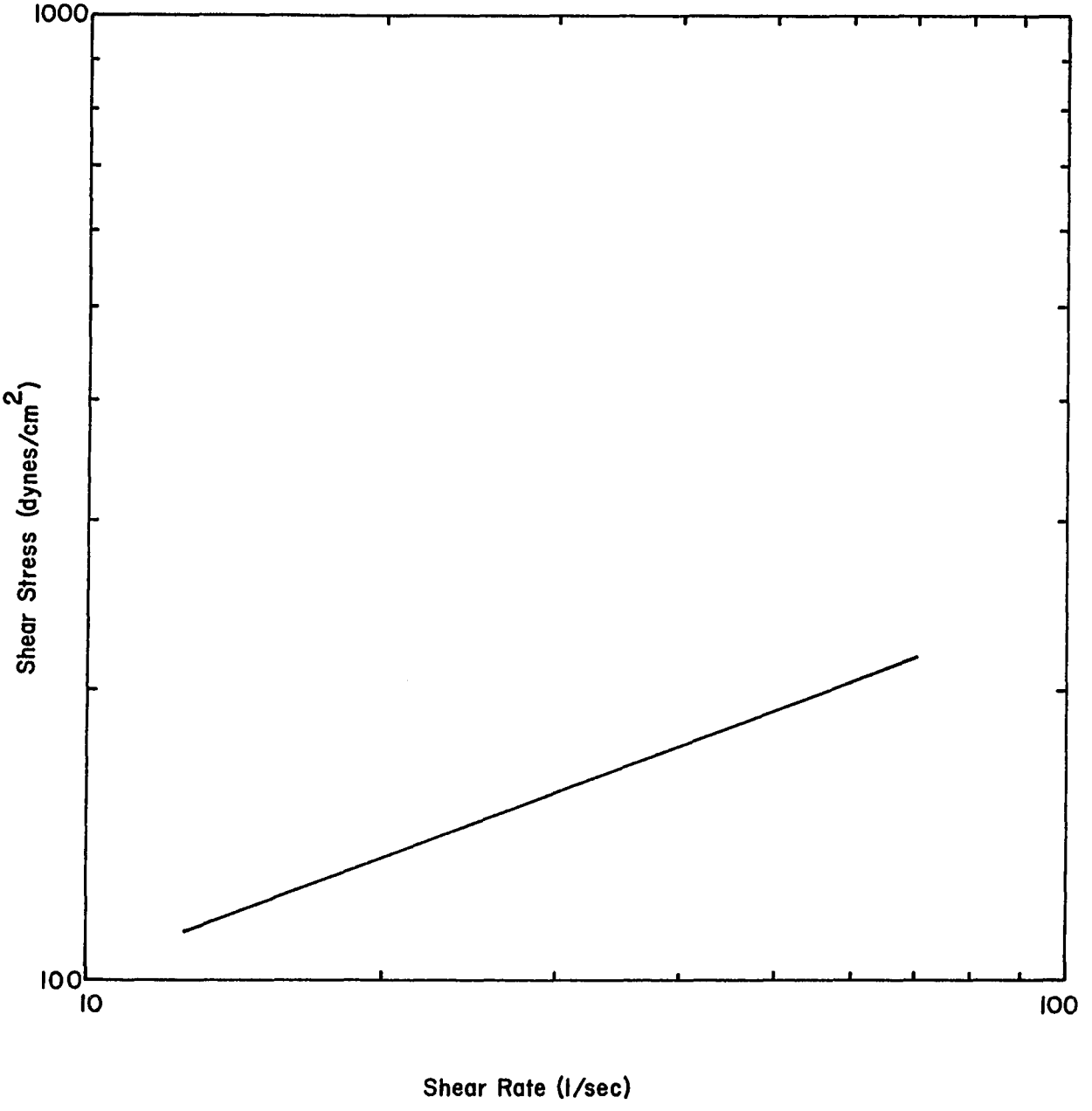

Figure 4-14. Log Plot of Run CBP025-9

Taking the logarithm of both sides of equation (4-1) gives:

$$\log \tau = -\log K + n \log \dot{\gamma} \qquad (4\text{-}2)$$

By plotting the log of shear stress versus the log of shear rate or shear stress vs. shear rate on log-log paper the flow behavior index could be determined from figure 4-14. For 0.25% Carbopol at 25°C the flow behavior index, n is equal to 0.38. Since the material was pseudoplastic this value had to be less than 1.0. Data for Carbopol in the literature is not complete, though a value of 0.37 for 0.25% Carbopol is given by Hagedorn (19) using a Brookfield viscometer. He mentions that the values might not completely agree from one investigator to another because the Carbopol resin varies slightly and the method of solution preparation and the degree of neutralization effect the values of the flow behavior properties. Therefore, the value determined from the instrument is well within reasonable error.

A dilatant material and a second pseudoplastic material were also tested with the instrument. Their flow curves are given in figures 4-15 and 4-16. The first material was a Goodyear vinyl rubber and showed a slight tendency to dilitancy. The apparent viscosity of the material increased as a function of shear rate and there was no hysteresis loop present. Finally, a motor oil additive, STP, was tested and found to be slightly pseudoplastic in nature.

Figure 4-15
Experimental Data Curve
Dilatant Material
Run GYVR-4

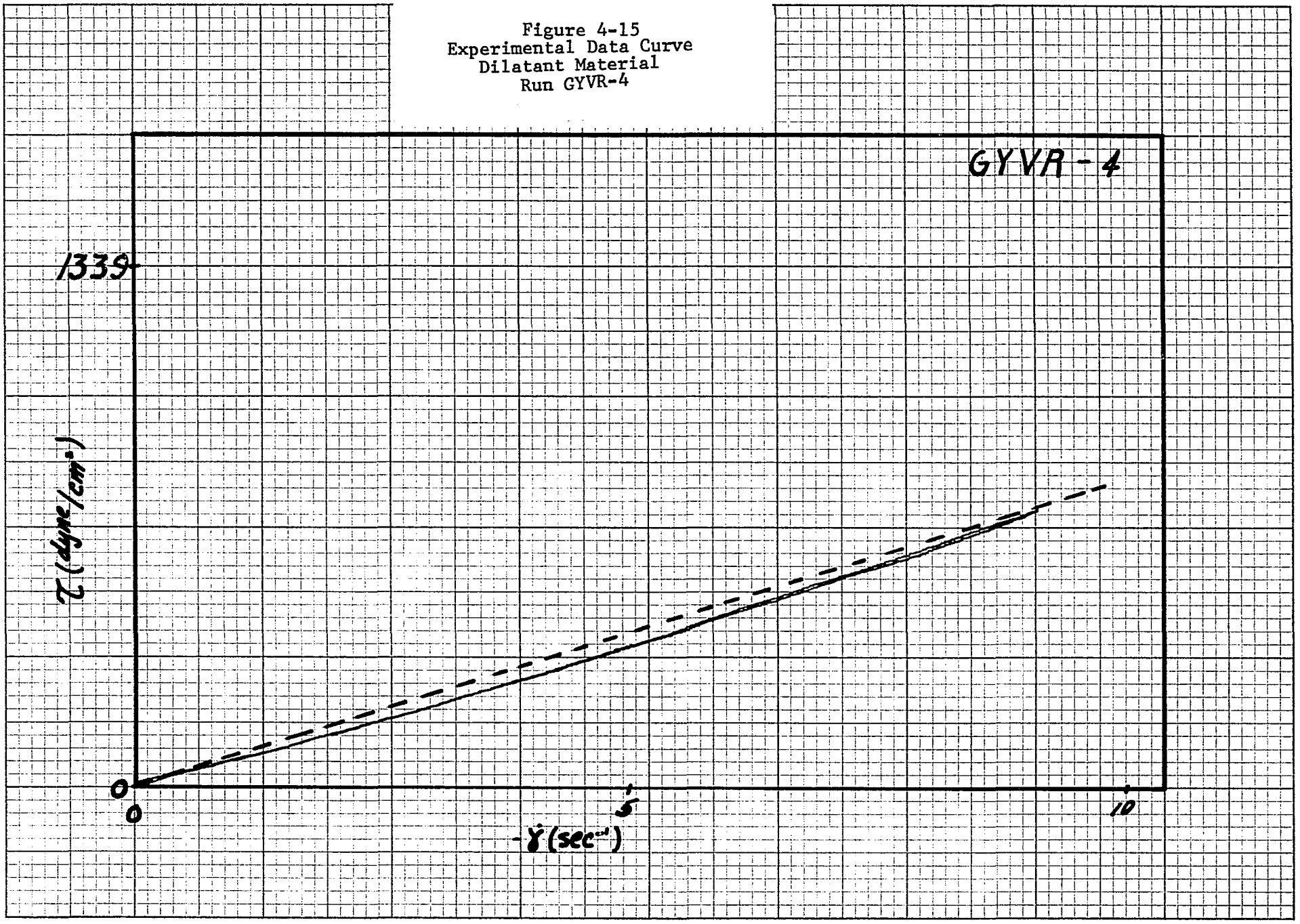

Figure 4-16
Experimental Data Curve
Pseudoplastic Material
Run STPPP-11

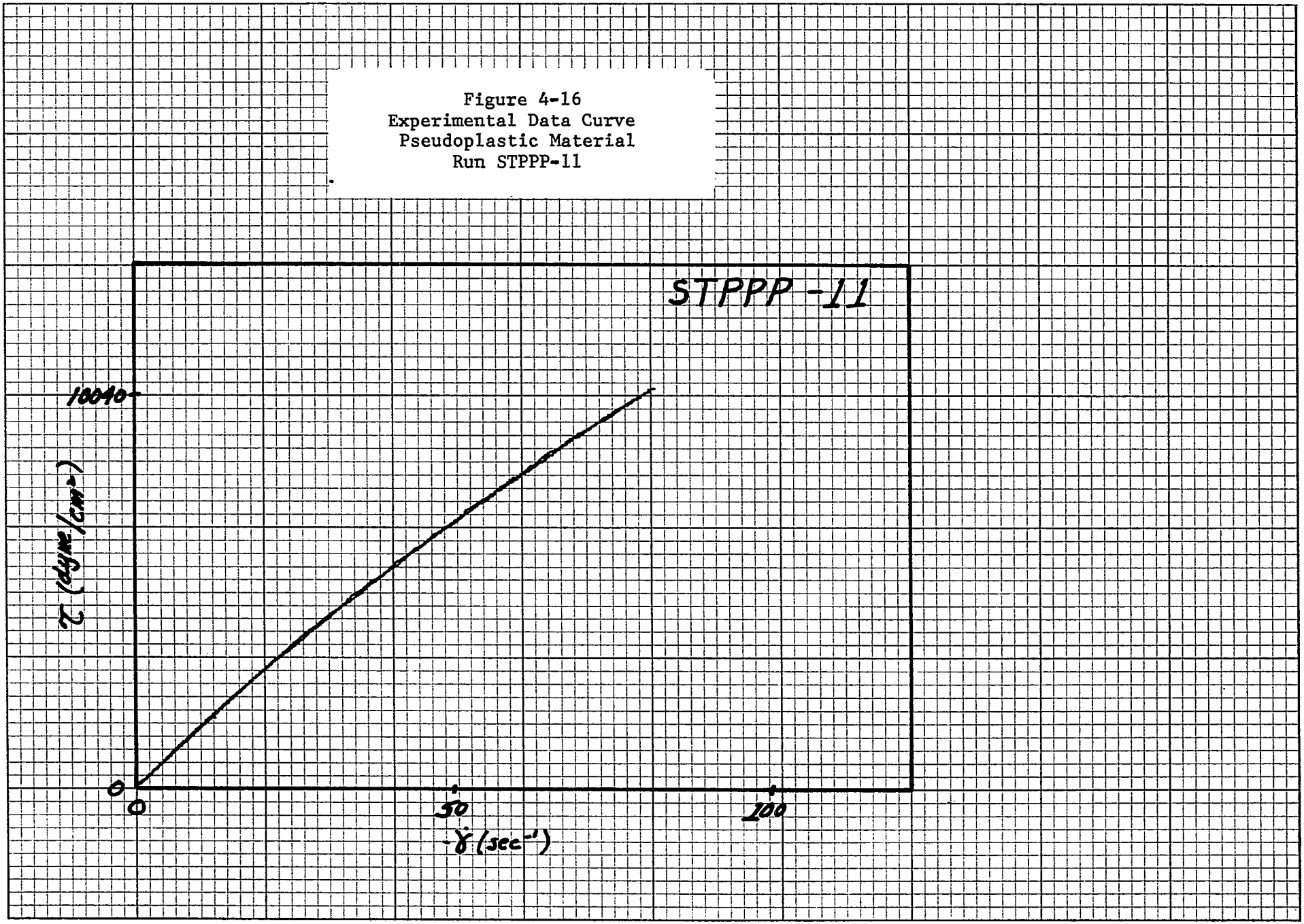

The quality of the curves added confidence to the accuracy and versatility of the instrument.

Thixotropic Materials

The final test for the modified Weissenberg Rheogoniometer was with thixotropic materials. Two types of thixotropic materials were used, a grease-oil mixture (1, 3, 21, 36, 39, 41) and a montmorillonite clay (3, 9, 27, 35). A brief description of the materials and the compositions used are included in Appendix E. These materials were known to have thixotropic characteristics and were thus chosen as test materials for the instrument. The ability of generating the characteristic rheograms described in Chapter 1 was chosen as the test criteria for the instrument. A single hysteresis loop (figure 1-2), multiple hysteresis loops (figure 1-3), and a hysteresis loop with a constant shear rate zone (figure 1-4) should all be obtainable by the instrument. Though important in characterizing thixotropic materials, a torque-decay curve (shear stress as a function of time of shearing at constant shear rate) was not considered during the testing of the instrument because this type of curve could be generated by the original Weissenberg Rheogoniometer and was not an objective with the modification of the instrument.

Sample results obtained with one particular silicone grease and oil mixture are shown in figures 4-17 through 4-20. The initial curve, figure 4-17, shows a single hysteresis loop which was generated by allowing the instrument to increase from zero to

SG0541-26

Figure 4-17
Experimental Data Curve
Thixotropic Material
Run SG0541-26

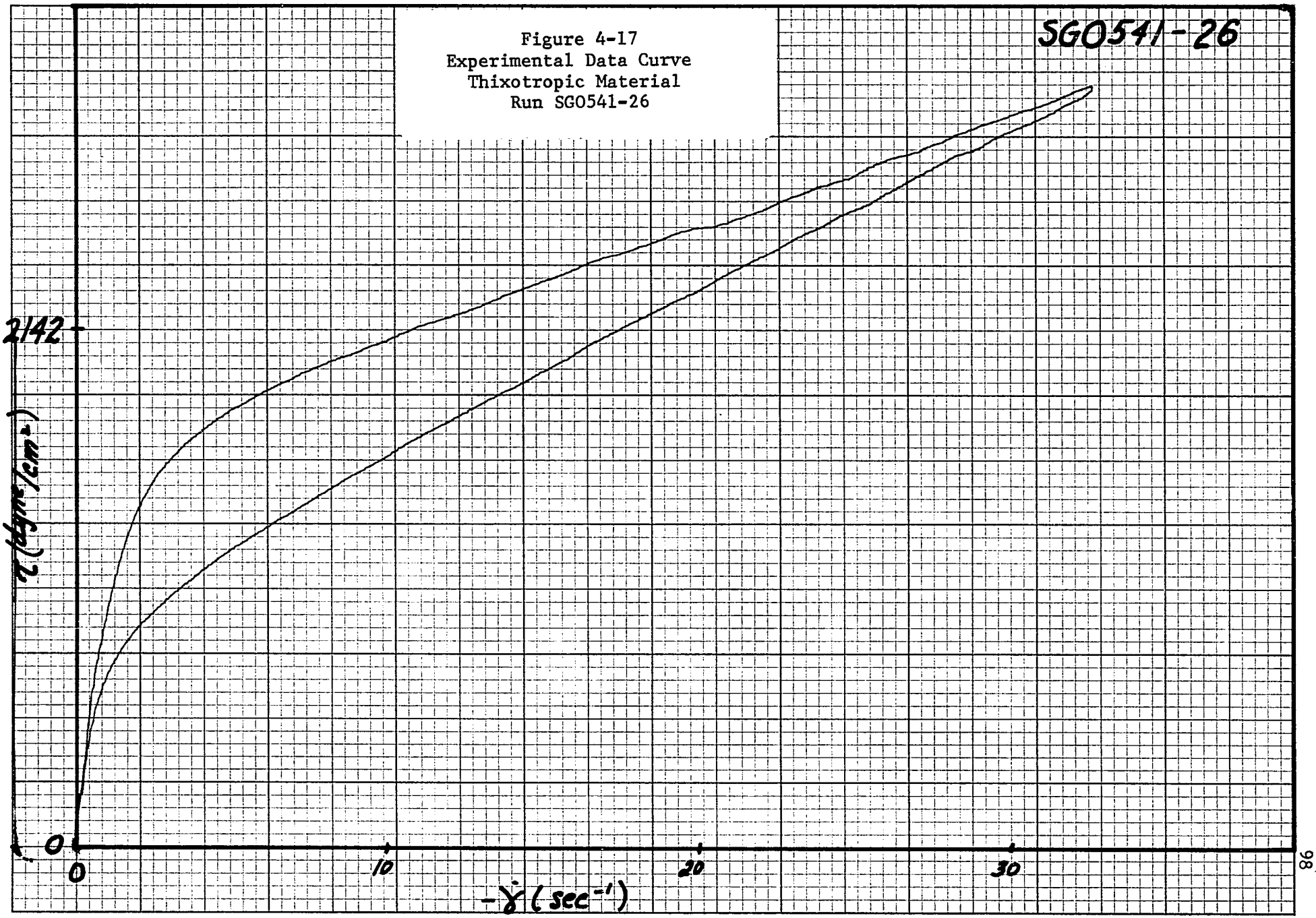

SGO 541-27

Figure 4-18
Experimental Data Curve
Thixotropic Material
Run SGO541-27

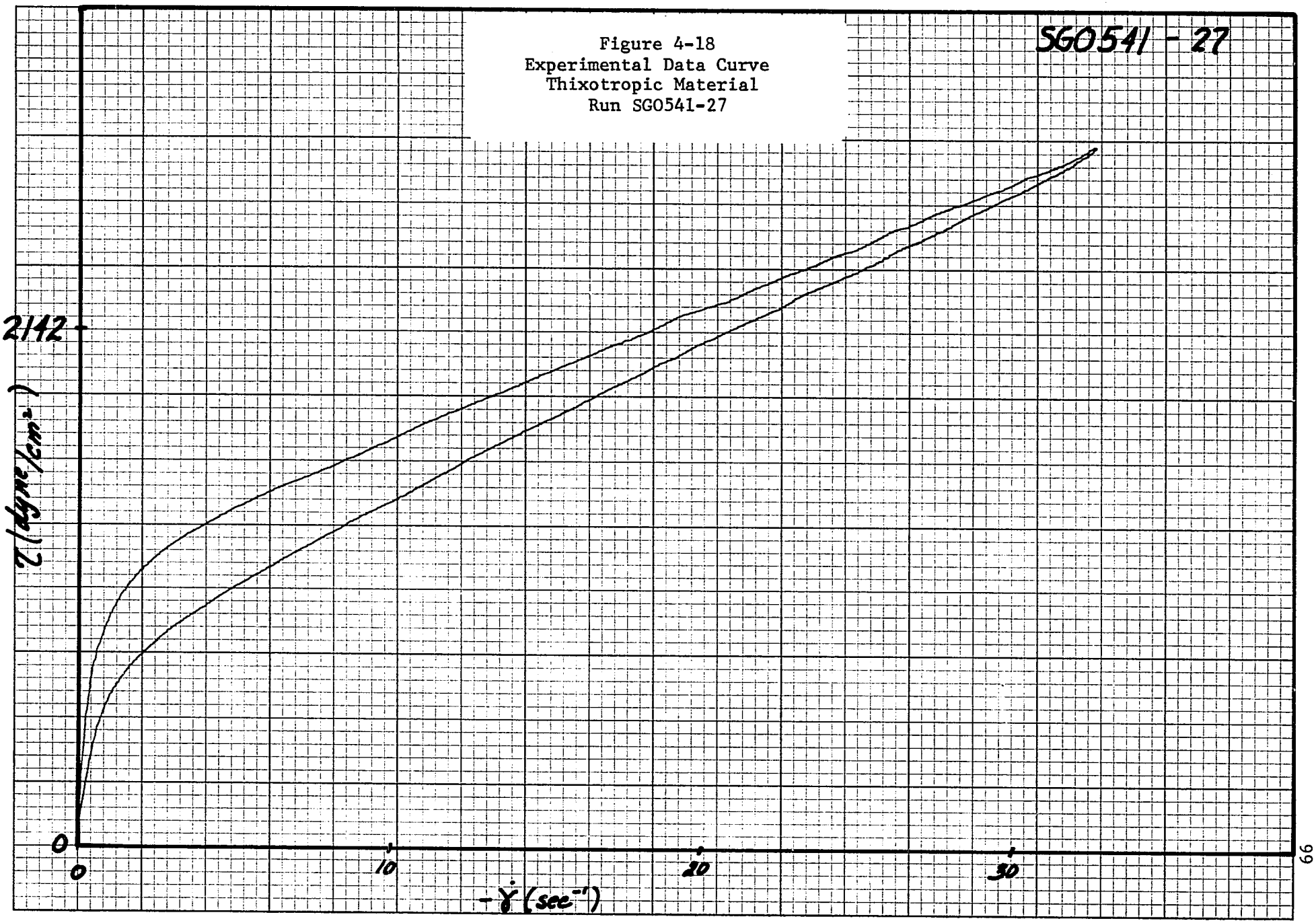

SG0541-42

Figure 4-19
Experimental Data Curve
Thixotropic Material
Run SG0541-42

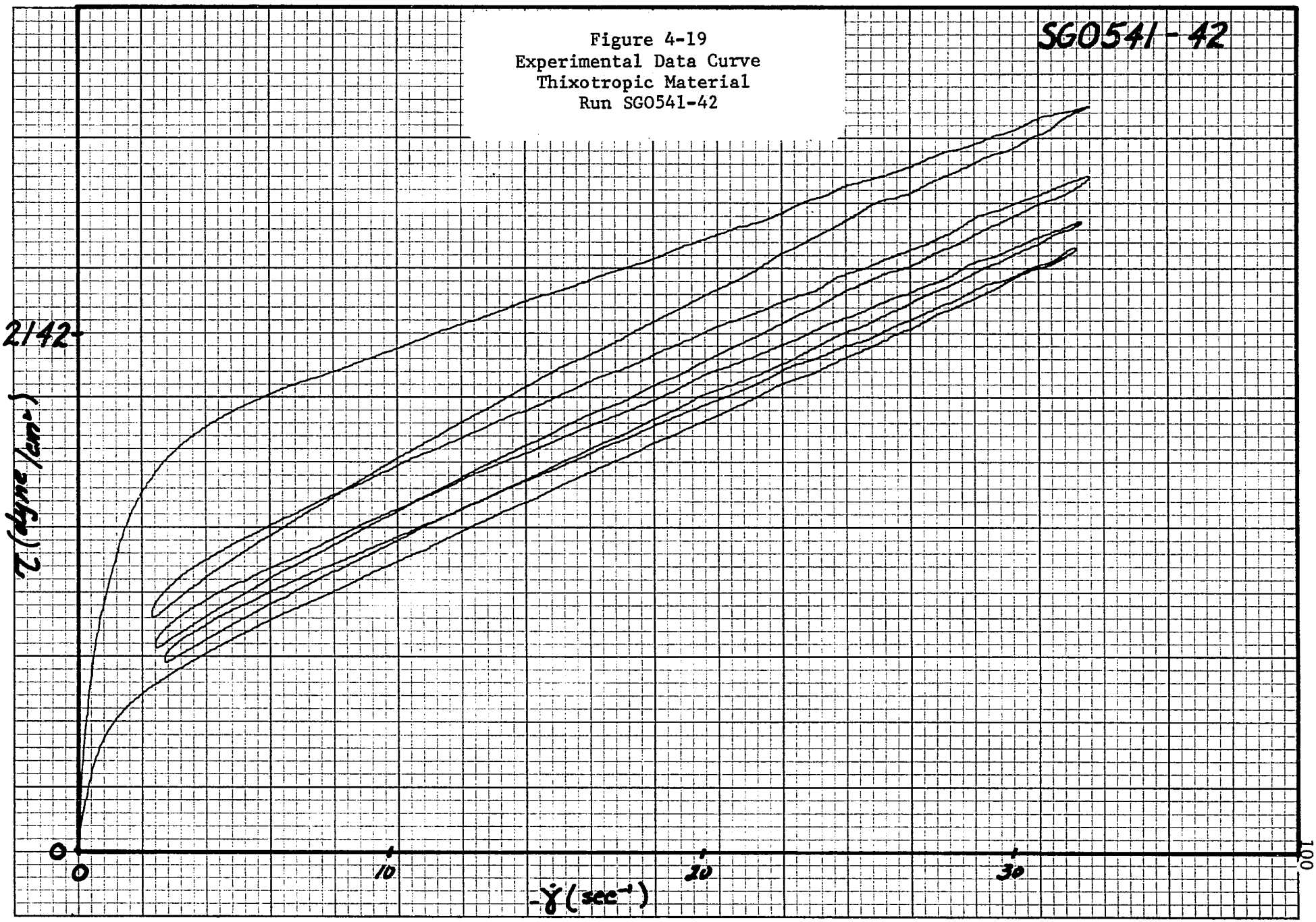

Figure 4-20
Experimental Data Curve
Thixotropic Material
Run SG0541-38

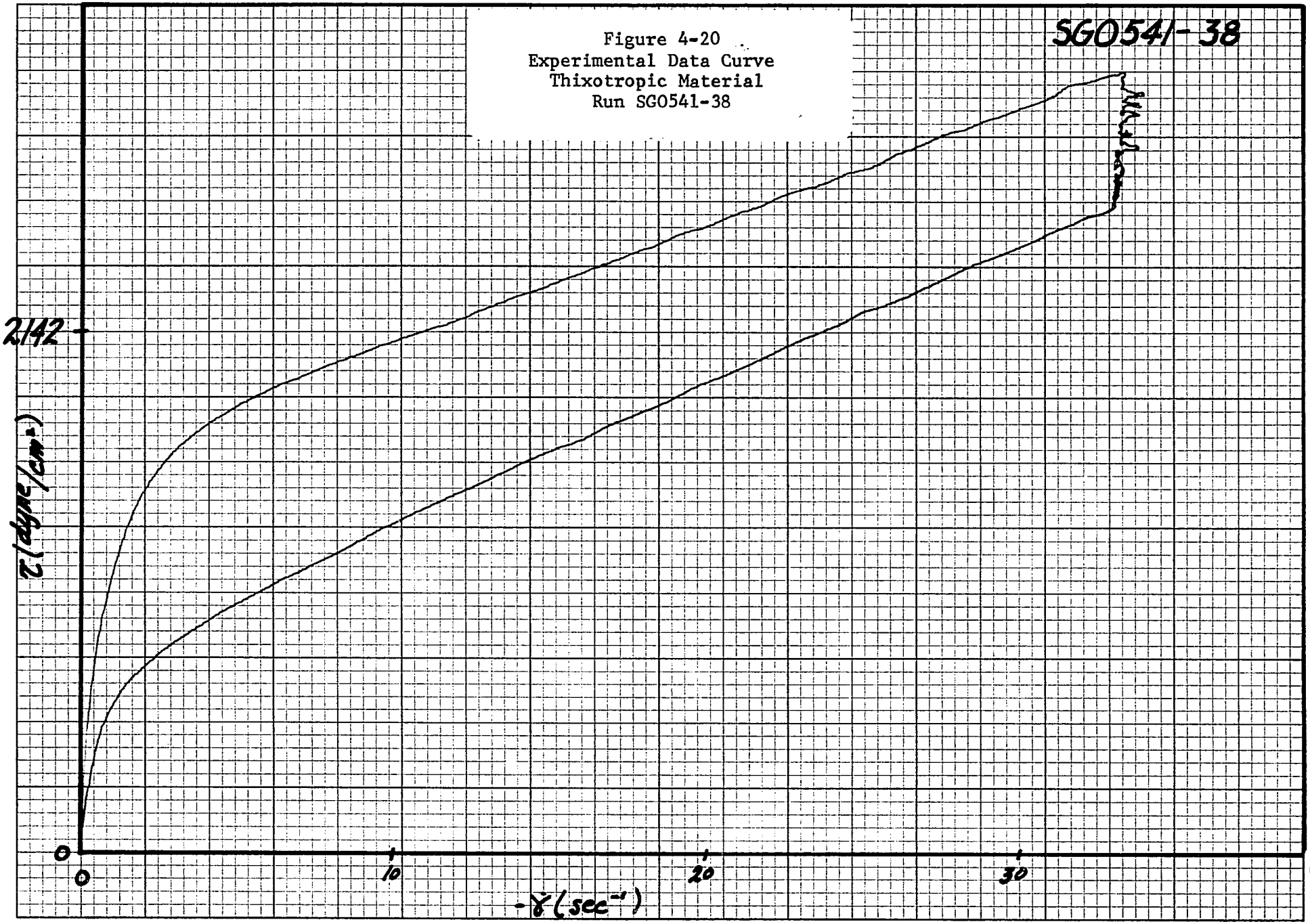

a maximum shear rate for the particular gearbox setting and then allow the shear rate to decrease and return to zero. The curve shown in figure 4-17 is the actual experimental hysteresis loop generated by the instrument. It should be noted that before the run could be made, a few tests were conducted to make certain that the correct diameter cone, cone angle, torsion bar size, and torsion bar-transducer meter setting were selected for the material being run. The variables associated with each run are given in Appendix F.

Two important results shown by figure 4-17 include a yield stress detected by the machine and the return to zero after the completion of the up-down cycle for the hysteresis loop. At the completion of Run SG0541-26 shown in figure 4-17, the paper was replaced in the recorder and a second hysteresis loop was generated, figure 4-18. The exact same experimental procedure was used to generate this curve. A definite difference can be seen between the two curves, most noticeably the maximum shear stress had decreased and the area enclosed by the hysteresis loop had decreased. The relative amount of thixotropy possessed by the fluid at the time the second loop had been generated, figure 4-18, was less than that present with the first loop, figure 4-17. This is a characteristic of thixotropic materials that have not been permitted to recover their original properties. Additional loops would show continued decrease in thixotropic properties for the material. An alternate method of generating a series of loops is shown in figure 4-19.

In this figure, rather than allowing the shear rate return to zero and changing the recorder paper, the shear rate was immediately increased to the maximum value and then decreased back toward zero. This up-down program was done 4 times to generate 4 hysteresis loops. In figure 4-19, the shear rate was not actually allowed to return to zero for clarity in following the loops. If this up-down looping procedure were continued, the hysteresis loop would disappear and the material would behave similar to a pseudoplastic material where the up-down looping procedure would result in a single curve. Finally, a hysteresis loop with a constant shear rate zone was generated, figure 4-20, using another sample of this same material. The constant shear rate section was generated by holding an essentially constant shear rate for a period of about 10 minutes. If figures 4-17, 4-19, and 4-20 were placed one on top of each other and viewed against bright light or with the aid of a light box, the upper curve of the first hysteresis loop would be very similar in all three cases with a fluctuation of less than 60 dynes/cm^2 for the three curves. Additional silicone grease and oil mixtures of different compositions are given in figures 4-21 and 4-22. The curves in figure 4-22 were allowed to return to zero before beginning the succeeding hysteresis loop.

A montmorillonite clay was also tested on the instrument, figures 4-23 through 4-25 and confirmed to be thixotropic in nature. A fresh sample of material at the same composition is

6/25/40

25 DCGGEO-23

Figure 4-21
Experimental Data Curve
Thixotropic Material
Run 25DCGGEO-23

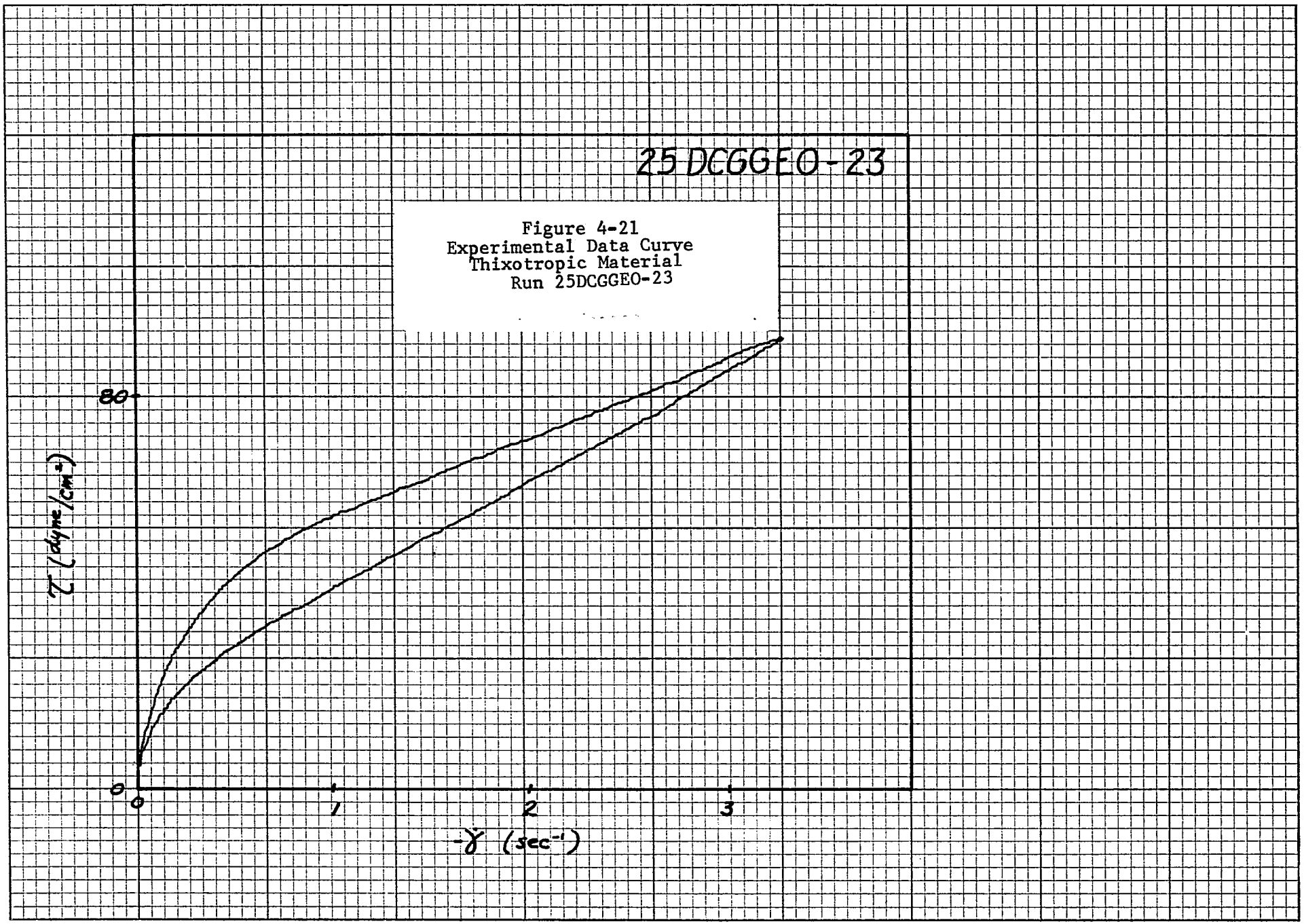

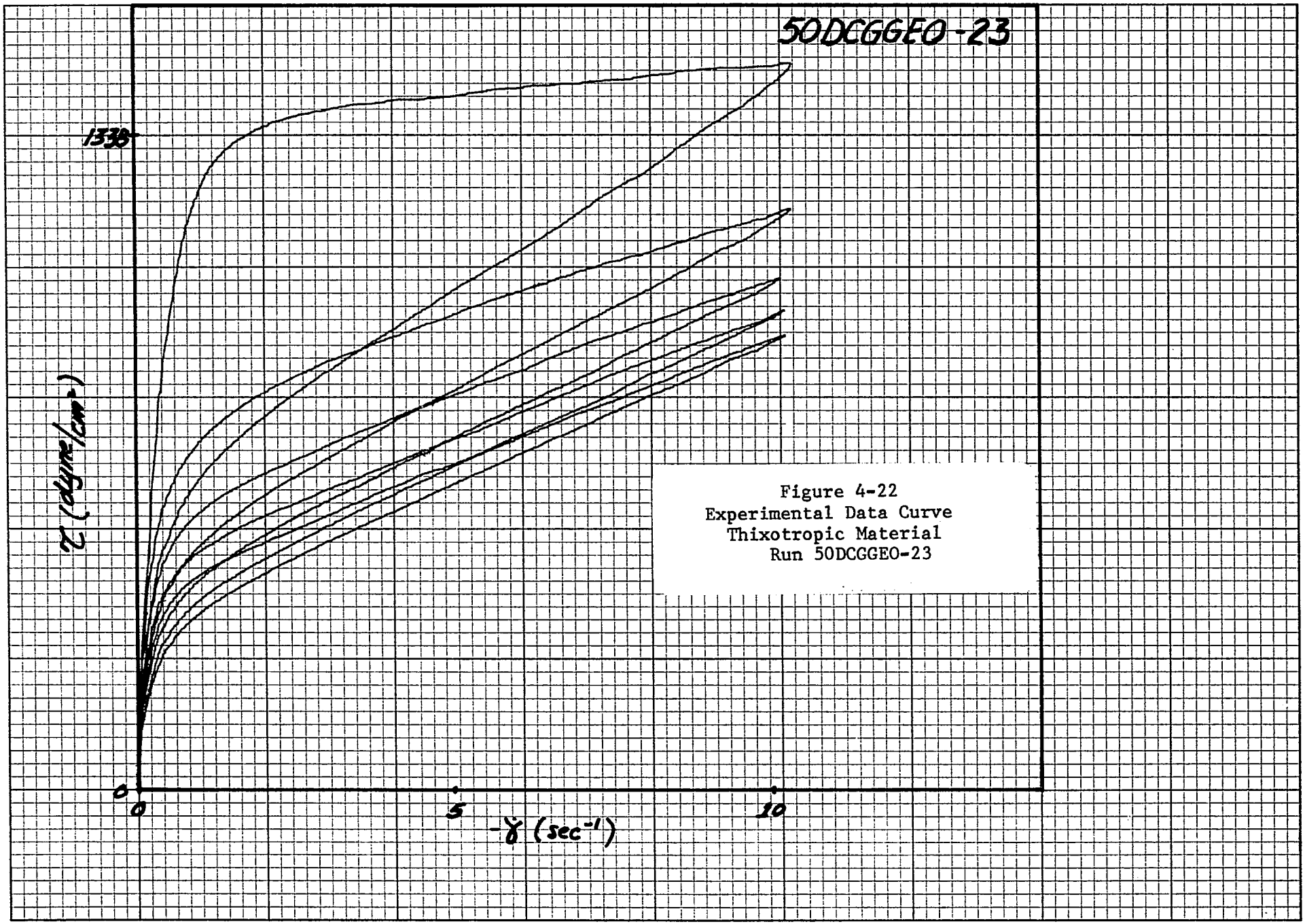

Figure 4-22
Experimental Data Curve
Thixotropic Material
Run 50DCGGEO-23

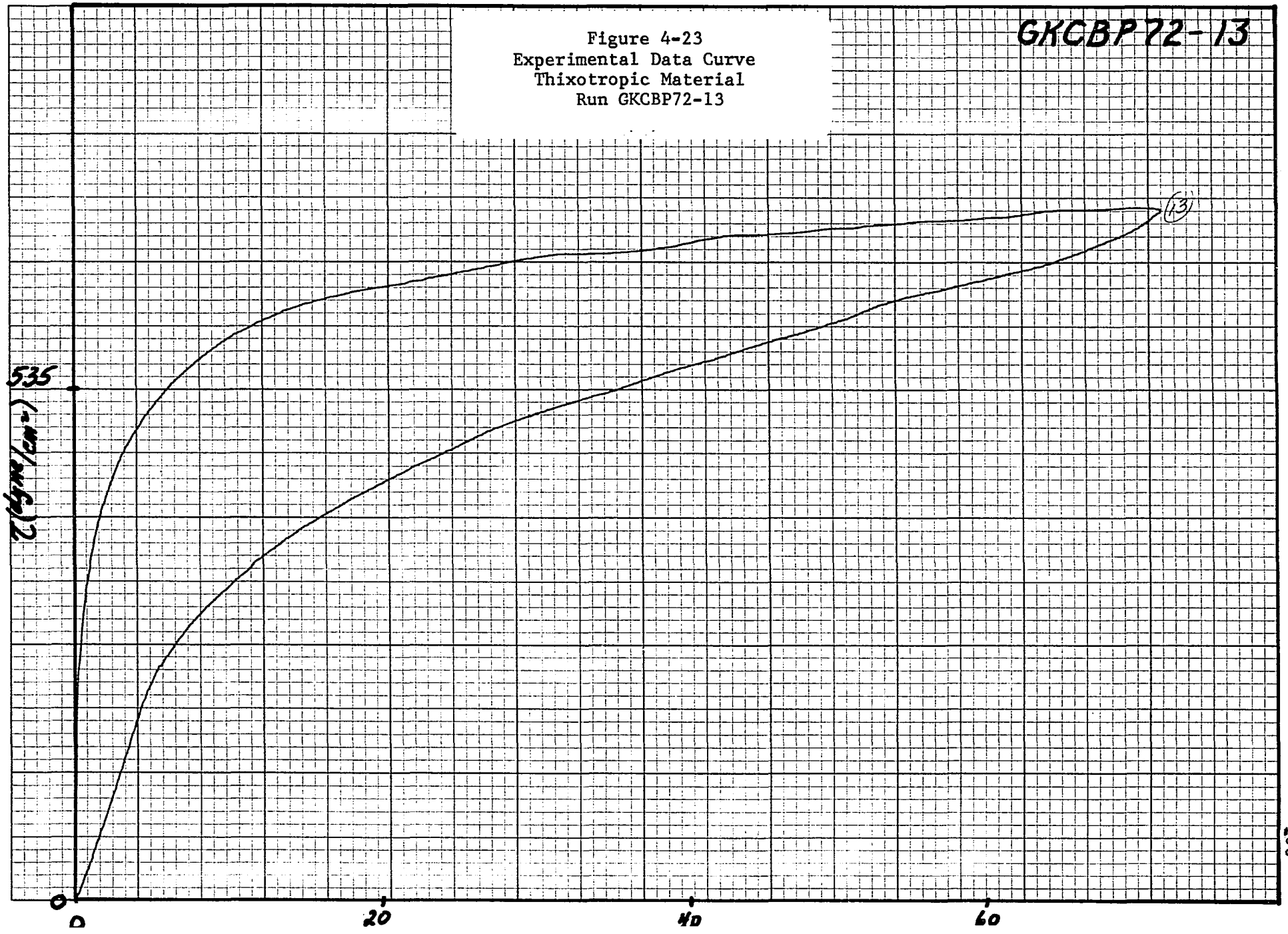

Figure 4-23
Experimental Data Curve
Thixotropic Material
Run GKCBP72-13

GKCBP7-

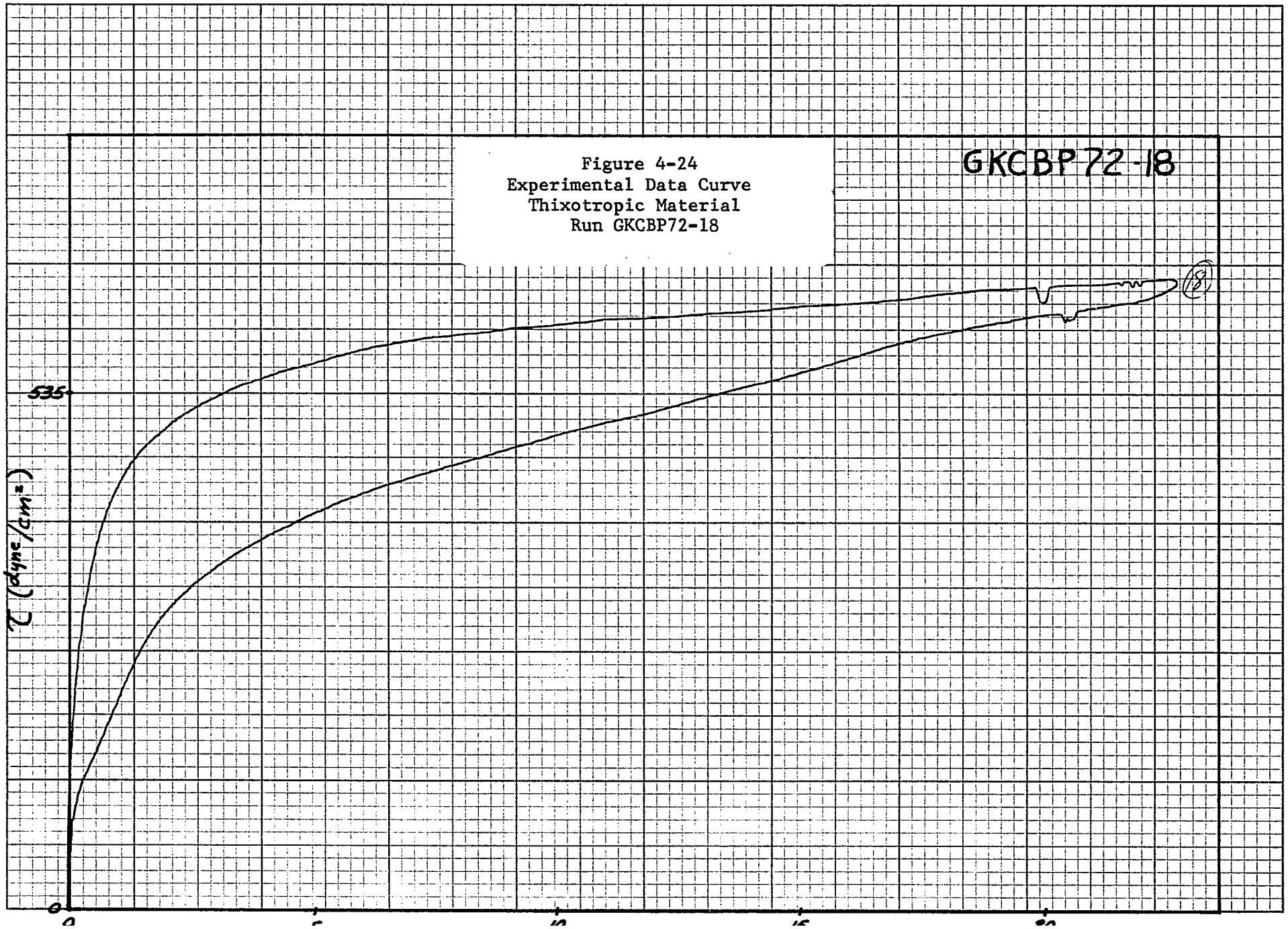

Figure 4-24
Experimental Data Curve
Thixotropic Material
Run GKCBP72-18

GKCBP72-21

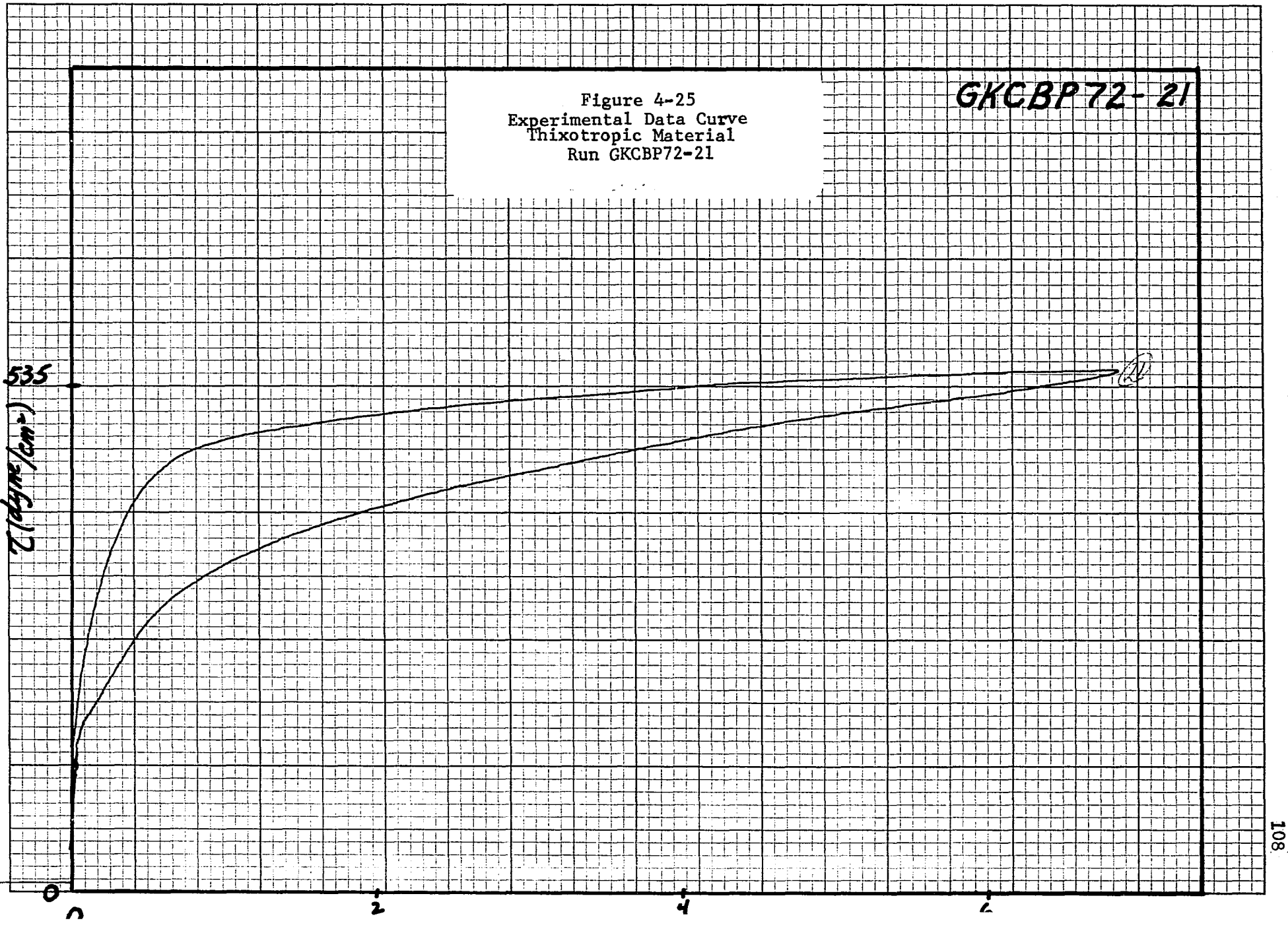

Figure 4-25
Experimental Data Curve
Thixotropic Material
Run GKCBP72-21

added to the instrument before the start of each curve. The difference between the various curves are in gearbox settings which give different maximum shear rates possible with each run. Thus, figure 4-25 represents about 1/3 of figure 4-24 which in turn represents about 1/3 of figure 4-23. A comparison of similar shear rate zones on each curve can be made for the upcurve but not for the downcurve, because of the difference in shear history between the various curves. For example, if the shear stress for the upcurves were read at a shear rate of 5 sec^{-1} in the three figures, values of 515, 566, and 542 dynes/cm^2 would correspond to figures 4-23, 4-24, and 4-25, respectively. The average of the three values 541 dynes/cm^2 are within 5% of the various readings. Similarly, for the downcurves would give shear stress values of 226, 410, and 503 dynes/cm^2 for figures 4-23, 4-24, and 4-25, respectively. The large differences in shear stress readings for the downcurves can be accounted for by considering the relative position on the curves for a chosen shear rate. In figure 4-25, a shear rate of 5 sec^{-1} is just at the start of the downcurve (the downcurve begins at right and goes toward zero shear rate) whereas in figure 4-23, this shear rate is near the end of the downcurve. In figure 4-23, the material has been subjected to a greater shear in going from 5 sec^{-1} on the upcurve, the 71 sec^{-1} (maximum shear rate), and finally back to 5 sec^{-1}. Therefore, the much lower reading on figure 4-23 is expected because the history of the shear applied to the material must enter into any analysis of the material.

Since the experimental results for known Newtonian and time-independent, non-Newtonian materials showed no hysteresis loops when tested, materials showing hysteresis loops could then be assumed to be thixotropic. Because of the ability of the instrument to generate accurate rheograms, it can be used to accurately identify thixotropic materials without suspect to equipment-caused loops. One such material was human blood, figure 4-26.

As late as 1961, researchers (38) considered blood to be a pseudo-plastic, non-Newtonian material. Experiments were performed in a point-wise manner, using capillary flow or rotational viscometers. Though viscosities varied with shear rate, no torque decay phenomena (figure 1-5) was detected when shear stress was measured as a function of time at constant rate of shear. By plotting shear stress as a function of shear rate for these pointwise measurements, a rheogram was obtained which was almost linear above shear rates of 10-20 sec^{-1} and curved toward the origin. Work was then directed toward getting data at low rates of shear (below 10 sec^{-1}). Cokelet, et al (5) found that below 4 sec^{-1}, a strip chart recording of shear stress as a function of time at constant shear rate, immediately increased to a maximum value followed by a decay in shear stress or torque. These results were confirmed by Dintenfass (7) and later by King and Copley (26), who observed torque decay curves at shear rates below 5 sec^{-1}.

Because of limitations to experimental equipment, none of these investigators were able to generate the characteristic hysteresis loop

for blood. Through the use of the modified Rheogoniometer, a hysteresis loop was obtained for blood containing CPD solution (citrate phosphate dextrose) as anticoagulant, figure 4-26. This rheogram is further evidence that blood is a thixotropic material.

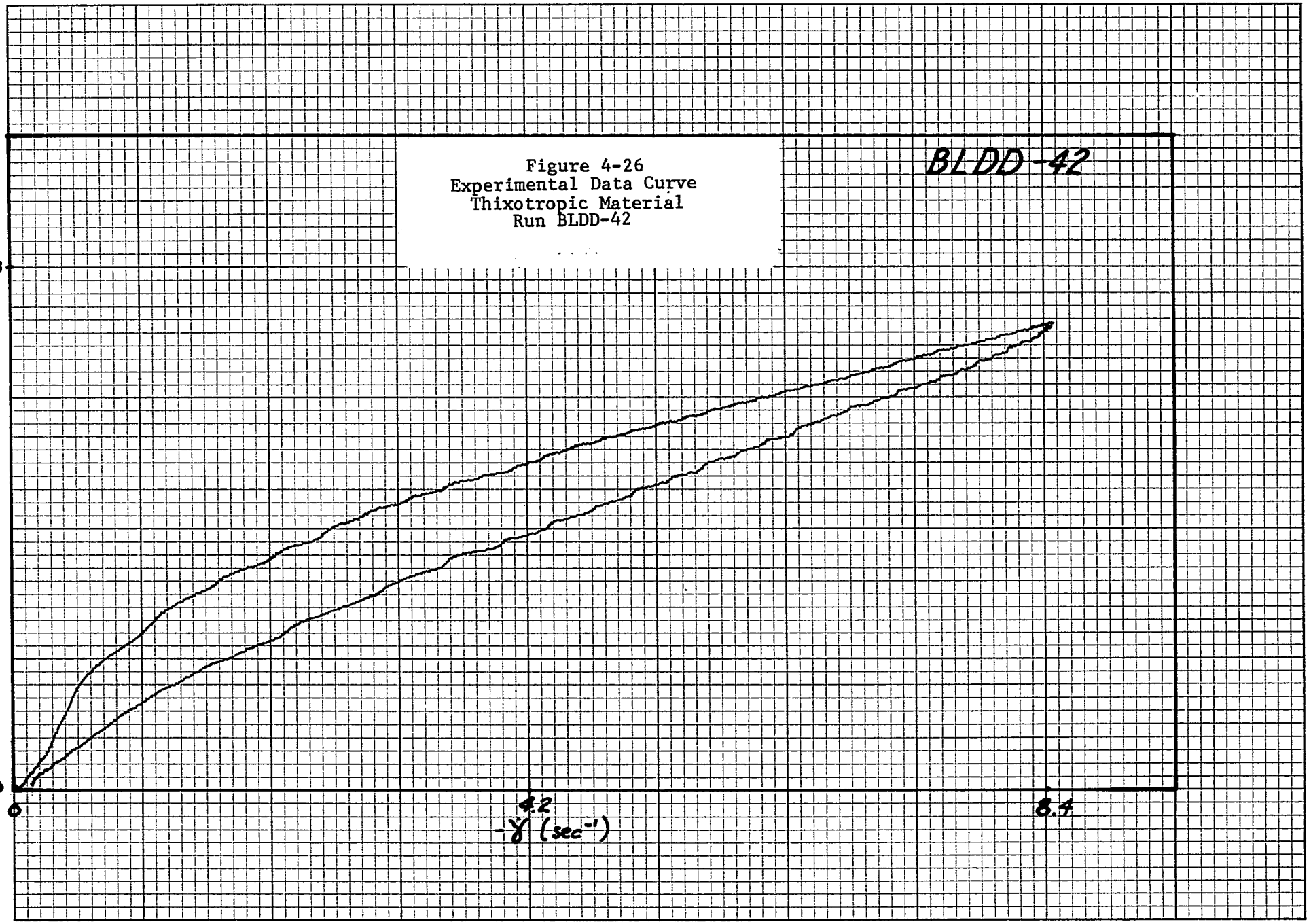

Figure 4-26
Experimental Data Curve
Thixotropic Material
Run BLDD-42

CHAPTER 5

ESTIMATION OF PARAMETERS IN THIXOTROPIC EQUATION

The various types of thixotropic materials described in Chapter 4: silicone grease and oil mixture, montmorillonite clay, and blood were used to test equation (2-68):

$$\tau = \tau_o - \mu\dot{\gamma} + C_1 \mathcal{B}_e |\dot{\gamma}|^n e^{-C_1 \int_o^t |\dot{\gamma}|^n dt} \qquad (2\text{-}68)$$

Equation (2-68) can be applied to a single hysteresis loop or multiple hysteresis loops as described in Appendix C and used in conjunction with the non-linear, least-squares computer program (Appendix D). For a single hysteresis loop, equation (2-68) can be rewritten, for the upcurve:

$$\tau = \tau_o + \mu\dot{\gamma} + C_1 \mathcal{B}_e \dot{\gamma}^n e^{-\frac{C_1}{a(n+1)}\dot{\gamma}^{n+1}} \qquad (5\text{-}1)$$

and for the downcurve:

$$\tau = \tau_o + \mu\dot{\gamma} + C_1 \mathcal{B}_e \dot{\gamma}^n e^{-\frac{C_1}{a(n+1)}\left\{2\dot{\gamma}(t_1)^{n+1} - \dot{\gamma}^{n+1}\right\}} \qquad (5\text{-}2)$$

where $\dot{\gamma}$, though negative by convention in equation (1-2), is assumed to be a positive number, thus changing the sign before the second term on the right-hand-side in the equations. In these equations, 'a' is the proportionality constant between the shear rate and the time of shearing, and depends upon the

gearbox reduction at the motor driving the control arm of the variable speed transmission, figure 3-7. The computer program determines the best values of the constants B_1, B_2, B_3, B_4, and B_5. The parameters in equations (5-1) and (5-2) are then evaluated from these constants, as follows:

$$\tau_o = B_1 \qquad n = B_5$$

$$\mu = B_2 \qquad \zeta\beta_e = B_3/C_1 \tag{5-3}$$

$$C_1 = |a| B_4$$

From the type of data collected in this paper, the individual constants, ζ and β_e, in the lumped term, $\zeta\beta_e$, cannot be explicitly evaluated.

When correlating equations (5-1) and (5-2) with the experimental data, the first term on the right-hand-side of the equation is the yield stress, the second term is the linear change in shear stress with shear rate (Newtonian contribution), and the third term is the non-Newtonian and time-dependent change in shear stress with shear rate. If the rheological curve displays a large area of thixotropy (region between the up and downcurves), the relative contribution of this term in the equation increases. Another condition which gives the non-Newtonian term in the equation a large relative weight, is a rheogram with a lot of curvature. Similarly, each of the other

terms in the equation may contribute to varying degrees to the overall characteristics of the material depending upon the actual shape of the experimental curve for the material under investigation. When a rheogram contains a large linear section following the portion of the loop which curves, an increase in the relative weight of the Newtonian term of the equation is noticed. Materials with a large yield stress, give increased importance to the first term of the thixotropic equation which then effects the overall results.

Good correlations between experimental data and the thixotropic equation would be obtained with those materials having low yield stresses, small Newtonian sections, and a continuing decrease in change of shear stress with increase in shear rate (decreasing slope with increase in shear rate). A poor correlation is obtained with those materials which have a large yield stress and a large decrease in the slope of the upcurve with a small increase in shear rate, followed by a linear section with a small slope, a relatively low value of μ in equation (5-1). In this case, the non-Newtonian portion of the equation would have its largest contribution at low shear rates after which the Newtonian portion of the equation makes an ever increasing contribution to the overall value of the shear stress. Under extreme situation a small portion of the curve, generated by the thixotropic equation may even generate a negative slope before the Newtonian term starts contributing a large weight to the overall shear stress.

This idea of relative weights associated with the various terms of equation (5-1) can be more easily seen by calculating each term separately in the equation. The results of this type of analysis are given in tables 5-1 and 5-2 and figures 5-1 and 5-2. An example of a poor correlation is demonstrated by run 50DCGGEO-23 in table 5-1 and figure 5-2, whereas an example of good correlation is seen with run BLDD-42 in table 5-2 and figure 5-2. When the various terms in equation (5-1) are calculated separately for run 50DCGGEO-23, the non-Newtonian portion of the equation quickly increased to a maximum and then decreased to form an asymptote with the abscissa, figure 5-1. Adding the terms, does not eliminate this negative slope because the relative contribution of the second, Newtonian term is small. That is, the third term in the equation is decreasing at a greater rate than the second term is increasing. In estimating the parameters, the computer program is looking for the best correlation for the complete hysteresis loop and not just a section of the curve. An additional problem with run 50DCGGEO-23 was that the rheogram was continued for a long period after the actual line had become linear. In contrast to this poor correlation, are the results for run BLDD-42. With this run, the third, non-Newtonian, term does not reach a maximum and has a positive slope in figure 5-2 throughout the shear rate range. In the original data curve, figure 4-26, there was no sharp curved portion for this run which made the correlation much better. Finally, the run was not continued into a region where the curve became linear with a small value for the slope.

TABLE 5-1

ESTIMATION OF VARIOUS TERMS IN THIXOTROPIC EQUATION

RUN NO. 50DCGGEO-23

where: $a = 0.08$ $\quad C_1 = 0.0138$

$\tau_o = 430$ $\quad n = 0.614$

$\mu = 108$ $\quad \xi\beta_e = 49{,}100$

$\dot{\gamma}$	τ_o	τ_1	τ_2	τ
0	430	0	0	430
1	"	108	607	1145
2	"	216	769	1415
3	"	324	707	1451
4	"	432	578	1440
5	"	540	433	1403
6	"	648	294	1372
7	"	756	185	1371
8	"	864	112	1406
9	"	972	62	1464
10	"	1080	35	1545

where: $\tau_1 = \mu\dot{\gamma} - \frac{C_1}{a(n+1)}\dot{\gamma}^{n+1}$

$\tau_2 = C_1 \xi\beta_e \dot{\gamma}^n e$

$\tau = \tau_o + \tau_1 + \tau_2$

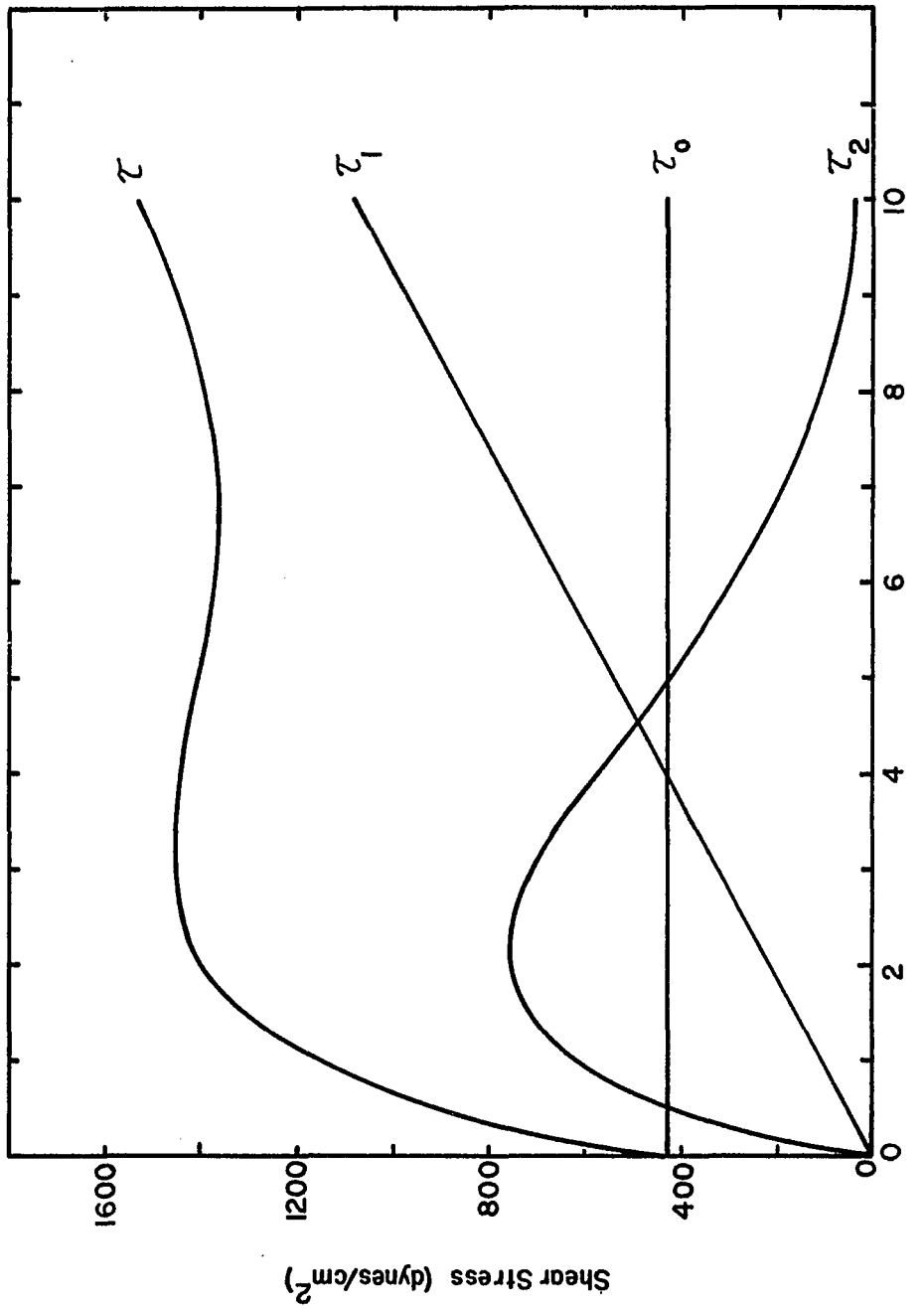

Figure 5-1. Summation of Upcurve for Run 50DCGGEO-23

TABLE 5-2

ESTIMATION OF VARIOUS TERMS IN THIXOTROPIC EQUATION

RUN NO. BLDD-42

where: $a = 0.08$ $\quad C_1 = 0.00175$

$\tau_o = 0.0$ $\quad n = 0.452$

$\mu = 0.0514$ $\quad \Sigma\beta_e = 145$

$\dot{\gamma}$	τ_o	τ_1	τ_2	τ
0	0.0	0.0	0.0	0.0
1	"	0.0514	0.249	0.3004
2	"	0.1028	0.330	0.4358
3	"	0.1542	0.387	0.5412
4	"	0.2056	0.413	0.6186
5	"	0.2570	0.448	0.7050
6	"	0.3084	0.464	0.7724
7	"	0.3598	0.473	0.8328
8	"	0.4112	0.482	0.8932

where: $\tau_1 = \mu\dot{\gamma}$

$\tau_2 = C_1 \Sigma\beta_e \dot{\gamma}^n e^{-\frac{C_1}{a(n+1)}\dot{\gamma}^{n+1}}$

$\tau = \tau_o + \tau_1 + \tau_2$

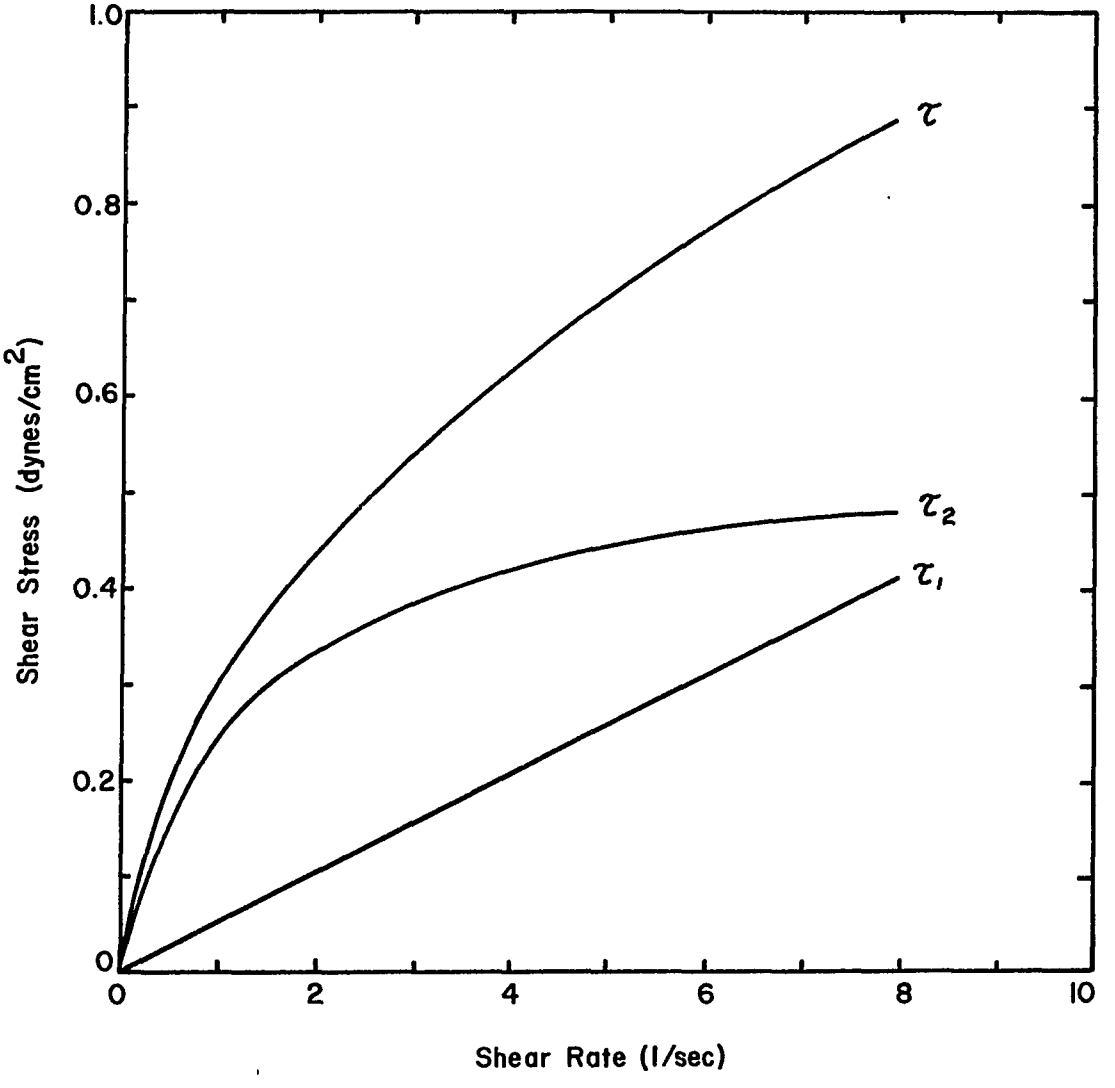

Figure 5-2. Summation of Upcurve for Run BLDD-42

Values for the parameters to equations (5-1) and (5-2) for the various materials which have been investigated are given in table 5-3. These parameters can be substituted back into equations (5-1) and (5-2) and the shear stress calculated as a function of shear rate. Figures 5-3 through 5-11 are plots of shear stress versus shear rate for these materials. The curves compare the actual experimental data (solid lines) with data calculated by the thixotropic equation (indicated by X's).

The goodness of fit (29) of the model to the data may be described by the standard error of the estimate

$$Se = (\phi/(N-k))^{1/2} \qquad (5\text{-}4)$$

where ϕ is the minimized sum of the squares of the differences of the experimental shear stress and the estimated shear stress, N is the number of data points, and k is the number of parameters. The non-linear least squares computer program calculates the values of ϕ and Se for each material. These values are presented in table 5-4. Because the magnitudes of the shear stresses are different for the various materials investigated, a comparison of the standard error is not a convenient method of determining the goodness of fit for these different materials. A better method of comparing the correlation of the equations to the materials is to divide the standard error by the mean shear stress, using the following dimensionless ratio:

$$\curvearrowright = \frac{Se}{Y_{mean}} (100) \qquad (5\text{-}5)$$

Values of $\curvearrowright$ and Y_{mean} are also given in table 5-4. The lower the value of $\curvearrowright$, the better the correlation between the experimental data and the thixotropic equation. Therefore, run BLDD-42 would be considered to have a good fit and the 50DCGGEO runs would have a poor fit.

Depending upon the particular material used, the results varied from good to poor. This is mainly due to the shape of the experimental curve. Looking at the silicone grease and oil mixtures, the results look good in figures 5-4 and 5-3, and poor in figure 5-5. In figure 5-4, there is only a small yield value for the material, a gentle increase in shear stress as a function of shear rate in the lower shear rate range, and an almost linear increase in shear stress with shear rate beyond the low shear rate region. This final linear region of the rheogram has a substantial slope(shear stress divided by shear rate) for both the upcurve and the downcurve. Run SG0541-26 in figure 5-3, behaves similarly to run 25DCGGEO-23 in figure 5-4, except for a more pronounced curvature in the low shear rate region. With this run, the curve did not become negative because the slope of the linear section to the right of the curved portion was significant. Reasons for the poor correlation of run 50DCGGEO-23 in figure 5-5 were discussed in figure 5-1.

TABLE 5-3

PARAMETERS IN THIXOTROPIC EQUATION

Run Number	τ_o	μ	C_1	n	$\xi\beta_e$	$C_1\xi\beta_e$
GKCBP72-13	42.6	1.85	0.000197	0.215	1,630,000	321
GKCBP72-18	92.6	1.63	0.000565	0.232	588,000	332
GKCBP72-21	112.0	0.307	0.00202	0.231	175,000	353
SG0541-26	828.0	71.2	0.00222	0.615	131,000	291
25DCGGEO-23	1.79	11.4	0.00218	0.342	20,200	44.1
50DCGGEO-23 (1 loop)	430.0	108.0	0.0138	0.614	49,100	676
50DCGGEO-23 (2 loops)	102.0	13.0	0.00134	0.233	729,000	976
50DCGGEO-23 (3 loops)	194.0	38.8	0.00158	0.195	535,000	844
BLDD-42	0.0	0.0514	0.00175	0.452	145	0.253

where

$|a| = 0.032$ Run 25DCGGEO-23

$|a| = 0.08$ All other runs

TABLE 5-4

STANDARD ERROR OF ESTIMATE

Run Number	N	Y_{mean}	Ø	Se	$\sqrt{}$
GKCBP72-13	47	519.74	67,900	40.21	7.74
GKCBP72-18	49	498.77	29,520	25.90	5.19
GKCBP72-21	47	440.28	15,370	19.13	4.34
SGO541-26	45	1959.69	209,900	72.43	3.70
25DCGGEO-23	53	50.73	95	1.407	2.77
50DCGGEO-23 (1 loop)	43	1118.43	319,300	91.66	8.20
50DCGGEO-23 (2 loops)	70	985.73	631,300	98.55	10.00
60DCGGEO-23 (3 loops)	96	903.85	927,200	100.90	11.16
BLDD-42	35	0.551	0.004243	0.01189	2.16

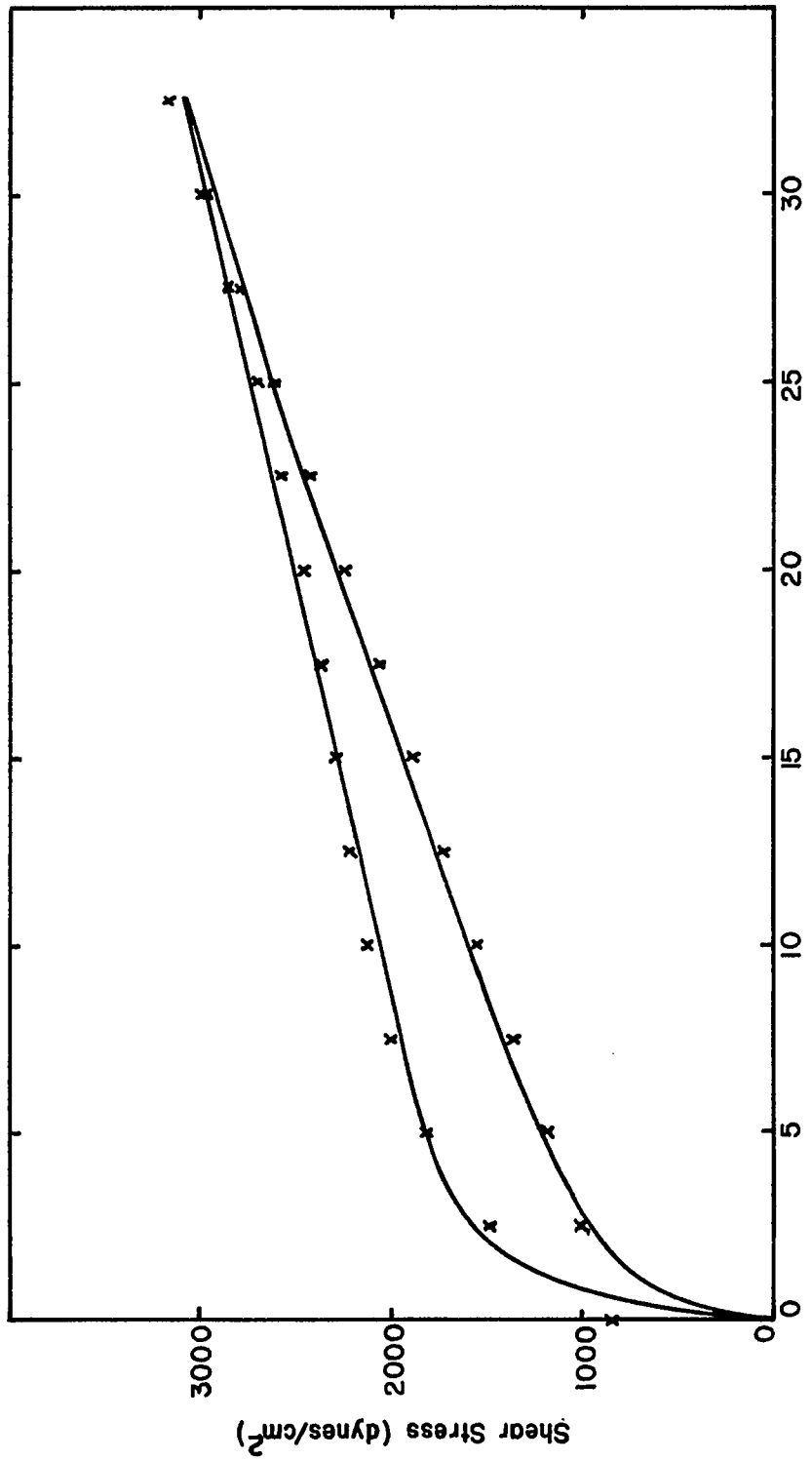

Figure 5-3. Correlation of Run SG0541-26

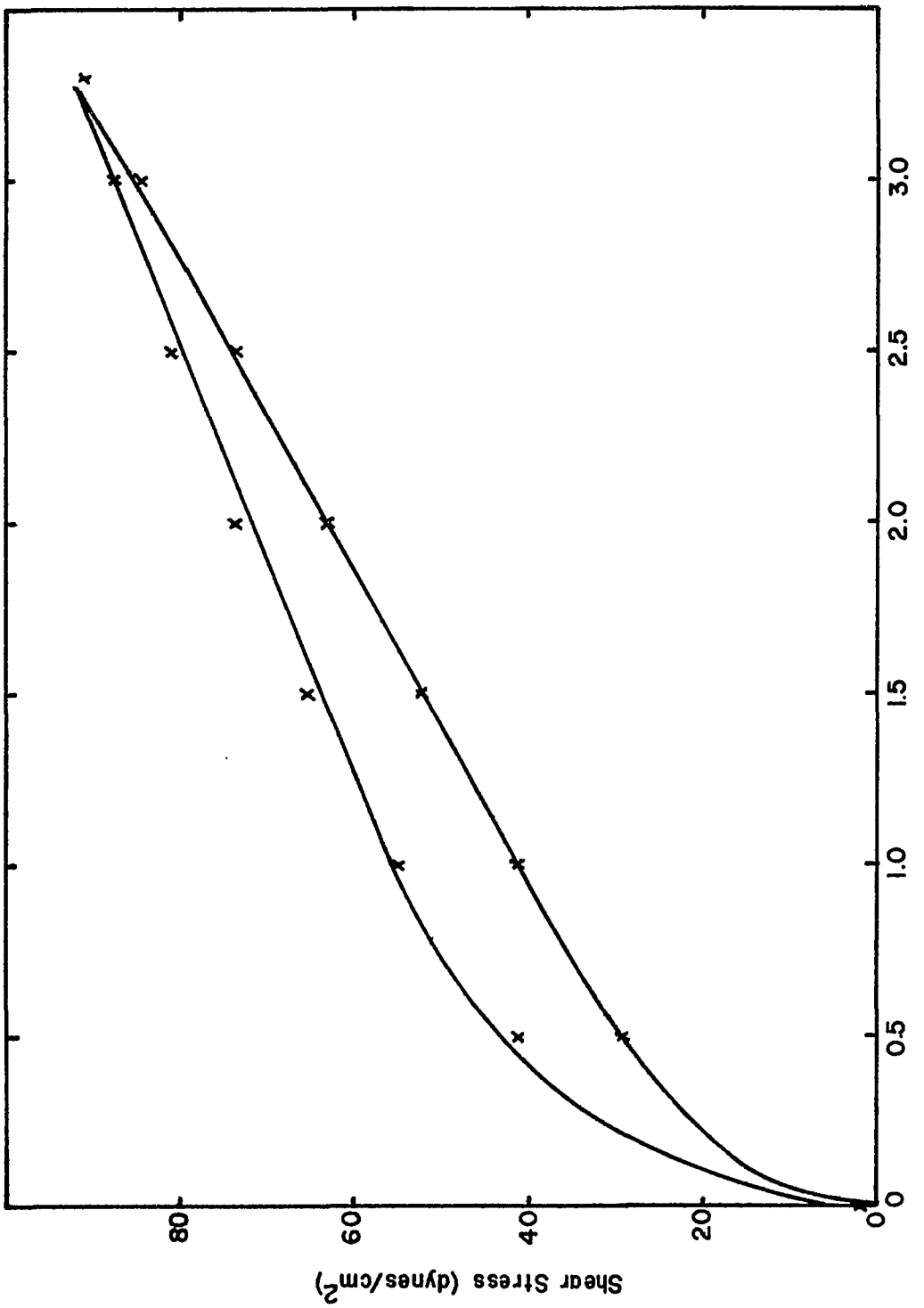

Figure 5-4. Correlation of Run 25DCGGEO-23

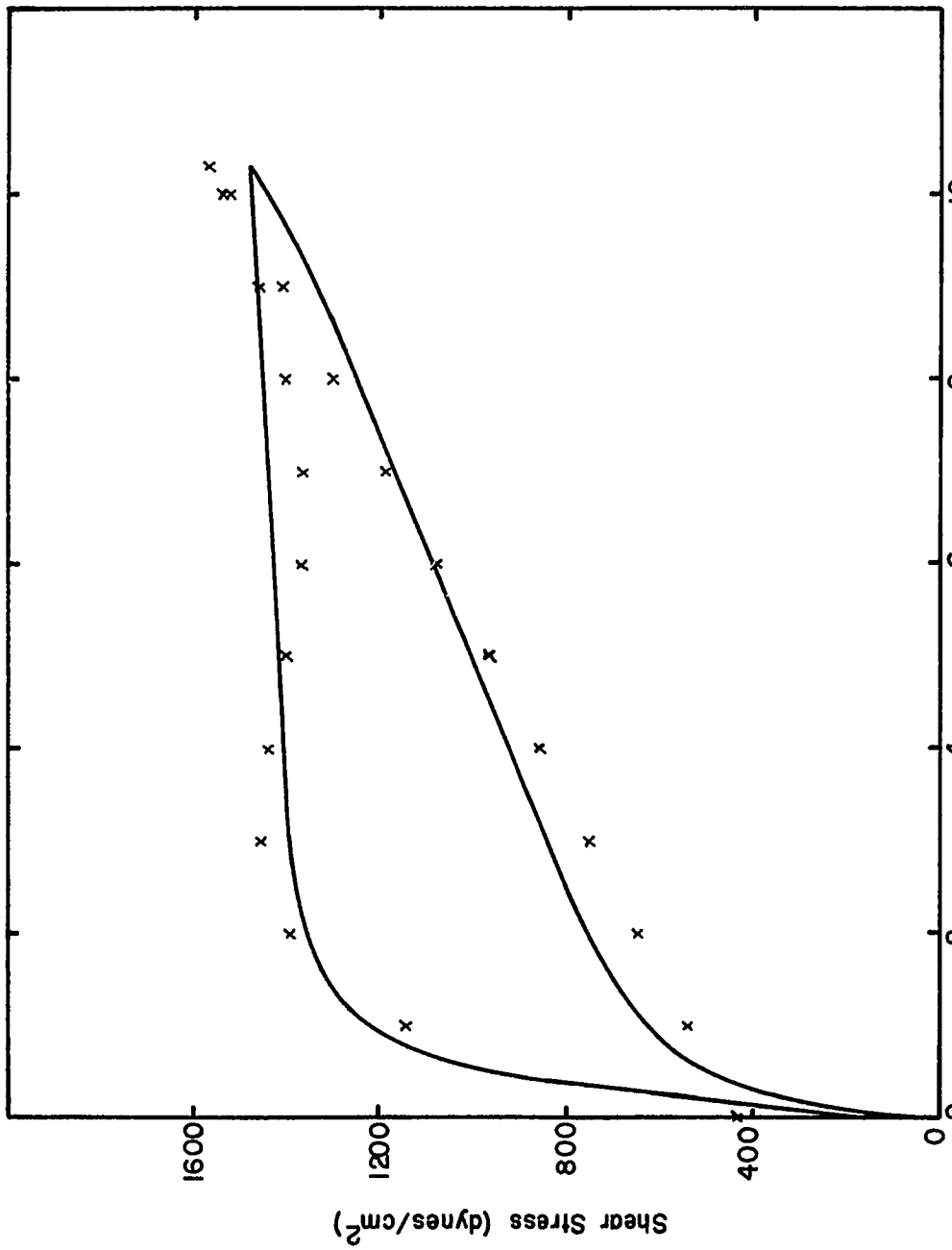

Figure 5-5. Correlation of Run 50DCGGEO-23 (1 loop)

Results for the montmorillonite clay, runs GKCBP72-13, 18, and 21, are shown in figures 5-6 through 5-8. As mentioned in Chapter 4, these runs were made using a fresh sample of the same material but shearing up to a different maximum shear rate. Run GKCBP72-21 (figure 5-8) represents about one-third of run GKCBP72-18 (figure 5-7) which in turn is about one-third of run GKCBP72-13 (figure 5-6). The parameters are reasonably consistent with 'n' and $C_1 \mathcal{S}\beta_e$ actually being constant. Multiplying C_1 by the maximum shear rate for each run gives 0.0139, 0.0129, and 0.01395 for runs GKCBP72-13, 18, and 21, respectively. The value for μ is nearly constant for the first two runs but low for GKCBP72-21. This could be anticipated since run GKCBP72 had the most curvature (figure 5-8) and would be expected to have the second term in the equation contribute a relative amount less than with runs GKCBP72-13 and 18. Finally, the time required to go from zero to the maximum shear rate on each curve is the same, since 'a' was constant in each of the runs. To go from zero to a shear rate of $6(sec^{-1})$ on each plot takes different periods of time, the quickest being run GKCBP72-13 and the longest being GKCBP72-21. Therefore, because of this shear history, sections of run GKCBP72-21 appears almost linear in figure 5-8 while at the same rate of shear, this section of run GKCBP72-13 is curved.

Figure 5-9 shows the results for run BLDD-42. As previously discussed, the shape of the curve obtained for this run, results in a good correlation between the experimental data (solid line)

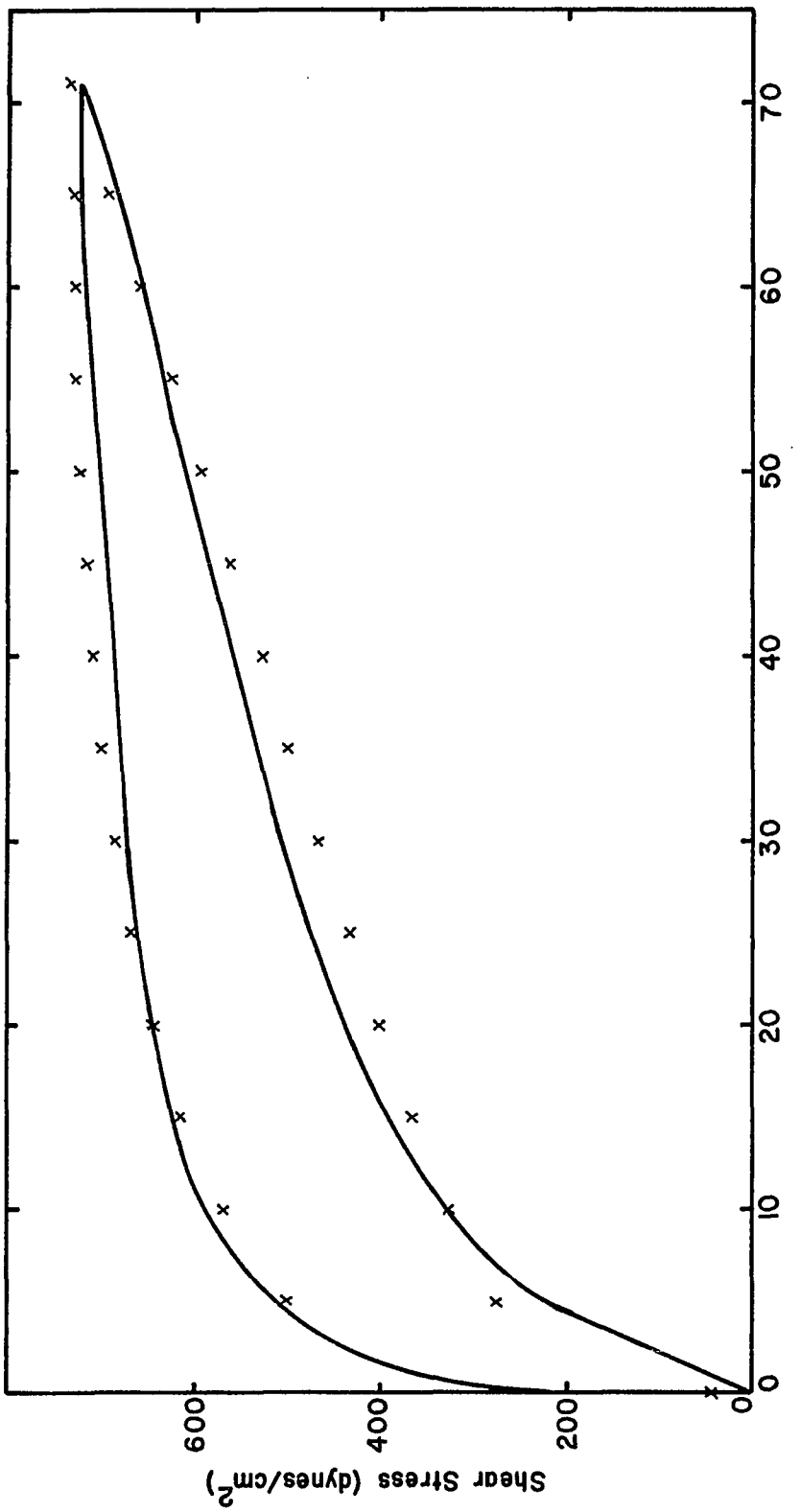

Figure 5-6. Correlation of Run GKCBP72-13

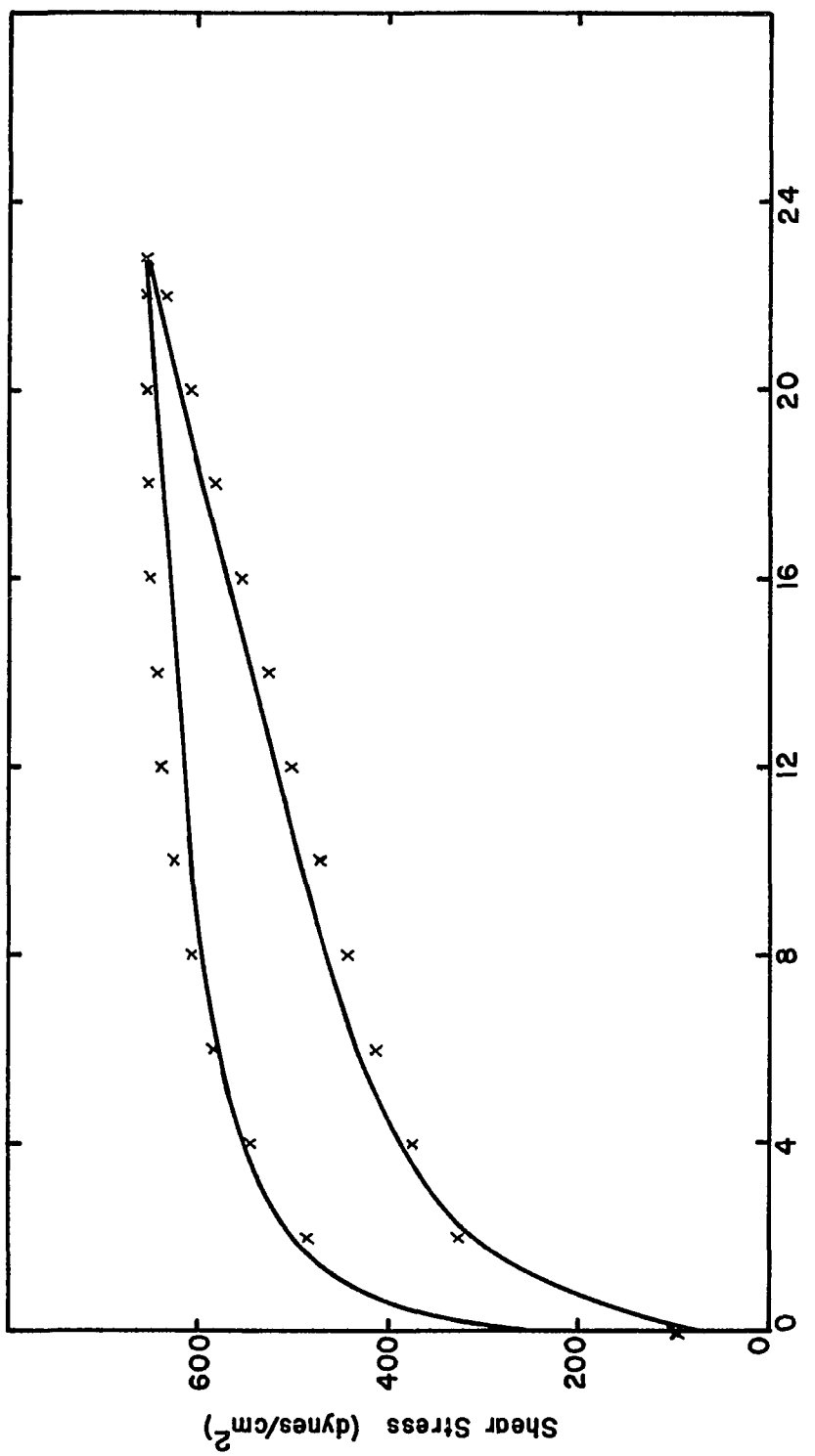

Figure 5-7. Correlation of Run GKCBP72-18

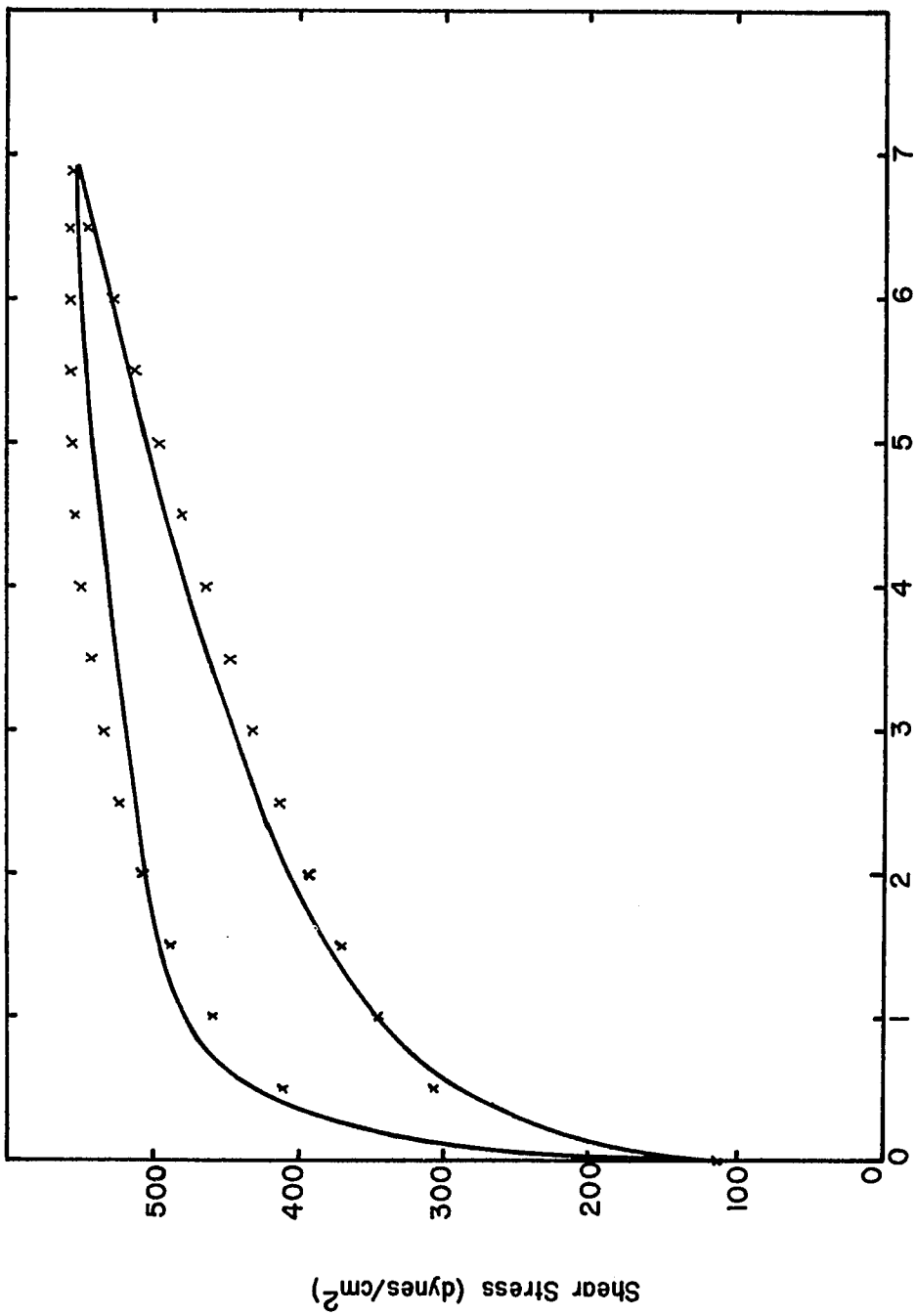

Figure 5-8. Correlation of Run GKCBP72-21

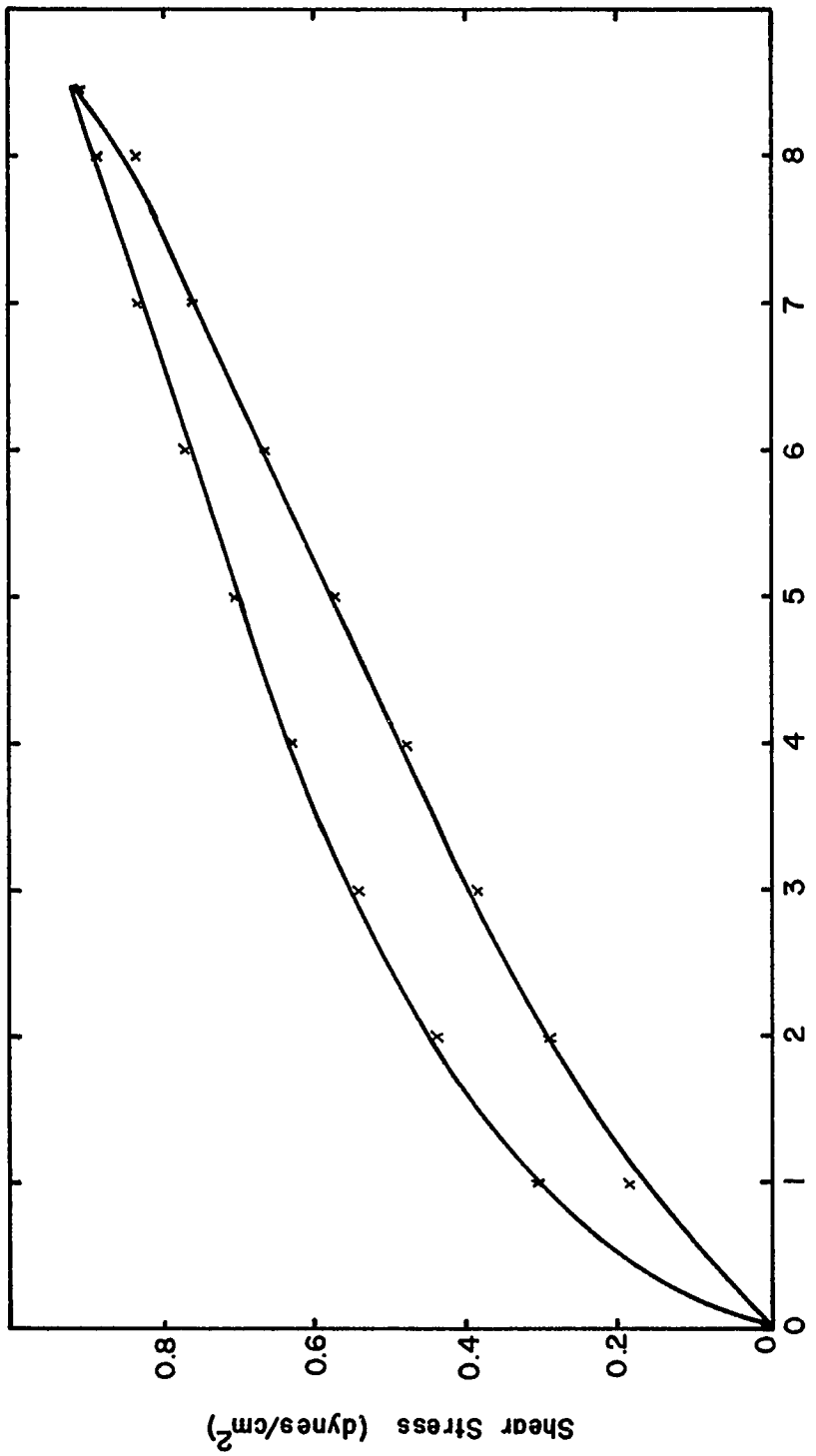

Figure 5-9. Correlation of Run BLDD-42

and data calculated from the thixotropic equations using the parameters in table 5-1. The parameters, μ and $C_1 \xi/\beta_e$, for this material were orders of magnitude less than corresponding parameters for the grease and clay samples. Blood is simply less viscous than the other materials studied.

The final two graphs, figures 5-10 and 5-11, contain multiple hysteresis loop data for run 50DCGGEO-23 (figure 4-22). Appendix C discusses how equation (2-68) can be manipulated to generate multiloop data. Though the system chosen for analysis was the one with the poorest results for one hysteresis loop, run 50DCGGEO-23 the equations were able to predict the general shape of the loops. The second and third loops do not show sharp curvature in the low shear rate region and have noticeably larger slopes at the higher shear rates than the first loop. Therefore, the effect of estimating the parameters based on all three loops, is to have a calculated first loop which has a slope that is greater than that of the experimental data for the first loop. Conversely, the first loop reduces the slope of the other calculated loops which can be seen in figure 5-11. In general, the calculated loops are smooth, curved, and increasing in slope in contradiction to the experimental data of run 50DCGGEO-23. It is quite possible, that the equation might do a much better job of characterizing multiple hysteresis loops, had a less viscous material been chosen.

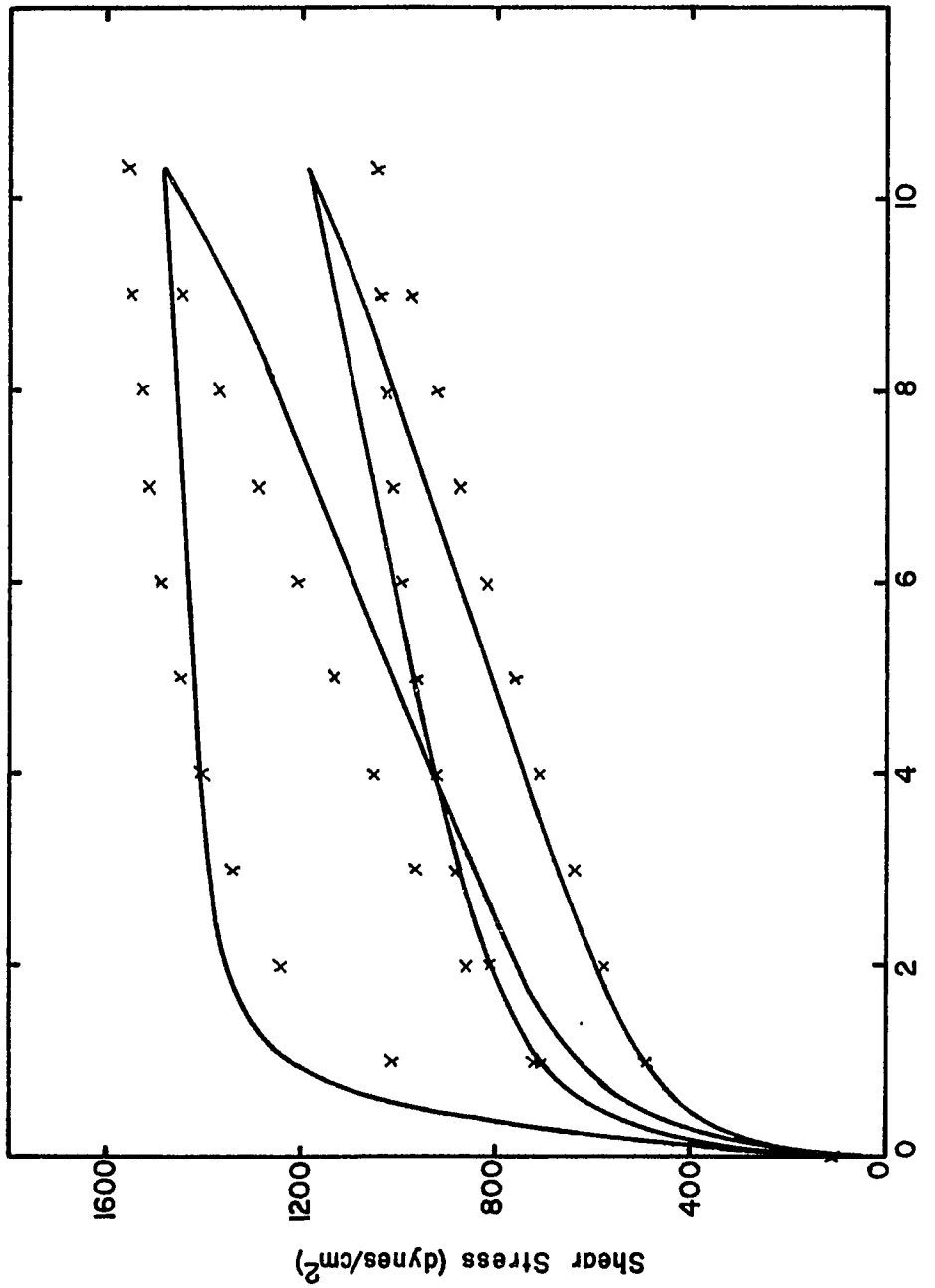

Figure 5-10. Multiloop Correlation of Run 50DCGGEO-23 (2 loops)

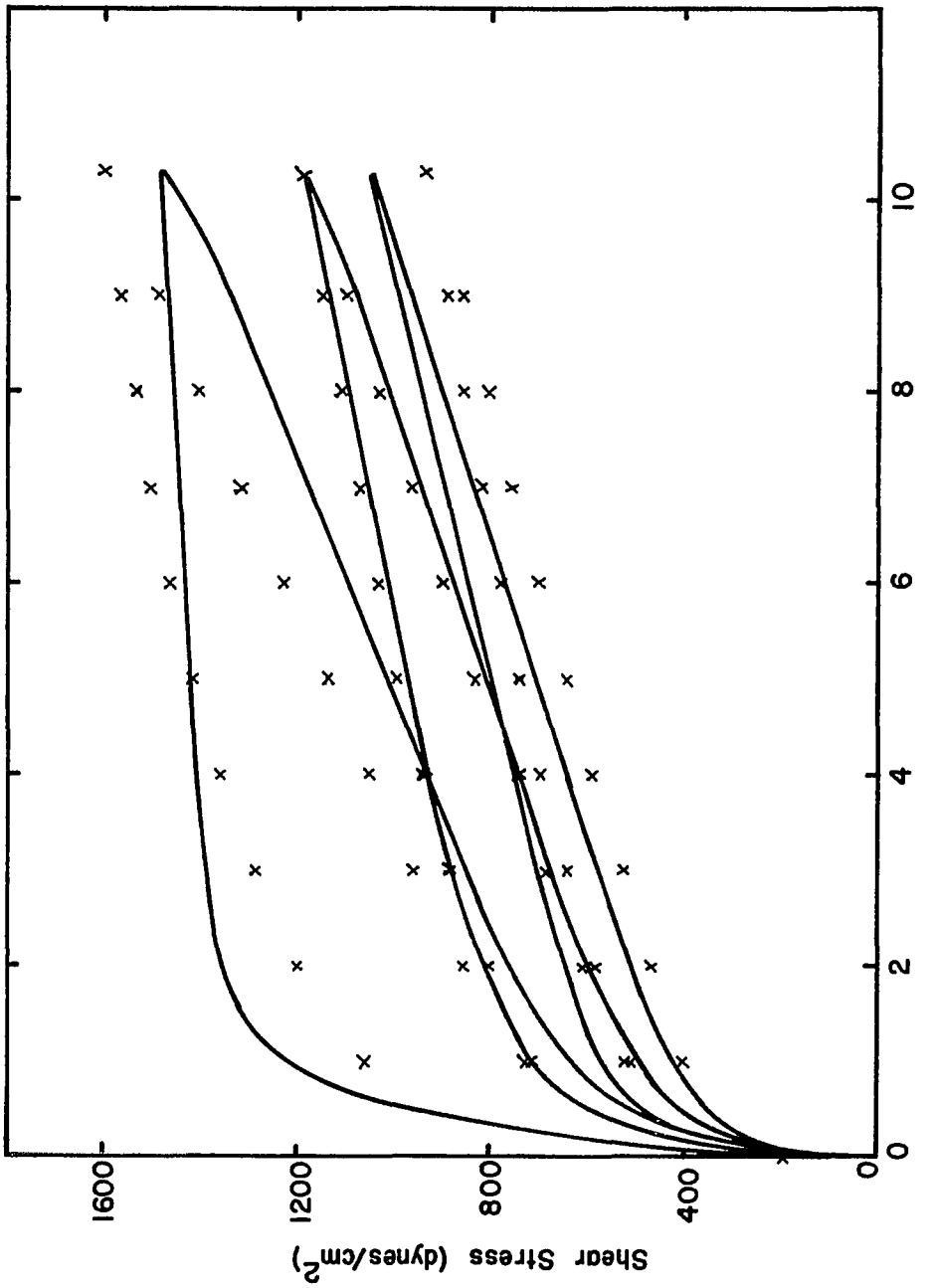

Figure 5-11. Multiloop Correlation of Run 50DCGGEO-23 (3 loops)

CONCLUSIONS

1. The Weissenberg Rheogoniometer was modified by adding a variable speed transmission to the drive train of the instrument. This modification enables the researcher to generate a complete rheological curve without stopping and starting the instrument to vary the shear rate. A number of Newtonian materials were run on the modified instrument to insure accuracy, convenience, and reproducibility. Samples of a known pseudoplastic material showed the instrument's capability of generating a time-independent curve without generating an inherent hysteresis loop.

2. Samples of a silicone grease-oil mixture, montmorillonite clay, and blood were tested by the instrument and shown to be thixotropic. The modified Rheogoniometer was able to generate all the characteristic thixotropic curves: single loop, multiple hysteresis loops, and hysteresis loop with constant shear rate zone.

3. The Huang rheological equation was tested and found able to accurately characterize most time-dependent, non-Newtonian materials, which were tested. Materials having large yield stresses and large decrease in slope of the upcurve with small increase in shear rate, followed by an essentially linear section with a small slope, did not exhibit good correlation of the thixotropic equation to the experimental data.

RECOMMENDATIONS

1. The instrument (modified Rheogoniometer) described in this paper should be automated. A means of preprogramming the instrument to draw the loop or loops of interest may be developed. This may be done mechanically or electrically.

2. The rheology of blood should be studied in greater detail. A correlation between the rheological properties of blood and an individual's health (heart disease, strokes, etc.) may exist.

3. Expansion of the thixotropic equation to include temperature and composition would provide additional information on time-dependent, non-Newtonian materials.

4. Because the equilibrium values of the molecular arrangement parameter, β_e, and the constant which relates the shear stress and the rate of molecular arrangement, ζ , cannot be explicitly determined from the present data, a study should be initialized to separate the lumped constant, $\zeta\beta_e$.

5. A study should be made to evaluate the ability of the thixotropic equation to characterize multiple hysteresis loops by studying additional materials which do not display some of the extreme slope changes displayed by some of the materials studied in this paper.

APPENDIX A

TABLE OF NOMENCLATURE

A = Area, constant in eq. 2-35,

a = Order of reaction, constant in eq. 2-12, material constant in eq. 2-33, proportionality constant between shear rate and time of shearing

B = Coefficient of thixotropic breakdown in eq. 2-8, parameter which is obtained from computer program

b = Constant in eq. 2-12, material constant in eq. 2-33

C = Rate constant

c = Material constant in eq. 2-14 and 2-33, constant in eq. 2-16

D = Derivative with respect to time

d = Diameter of cone and platen

F = Force, calculated value of shear stress in computer program

h = Height of bob

K = Proportionality constant for forward reaction in eq. 2-2

K' = Instrument constant, specific rate of flow with no stress,

k = Fluid consistency index in eq. 2-6

k' = Constant in eq. 2-3

k'' = Proportionality constant for backward reaction in eq. 2-1

k_b = Specific rate for the reverse reaction at zero stress

k_f = Specific rate for the forward reaction at zero stress

k_T = Torsion bar constant

M = Coefficient of thixotropic breakdown with shear rate, torque,

N = Number of data points analyzed by computer program

n = Flow behavior index, order of rate equation, RPM

q = Heat flux

R = Radius of cone and platen

R_b = Radius of bob

R_c = Radius of cylinder

r = Distance from axis

S = Specific entropy

S_e = Standard error of estimate

T = Absolute temperature, torque

t = Time

U = Specific internal energy

V = Velocity

v = Linear velocity, specific volume

X = Total volume of cells per unit volume

X_1 = Shear rate data in computer program

X_2 = Maximum shear rate in computer program

Xm = Maximum volume of cells per unit volume

Y = Distance, shear stress data in computer program

α = Coefficient in eq. 1-7, cone angle

β = Coefficient in eq. 1-7, relaxation time, molecular arrangement parameter, angular rotation of platen

β_e = Equilibrium value of molecular arrangement parameter

γ = Strain

$\gamma_{\alpha\beta}$ = Total strain tensor

$\dot{\gamma}$ = Shear rate or rate of shear

$\dot{\gamma}_o$ = Shear rate at time = 0

$\dot{\gamma}_m$ = Maximum shear rate at end of upcurve

Δ_T = Movement of torsion head transducer

$\delta_{\alpha\beta}$ = Kronecker's delta

ζ = Rate constant coefficient of shear stress with molecular arrangement parameter

η = Apparent viscosity

η_{a_o} = Yield value of apparent viscosity

η_{ae} = Apparent viscosity at equilibrium

η_o = Apparent viscosity at equilibrium, viscosity of completely broken down state, material constant in eq. 2-33

η_{pl} = Coefficient of rigidity, plastic viscosity

θ = Coefficient of thixotropy

K = Boltzmann's constant

λ = Linkage, fraction linkage of completely built upstate, structural parameter, thermal conductivity, linkage at time = 0

λ_i = Fraction of area occupied by i^{th} kind of flow units, parameters in Eyring's theory of flow

λ_o = Structural parameter at time = 0

μ = Proportionality constant, Newtonian viscosity, reaction constant

ξ = State variable representing structural breakdown

ρ = Experimental constant in eq. 2-17, density

σ = Rate of generation of entropy

τ = Shear stress

τ_b = Shear stress at bob

τ_c = Shear stress at cylinder

τ_e = Equilibrium shear stress at constant shear rate

τ_o = Yield stress

τ_1 = Shear stress due to Newtonian portion of curve

τ_2 = Shear stress due to non-Newtonian portion of curve

$\tau_{\alpha\beta}^{def}$ = Stress tensor for deformation

$\tau_{\alpha\beta}^{des}$ = Stress tensor for destruction of internal structure

$\tau_{\alpha\beta}^{eq}$ = Equilibrium stress tensor

$\tau_{\alpha\beta}^{v}$ = Viscous stress tensor

ϕ = Angle in plane of rotation, sum of squares of differences in computer program convergence routine

ω = Angular velocity

Λ = Dimensionless ratio in equation 5-5

APPENDIX B

CONVERSION OF DATA

Though the recorder X Y output is the actual rheological curve for a material, a number of instrument and recorder settings and constants influence the numbers which appear on the curves. The equation which change a recorder scale division reading into actual shear rate data is from Chapter 3:

$$(-\dot{\gamma}) = \frac{2.58.15\ (\text{XRANGE})\ (\text{XDIV})}{(\alpha)\ (\text{GBR})} \qquad \text{(B-1)}$$

where α is the angle of the cone in degrees, GBR is the gear reduction before the instrument, XRANGE is the recorder X-scale setting in volts/division, and XDIV is the reading on the curve that is to be converted to shear rate. Similarly, the equation for shear stress from Chapter 3 is:

$$\tau = \frac{12\ (k_T)\ (\text{MS})\ (\text{YDIV})}{\pi\,(d)^3\ (\text{FSD})} \qquad \text{(B-2)}$$

where d is diameter of cone in cm., FSD is the reading on the recorder in inches which is equivalent to the full scale deflection of the meter, k_T is the torsion bar constant, MS is the meter setting in microns, and YDIV is the reading on the curve that is to be converted to shear rate. For Newtonian materials only one point is required to be calculated to fully describe the material. However, for non-Newtonian materials, it would be rather tedious to calculate the necessary number of points. A data conversion program follows.

```
C  PROGRAM DTCNV
       READ(2,9) A,B,C,D,E,F
9      FORMAT(6A4)
       WRITE(6,10)A,B,C,D,E,F
10     FORMAT(5X,6A4)
       READ(2,11)AA
11     FORMAT(F10.0)
       READ(2,1)XKT,XMS,DIAM,FSD,XRNGE,ALPHA,GBR
1      FORMAT(F10.0,F6.0,F4.0,F6.0,F4.0,2F10.0)
       WRITE(6,12)AA
12     FORMAT(5X,3HAA=,F10.6)
       WRITE(6,3)XKT,XMS,DIAM,FSD,XRNGE,ALPHA,GBR
3      FORMAT(5X,4HXKT=,F10.3,2X,4HXMS=,F6.1,2X,5HDIAM=,F4.1,2X,4HFSD=,
      1F6.3,2X,6HXRNGE=,F4.2,2X,6HALPHA=,F10.6,2X,4HGBR=,F10.6/)
       WRITE(6,5)
5      FORMAT(4X,1HI,12X,5HDIVTA,14X,5HDIVGM,14X,5HGAMDT,15X,3HTAU,16X,
      24HTIME,15X,4HHIST/)
       TMP=0.0
       TEMP=0.0
       HIST=0.0
       GMDT=0.0
       GMDT=0.0
       DO 100 I=1,100
       READ(2,7)DIVGM,DIVTA
7      FORMAT(2F10.0)
       IF(DIVGM) 101,102,102
102    TAU=((3.819719*XKT*XMS)/((DIAM**3)*FSD))*DIVTA
       GAMDT=(258.15*XRNGE*DIVGM)/(ALPHA*GBR)
       TIME=GAMDT/AA
       TEMP=TIME-TMP
       HIST=HIST+ABS(TEMP)
       TMP=TIME
       WRITE(6,8)I,DIVTA,DIVGM,GAMDT,TAU,TIME,HIST
8      FORMAT(2X,I3,5X,F14.6,5X,F14.6,5X,F14.6,5X,F14.6,5X,F14.6,5X,
      3F14.6)
       IF(GAMDT-GMDT) 110,111,111
111    WRITE(5,22)TAU,GAMDT
22     FORMAT(2F10.5)
       GMDT=GAMDT
       GO TO 100
110    WRITE(5,22) TAU,GAMDT
100    CONTINUE
101    CONTINUE
       CALL EXIT
       END
```

APPENDIX C

MANIPULATION OF THIXOTROPIC EQUATION

Equation (2-68) is the generalized equation for time-dependent, non-Newtonian (thixotropic) materials:

$$\tau = \tau_o - \mu\dot{\gamma} + C_1 \xi/\beta_e |\dot{\gamma}|^n e^{-c \int_o^t |\dot{\gamma}|^n dt} \qquad (3\text{-}19)$$

For the analysis of the experimental data, the numerical value of the shear rate, $\dot{\gamma}$, will be assumed a positive number, though it is actually negative based on equation (2-55). Equation (2-68) can now be rewritten as follows:

$$\tau = \tau_o + \mu\dot{\gamma} + C_1 \xi/\beta_e \dot{\gamma}^n e^{-C_1 \int_o^t \dot{\gamma}^n dt} \qquad (C\text{-}1)$$

Where $(-\mu\dot{\gamma})$ is now rewritten as $(+\mu\dot{\gamma})$ since the numerical value of shear rate is assumed positive. Combining the constants in the third term of equation (C-1)

$$C_2 = C_1 \xi/\beta_e \qquad (C\text{-}2)$$

and substituting back into equation (C-1) gives

$$\tau = \tau_o + \mu\dot{\gamma} + C_2 \dot{\gamma}^n e^{-C_1 \int_o^t \dot{\gamma}^n dt} \qquad (C\text{-}3)$$

The exponential part of the third term can be integrated for multiloop, hysteresis curves.

The shear rate varies linearly with time (constant acceleration) and can be written:

$$\dot{\gamma} = at \tag{C-4}$$

where a is the proportionality constant between shear rate and time of shear. Actually, a will be a negative number in equation (C-4), since shear rate is negative. The sign of a will not be carried through the derivation, but simply recalled at the end. For the first hysteresis loop, $o \leq t \leq 2t_1$, where t_1, is the time of shearing to reach the maximum shear rate. Therefore, the shear rate for the upcurve is:

$$\dot{\gamma} = at \qquad o \leq t \leq t_1 \tag{C-5}$$

which can be substituted into the integral of equation (C-3) and integrated as follows:

$$C_1 \int_o^t \dot{\gamma}^n dt = \frac{C_1}{a} \int_o^{\dot{\gamma}} \dot{\gamma}^n d\dot{\gamma} = \frac{C_1}{a(n+1)} \dot{\gamma}^{n+1} \tag{C-6}$$

Substituting equation (C-6) into equation (C-3), gives:

$$\tau = \tau_o + \mu\dot{\gamma} + C_2 \dot{\gamma}^n e^{-\frac{C_1 \dot{\gamma}^{n+1}}{a(n+1)}} \tag{C-7}$$

The shear rate for the downcurve is:

$$\dot{\gamma} = 2at_1 - at \qquad t_1 \leq t \leq 2t_1 \qquad \text{(C-8)}$$

which can be substituted into equation (C-3) and integrated

$$C_1 \int_o^t \dot{\gamma}^n dt = C_1 \int_o^t \dot{\gamma}^n dt + C_1 \int_t^{2t_1} \dot{\gamma}\, dt$$

$$= \frac{C_1}{a} \int_o^{\dot{\gamma}(t_1)} \dot{\gamma}^n dt + \frac{C_1}{a} \int_{\dot{\gamma}(t_1)}^{\dot{\gamma}(t)=\dot{\gamma}} \dot{\gamma}^n (-d\dot{\gamma})$$

$$= \frac{C_1}{a(n+1)} \left(\dot{\gamma}(t_1)^{n+1}\right) - \frac{C_1}{a(n+1)} \left\{\dot{\gamma}^{n+1} - \dot{\gamma}(t_1)^{n+1}\right\}$$

$$= \frac{C_1}{a(n+1)} \left\{2\,\dot{\gamma}(t_1)^{n+1} - \dot{\gamma}^{n+1}\right\} \qquad \text{(C=9)}$$

In equation (C-9), $\dot{\gamma}(t_1)$ is the maximum shear rate for the particular hysteresis loop. Substituting equation (C-9) into equation (C-3) gives the shear stress-shear rate expression for the downcurve of the first hysteresis loop.

$$\tau = \tau_o + \mu\dot{\gamma} + C_2 \dot{\gamma}^n e^{-\frac{C_1}{a(n+1)} \left\{2\,\dot{\gamma}(t_1)^{n+1} - \dot{\gamma}^{n+1}\right\}} \qquad \text{(C-10)}$$

Similarly, the expressions for the second loop can be obtained for the upcurve:

$$\dot{\gamma} = at \qquad 2t_1 \leq t \leq 3t_1 \tag{C-11}$$

and

$$\tau = \tau_o + \mu\dot{\gamma} + C_2\dot{\gamma}^{n_e} - \frac{C_1}{a(n+1)}\left\{2\dot{\gamma}(t_1)^{n+1} + \dot{\gamma}^{n+1}\right\} \tag{C-12}$$

and downcurve:

$$\dot{\gamma} = 4at_1 - at \qquad 3t_1 \leq t \leq 4t_1 \tag{C-13}$$

and

$$\tau = \tau_o + \mu\dot{\gamma} + C_2\dot{\gamma}^{n_e} \frac{C_1}{a(n+1)}\left\{4\dot{\gamma}(t_1)^{n+1} - \dot{\gamma}^{n+1}\right\} \tag{C-14}$$

In general, with k = loop number the equations are

Upcurve:

$$\tau = \tau_o + \mu\dot{\gamma} + C_2\dot{\gamma}^{n_e} - \frac{C_1}{a(n+1)}\left\{(2k-2)\dot{\gamma}(t_1)^{n+1} + \dot{\gamma}^{n+1}\right\} \tag{C-15}$$

Downcurve:

$$\tau = \tau_o + \mu\dot{\gamma} + C_2\dot{\gamma}^{n_e} - \frac{C_1}{a(n+1)}\left\{(2K)\dot{\gamma}(t_1)^{n+1} - \dot{\gamma}^{n+1}\right\} \tag{C-16}$$

For the single loop, thixotropic data, equation (C-7) and (C-10) can be rewritten into a form used by the computer program in analysis of the experimental data. The equation will be inserted

into the computer and experimental data submitted for evaluation. A 'best fit' solution for determining the equation's constants will then be evaluated by the computer. For the upcurve:

$$Y = B_1 + B_2X_1 + B_3X_1^{B_5} e^{-\frac{B_4}{B_5+1}\left\{X_1^{B_5+1}\right\}} \qquad \text{(C-17)}$$

and for the downcurve:

$$Y = B_1 + B_2X_1 + B_3X_1^{B_5} e^{-\frac{B_4}{B_5+1}\left\{2X_2^{B_5+1} - X_1^{B_5+1}\right\}} \qquad \text{(C-18)}$$

where:

$Y = \tau$ $\qquad$ $B_2 = \mu$

$X_1 = \dot{\gamma}$ $\qquad$ $B_3 = C_2 = C_1 \xi/\beta e$

$X_2 = \dot{\gamma}(t_1)$ $\qquad$ $B_4 = C_1/a$

$B_1 = \tau_o$ $\qquad$ $B_5 = n$

A non-linear, least squares, curve fitting, computer program can now be used to determine the constants in equations (C-17) and (C-18) for various thixotropic materials. The original work was done by D. W. Marquardt (28) and adapted by the present author to the particular computer and type of equation under investigation. Initial gueses for the parameters B_1, B_2, B_3, B_4, and B_5 are entered with the experimental shear stress, Y_i, and shear rate, X_i, data. The program will then adjust the values for B until the following relationship is minimized:

$$\phi = \sum_{i=1}^{N} (Y_i - F_i)^2 \qquad \text{(C-19)}$$

where Y_i is the experimental value of shear stress for a particular rate of shear, F_i is the calculated value of shear stress at the same rate of shear for the present value of the parameters-B, and N is the number of data points being analyzed.

The computer program also calculates the standard error of estimate of F_i:

$$S_e = \left[\frac{\phi}{N-k}\right]^{\frac{1}{2}} \qquad \text{(C-20)}$$

where k is the number of parameters in the non-linear equation.

A working copy of the computer program adapted for TSO (Time-Sharing Option) usage with an IBM 360 computer is included in Appendix D. The values of F_i are calculated in subroutine FCODE of the program. The particular set of equations given in FCODE in Appendix D are for estimating the parameters associated with 3 hysteresis loops, though this subroutine could just as easily be used to estimate the parameters of a single hysteresis loop by simply putting in the correct control data. The program in Appendix D can also be modified to estimate parameters of different non-linear equations by inserting the desired equation in subroutine FCODE and changing a few input data cards requested by the program.

APPENDIX D

NON-LINEAR LEAST SQUARES COMPUTER PROGRAM

```
C  PROGRAM NLIN
C  NONLINEAR LEAST SQUARES - REPROGRAMMED BY PAUL J. OROSZ
C  ORIGINAL VERSION BY D. W. MARQUARDT
      DATA IBCH/' '/,IOCH/'0'/,IPCH/'P'/,IYCH/'Y'/,IXCH/'X'/
      DIMENSION BS(5),DB(5),BA(5),G(5),IB(4),SA(5),P(5),A(10,6),B(5)
      DIMENSION X(100,2),Y(100),CONS(5),PRNT(5)
C  .....
C  MAXIMUM NUMBER OF PARAMETERS IS K=5
C  MAXIMUM NUMBER OF INDEPENDENT VARIABLES IS M=2
C  MAXIMUM NUMBER OF OBSERVATIONS IS N=100
C  NUMBER OF OMITTED PARAMETERS IS GIVEN BY IP
C  SET IFP = 1 FOR PLOT OF Y AND F, IFP = 0 FOR NO PLOT
C  SETTINGS OF SENSE SWITCHES: IWS2,IWS3,AND IWS4; OTHERS SET TO 0
C  SWITCH     OFF(EQUAL TO 0)       ON(EQUAL TO A #)
C    2      ANALYTIC DERIVATIVES  ESTIMATED DERIVATIVES
C    3      ABBREVIATED PRINTOUT  DETAILED PRINTOUT = #
C    4      NO FORCE OFF          FORCE OFF AFTER # ITERATIONS
C  CALL SUBZ
C     CODING FOR CASE INITIALIZATION GOES HERE
C  CALL FCODE
C     THE EQUATION TO BE TESTED IS WRITTEN HERE AND SET EQUAL TO F(YHAT)
C     NPRNT IS THE NUMBER OF OTHER WORDS TO BE PRINTED
C     THE WORDS TO BE PRINTED ARE IN PRNT(1).....PRNT(5)
C  CALL PCODE
C     THIS SUBROUTINE IS FOR USE WITH ANALYTICAL PARTIAL DERIVATIVES
C     CODING TO MAKE DF/DB GOES HERE.  MAKE K OF THEM.  CALL THEM P(J).
C     THEY ARE MADE FROM X(I,L) AND B(J).
C  .....
C  INSERT THE NAME OF DATASET TO BE USED
      READ(5,961) Z1,Z2,Z3,Z4,Z5,Z6
961   FORMAT(6A4)
C  .....
      NPRNT=0
10    ITCT=0
      IBOUT=0
C  INSERT VARIOUS CONTROLS FOR LOOPS AND UPCURVES AND DOWNCURVES
      READ(5,950) IXP,IXP2,IXP3,IXP4,IXP5
      READ(5,900) N,K,IP,M,IFP,NCONS
      NTLDA=N+NCONS
      XNT=NTLDA
      IF(N) 660,660,7000
7000  READ(5,900) IWS1,IWS2,IWS3,IWS4,IWS5,IWS6
      WRITE(6,932)
      WRITE(6,962) Z1,Z2,Z3,Z4,Z5,Z6
962   FORMAT(/54X,6A4)
      IF(IFP) 22,22,7001
7001  READ(5,930) YMN,SPRD
22    IF(IP) 30,30,7002
7002  READ(5,900) (IB(I),I=1,IP)
      DO 26 I=1,IP
```

```
      IF(IB(I)) 7003,7003,26
7003  WRITE(6,926)
      IBOUT=1
26    CONTINUE
30    CONTINUE
C  DUB IN INPUT CONSTANTS IF NOT SUPPLIED
C  (XL IS CHECKED IN FIRST ITERATION)
      READ(5,931) FF,T,E,TAU,XL,GAMCR,DEL,ZETA
      IF(FF) 7004,7004,34
7004  FF=4.0
34    IF(E) 7005,7005,37
7005  E=0.00005
37    IF(TAU) 7006,7006,39
7006  TAU=0.001
39    IF(T) 7007,7007,50
7007  T=2.0
50    IF(GAMCR) 7008,7008,52
7008  GAMCR=45.0
52    IF(DEL) 7009,7009,55
7009  DEL=0.00001
55    IF(ZETA) 7010,7010,53
7010  ZETA=0.1E-30
53    CONTINUE
      XKDB=1.0
C  READ IN INITIAL B GUESSES
      READ(5,901) (B(I),I=1,K)
      READ(5,970) XI2
970   FORMAT(F10.0)
      DO 8000 I=1,IXP
8000  X(I,2)=0.0
      IXPP=IXP+1
      DO 7999 I=IXP,N
7999  X(I,2)=XI2
      DO 56 I=1,N
56    READ(5,931) Y(I),(X(I,L),L=1,M)
      CALL SUBZ(Y,X,B,PRNT,NPRNT,N)
      IF(IBOUT) 10,7011,10
7011  IBKA=1
C  START THE CALCULATION OF THE PTP MATRIX
      IF(IFP) 61,61,8031
8031  WRITE(6,907) N,K,IP,M,IFP,GAMCR,DEL,FF,T,E,TAU,XL,ZETA
      GO TO 61
60    IWS3=IWS3-1
      IDUM=IWS3
      IF(IDUM) 7012,7012,7013
7012  IWS3=0
      GO TO 61
7013  IWS3=IDUM
61    DO 62 I=1,K
      G(I)=0.0
      DO 62 J=1,K
62    A(I,J)=0.0
      WRITE(6,908) ITCT,(B(J),J=1,K)
      IF(IWS3) 7014,73,7014
7014  IF(IFP) 68,68,7015
7015  WS=YMN+SPRD
      WRITE(6,906) YMN,WS
      GO TO 73
68    WRITE(6,910)
73    I=1
```

```
      PHI=0.0
      PHIN=0.0
      ICONS=1
C  GET P. S. AND F
72    IF(IWS2-1) 7016,602,7016
C  THIS IS THE ANALYTICAL P. S. ROUTINE
7016  CALL FCODE(Y,X,B,PRNT,F,I,RES,IXP,IXP2,IXP3,IXP4,IXP5)
      CALL PCODE(P,X,B,PRNT,F,I,IXP)
      IF(IP) 80,80,7017
7017  DO 77 II=1,IP
      KWS=IB(II)
77    P(KWS)=0.0
      GO TO 80
C  END OF THE ANALYTICAL P. S. ROUTINE
C  THIS IS THE ESTIMATED P. S. ROUTINE
602   CALL FCODE(Y,X,B,PRNT,F,I,RES,IXP,IXP2,IXP3,IXP4,IXP5)
      RWS=RES
      FSAVE=F
      J=1
608   IF(IP) 618,618,7018
7018  DO 612 II=1,IP
      IF(J-IB(II)) 612,621,612
612   CONTINUE
618   DBW=B(J)*DEL
      TWS=B(J)
      B(J)=B(J)+DBW
      CALL FCODE(Y,X,B,PRNT,F,I,RES,IXP,IXP2,IXP3,IXP4,IXP5)
      B(J)=TWS
      P(J)=-(RES-RWS)/DBW
      GO TO 622
621   P(J)=0.0
622   J=J+1
      IF(J-K) 608,608,7019
7019  RES=RWS
      F=FSAVE
C  END OF THE ESTIMATED P. S. ROUTINE
C  NOW USE THE P. S. TO MAKE PARTIALS MATRIX
80    DO 82 JJ=1,K
      G(JJ)=G(JJ)+RES*P(JJ)
      DO 82 II=JJ,K
      A(II,JJ)=A(II,JJ)+P(II)*P(JJ)
82    A(JJ,II)=A(II,JJ)
      IF(IFP) 318,318,7020
7020  IF(IWS3) 7021,314,7021
7021  IF(I-N) 7022,7022,314
C  PLOTTING Y(I),F
7022  IO=(Y(I)-YMN)*100.0/SPRD
      IPP=(F-YMN)*100.0/SPRD
      IF(IO-IPP) 7023,808,812
C  Y(I) OUT FIRST
7023  IP1=IOCH
      IP2=IPCH
      I1=IO
      I2=IPP
      GO TO 816
C  ONLY ONE CHARACTER
808   IP1=IYCH
      IP2=IBCH
      I1=IO
      I2=IPP
```

```
      GO TO 816
C  F OUT FIRST
812   IP1=IPCH
      IP2=IOCH
      I1=IPP
      I2=IO
C  ZERO PLOTS IN THE LEFT HAND COLUMN, SO I1 IS ITS OWN BLANK COUNTER,
C  OVERFLOWS PLOT X IN COLUMN 102, UNDERFLOWS ALSO PLOT X IN COLUMN ZERO
816   IF(I2-101) 819,819,7123
7123  I2=101
      IP2=IXCH
      IF(I1-101) 819,7024,7024
7024  I1=101
      IP1=IXCH
      IP2=IBCH
      GO TO 825
819   IF(I1) 7025,825,825
7025  I1=0
      IP1=IXCH
      IF(I2) 7026,7026,825
7026  I2=1
      IP2=IBCH
825   I1M1=I1
      I1M2=I2-I1-1
      IF(I1M1) 7027,7027,832
7027  IF(I1M2) 7028,7028,828
7028  WRITE(6,928) IP1,IP2
      GO TO 314
828   WRITE(6,928) IP1,(IBCH,II=1,I1M2),IP2
      GO TO 314
832   IF(I1M2) 7029,7029,840
7029  WRITE(6,928) (IBCH,II=1,I1M1),IP1,IP2
      GO TO 314
840   WRITE(6,928)(IBCH,II=1,I1M1),IP1,(IBCH,II=1,I1M2),IP2
      GO TO 314
318   WS=RES
      IF(IWS3) 7030,314,7030
7030  IF(I-N) 7031,7031,314
7031  IF(NPRNT) 7032,7032,312
7032  WRITE(6,925) Y(I),F,WS
      GO TO 314
312   WRITE(6,925)Y(I),F,WS,(PRNT(JJ),JJ=1,NPRNT)
314   WS=RES
      PHI=PHI+WS*WS
      IF(I-N) 7033,7033,313
7033  PHIN=PHIN+WS*WS
      GO TO 315
313   CONS(ICONS)=RES
      ICONS=ICONS+1
315   I=I+1
      IF(I-NTLDA) 72,72,7034
7034  IF(IP) 88,88,7035
7035  DO 87 JJ=1,IP
      KWS=IB(JJ)
      DO 86 II=1,K
      A(KWS,II)=0.0
86    A(II,KWS)=0.0
87    A(KWS,KWS)=1.0
88    GO TO (90,704,703),IBKA
C  SAVE THE SQUARE ROOTS OF THE DIAGONAL ELEMENTS
```

```
90      DO 92 I=1,K
92      SA(I)=SQRT(A(I,I))
        DO 106 I=1,K
        DO 100 J=1,K
        WS=SA(I)*SA(J)
        IF(WS) 7036,7036,98
7036    A(I,J)=0.0
        GO TO 100
98      A(I,J)=A(I,J)/WS
100     CONTINUE
        IF(SA(I)) 7037,7037,104
7037    G(I)=0.0
        GO TO 106
104     G(I)=G(I)/SA(I)
106     CONTINUE
        DO 110 I=1,K
110     A(I,I)=1.0
        PHIZ=PHI
C   NOW WE HAVE PHI ZERO
        DO 1133 II=1,K
        III=II+5
        DO 1133 JJ=1,K
1133    A(III,JJ)=A(II,JJ)
        IF (ITCT) 163,7038,163
C   FIRST ITERATION
7038    IF(XL) 7039,7039,154
7039    XL=0.01
154     DO 161 J=1,K
161     BS(J)=B(J)
C   BS(J) CORRESPONDS TO PHIZ
163     IBK1=1
        WS=N-K+IP
        ITCT=ITCT+1
        SE=SQRT(PHIN/WS)
        IF(IWS3) 7040,7040,165
7040    IF(IWS2) 7041,168,7041
7041    WRITE(6,911) PHIZ, SE,XLL,GAMMA,XL
        GO TO 200
168     WRITE(6,912) PHIZ,SE,XLL,GAMMA,XL
        GO TO 200
165     IF(NCONS) 7042,166,7042
7042    WRITE(6,938) (JJ,CONS(JJ),JJ=1,NCONS)
166     WRITE(6,939)
        DO 114 I=1,K
        WRITE(6,937) I,(A(I,J),J=1,K)
114     CONTINUE
        IF(IWS2) 7043,1661,7043
7043    WRITE(6,903) PHIZ,SE,XL
        GO TO 200
1661    WRITE(6,909) PHIZ,SE,XL
        GO TO 200
164     PHIL=PHI
C   WE NOW HAVE PHI LAMDA
        DO 170 J=1,K
        IF(ABS(DB(J)/(ABS(B(J))+TAU))-E) 170,172,172
170     CONTINUE
        WRITE(6,923)
        GO TO 700
172     IF(IWS4) 7044,173,7044
7044    IF(IWS4-1) 7045,171,7045
```

```
7045  IWS4=IWS4-1
      GO TO 173
171   WRITE(6,924)
      GO TO 700
173   XKDB=1.0
      IF(PHIL-PHIZ) 7046,7046,190
7046  XLS=XL
      DO 176 J=1,K
      BA(J)=B(J)
176   B(J)=BS(J)
      IF(XL-0.00000001) 7047,7047,175
7047  DO 1176 J=1,K
      B(J)=BA(J)
1176  BS(J)=B(J)
      GO TO 60
175   XL=XL/10.0
      IBK1=2
      GO TO 200
177   PHL4=PHI
C  WE NOW HAVE PHI(LAMDA/10.0)
      IF(PHL4-PHIZ) 7048,7048,184
7048  DO 183 J=1,K
183   BS(J)=B(J)
      GO TO 60
184   XL=XLS
      DO 186 J=1,K
      BS(J)=BA(J)
186   B(J)=BA(J)
      GO TO 60
190   IBK1=4
      XLS=XL
      XL=XL/10.0
      DO 185 J=1,K
185   B(J)=BS(J)
      GO TO 200
187   IF(PHI-PHIZ) 196,196,7049
7049  XL=XLS
      IBK1=3
192   XL=XL*10.0
195   DO 193 J=1,K
193   B(J)=BS(J)
      GO TO 200
194   PHIT4=PHI
C  WE NOW HAVE PHI(10.0*LAMDA)
      IF(PHIT4-PHIZ) 196,196,198
196   DO 197 J=1,K
197   BS(J)=B(J)
      GO TO 60
198   IF(GAMMA-GAMCR) 7050,192,192
7050  XKDB=XKDB/2.0
      DO 1199 J=1,K
      IF(ABS(DB(J)/(ABS(B(J))+TAU))-E) 1199,195,195
1199  CONTINUE
      DO 1200 J=1,K
1200  B(J)=BS(J)
      WRITE(6,934)
      GO TO 700
C  SET UP FOR MATRIX INVERSION
200   CONTINUE
      DO 1103 II=1,K
```

```
      III=II+5
      DO 1103 JJ=1,K
1103  A(II,JJ)=A(III,JJ)
      DO 202 I=1,K
202   A(I,I)=A(I,I)+XL
C  GET INVERSE OF A AND SOLVE FOR DB(J)'S
      IBKM=1
C  THIS IS THE MATRIX INVERSION ROUTINE, K IS THE SIZE OF THE MATRIX
404   CALL GJR(A,K,ZETA,MSING)
      GO TO (415,10),MSING
415   GO TO (416,710),IBKM
C  END OF MATRIX INVERSION, SOLVE FOR DB(J)
416   CONTINUE
      DO 420 I=1,K
      DB(I)=0.0
      DO 421 J=1,K
421   DB(I)=A(I,J)*G(J)+DB(I)
420   DB(I)=XKDB*DB(I)
      XLL=0.0
      DTG=0.0
      GTG=0.0
      DO 250 J=1,K
      XLL=XLL+DB(J)*DB(J)
      DTG=DTG+DB(J)*G(J)
      GTG=GTG+G(J)*G(J)
      DB(J)=DB(J)/SA(J)
250   B(J)=B(J)+DB(J)
      KIP=K-IP
      IF(KIP-1) 7051,1257,7051
7051  CGAM=DTG/SQRT(XLL*GTG)
      JGAM=1
      IF(CGAM-0.0) 7052,7052,253
7052  CGAM=ABS(CGAM)
      JGAM=2
253   GAMMA=57.2958*(1.57073+CGAM*(-0.212114+CGAM*(0.074261-CGAM
     1*0.0187293)))*SQRT(1.0-CGAM)
      GO TO (257,255) ,JGAM
255   GAMMA=180.0-GAMMA
      IF(XL-1.0) 257,7053,7053
7053  WRITE(6,922) XL,GAMMA
      GO TO 700
1257  GAMMA=0.0
257   XLL=SQRT(XLL)
7100  IBK2=1
      GO TO 300
252   IF(IWS3) 7054,256,7054
7054  WRITE(6,904) (DB(J),J=1,K)
      WRITE(6,905) PHI,XL,GAMMA,XLL
256   GO TO (164,177,194,187),IBK1
C  CALCULATE PHI
300   I=1
      PHI=0.0
      PHIN=0.0
800   CALL FCODE(Y,X,B,PRNT,F,I,RES,IXP,IXP2,IXP3,IXP4,IXP5)
      PHI=PHI+(RES**2)
      IF(I-N) 7055,7055,305
7055  PHIN=PHIN+RES*RES
305   I=I+1
      IF(I-NTLDA) 800,800,7056
7056  GO TO (252,7067,704,7067,7067,7067),IBK2
```

```
C  THIS IS THE CONFIDENCE LIMIT CALCULATION
700    DO 702 J=1,K
702    B(J)=BS(J)
       IF(IFP) 8033,8033,8034
8034   WRITE(6,933) N,K,IP,M,FF,T,E,TAU
8033   IBKA=2
       NTLDA=N
C  THIS WILL PRINT THE Y, YHAT, DELTA Y
       ITCT=ITCT-1
       IWS3=1
       GO TO 61
704    IF(IFP) 703,703,7057
7057   IBKA=3
       IFP=0
       GO TO 61
703    IF(NCONS) 7058,706,7058
7058   WRITE(6,938) (JJ,CONS(JJ),JJ=1,NCONS)
706    WS=N-K+IP
       SE=SQRT(PHI/WS)
       PHIZ=PHI
       IF(IWS2) 7059,709,7059
7059   WRITE(6,903) PHIZ,SE,XL
       GO TO 708
709    WRITE(6,909) PHIZ,SE,XL
C  NOW WE HAVE MATRIX A
708    DO 1123 II=1,K
       III=II+5
       DO 1123 JJ=1,K
1123   A(III,JJ)=A(II,JJ)
       IBKM=2
       GO TO 404
C  WE NOW HAVE C=A INVERSE
710    DO 711 J=1,K
       IF(A(J,J)) 713,711,711
711    SA(J)=SQRT(A(J,J))
       GO TO 715
713    IBOUT=1
715    KST=-4
       WRITE(6,916)
234    KST=KST+5
       KEND=KST+4
       IF(KEND-K) 719,7060,7060
7060   KEND=K
719    DO 712 I=1,K
712    WRITE(6,918) I,(A(I,J),J=KST,KEND)
       IF(KEND-K) 234,7061,7061
7061   IF(IBOUT) 7062,717,7062
7062   WRITE(6,936)
       GO TO 10
717    DO 718 I=1,K
       DO 718 J=1,K
       WS=SA(I)*SA(J)
       IF(WS) 7063,7063,716
7063   A(I,J)=0.0
       GO TO 718
716    A(I,J)=A(I,J)/WS
718    CONTINUE
       DO 720 J=1,K
720    A(J,J)=1.0
       WRITE(6,917)
```

```
      KST=-9
721   KST=KST+10
      KEND=KST+9
      IF(KEND-K) 722,7064,7064
7064  KEND=K
722   DO 724 I=1,K
724   WRITE(6,935) I,(A(I,J),J=KST,KEND)
      IF(KEND-K) 721,7065,7065
C  GET T*SE*SQRT(C(I,I))
7065  DO 726 J=1,K
726   SA(J)=SE*SA(J)
      DO 1113 II=1,K
      III=II+5
      DO 1113 JJ=1,K
1113  A(II,JJ)=A(III,JJ)
      WRITE(6,919)
      WS=K-IP
      DO 750 J=1,K
      IF(IP) 743,743,7066
7066  DO 742 I=1,IP
      IF(J-IB(I)) 742,746,742
742   CONTINUE
743   CONTINUE
      HJTD=SQRT(WS*FF)*SA(J)
      STE=SA(J)
      OPL=BS(J)-SA(J)*T
      OPU=BS(J)+SA(J)*T
      SPL=BS(J)-HJTD
      SPU=BS(J)+HJTD
      WRITE(6,927) J,STE,OPL,OPU,SPL,SPU
      GO TO 7200
746   WRITE(6,913) J
C  NONLINEAR CONFIDENCE LIMIT
7200  IF(IWS6-1) 750,10,750
750   CONTINUE
7067  CONTINUE
      GO TO (7101,780,7101,762,766,772),IBK2
7101  WS=K-IP
      WS1=N-K+IP
      PKN=WS/WS1
      PC=PHIZ*(1.0+FF*PKN)
      WRITE(6,920) PC
      WRITE(6,921)
      IWS3=1
      DO 790 J=1,K
      IBKP=1
      DO 752 JJ=1,K
752   B(JJ)=BS(JJ)
      IF(IP) 758,758,7068
 7068  DO 756 JJ=1,IP
      IF(J-IB(JJ)) 756,787,756
756   CONTINUE
758   DD=-1.0
      IBKN=1
760   D=DD
      B(J)=BS(J)+D*SA(J)
      IBK2=4
      GO TO 300
762   PHI1=PHI
      IF(PHI1-PC) 764,770,770
```

```
764   D=D+DD
      IF(D/DD-5.0) 7069,788,788
7069  B(J)=BS(J)+D*SA(J)
      IBK2=5
      GO TO 300
766   PHID=PHI
      IF(PHID-PC) 764,7070,7070
7070  IF(PHID-PC) 770,778,778
770   D=D/2.0
      IF(D/DD-0.001) 788,788,7071
7071  B(J)=BS(J)+D*SA(J)
      IBK2=6
      GO TO 300
772   PHID=PHI
      IF(PHID-PC) 778,778,770
778   XK1=PHIZ/D+PHI1/(1.0-D)+PHID/(D*(D-1.0))
      XK2=-(PHIZ*(1.0+D)/D+D/(1.0-D)*PHI1+PHID/(D*(D-1.0)))
      XK3=PHIZ-PC
      BC=(SQRT(XK2*XK2-4.0*XK1*XK3)-XK2)/(2.0*XK1)
      GO TO (779,784),IBKN
779   B(J)=BS(J)-SA(J)*BC
      GO TO 781
784   B(J)=BS(J)+SA(J)*BC
781   IBK2=2
      GO TO 300
780   GO TO (782,786),IBKN
782   IBKN=2
      DD=1.0
      BL=B(J)
      PL=PHI
      GO TO 760
786   BU=B(J)
      PU=PHI
      GO TO (783,795,785,789),IBKP
783   WRITE(6,918) J,BL,PL,BU,PU
      GO TO 790
795   WRITE(6,915) J,BU,PU
      GO TO 790
785   WRITE(6,918) J,BL,PL
      GO TO 790
787   WRITE(6,913) J
      GO TO 790
789   WRITE(6,914) J
      GO TO 790
788   GO TO (791,792) ,IBKN
C  DELETE LOWER PRINT
791   IBKP=2
      GO TO 780
792   GO TO (793,794),IBKP
C  DELETE UPPER PRINT
793   IBKP=3
      GO TO 780
C  LOWER PRINT IS ALREADY DELETED, SO DELETE BOTH
794   IBKP=4
      GO TO 780
790   CONTINUE
      GO TO 10
660   CALL EXIT
900   FORMAT(2513)
901   FORMAT(7F10.0)
```

```
903   FORMAT(/13X,4H PHI,14X,4H S E,9X,7H  LAMDA,6X,25H ESTIMATED PARTIA
     1LS USED          /5X,2E18.8,E13.3)
904   FORMAT(/12H INCREMENTS ,5E18.8/(12X,5E18.8))
905   FORMAT(13X,4H PHI,10X,7H  LAMDA,6X,7H GAMMA ,6X,7H LENGTH/5X,
     1E18.8,3E13.3)
906   FORMAT(1X,E9.2,86X,E9.2,/1X,1H+,99X,1H+)
907   FORMAT(5HON = ,I3.5X,5H K = ,I3,5X,5H P = ,I3,5X,5H M = ,I3,5X
     1,7H IFP = ,I3,5X,13HGAMMA CRIT = ,E10.3,5X,6HDEL = ,E10.3/6H FF =
     2,E10.3,5X,5H T = ,E10.3,5X,5H E = ,E10.3,5X,7H TAU = ,E10.3,5X,
     36H XL = ,E10.3,4X,7HZETA = ,E10.3/)
908   FORMAT(3H  (,I3,13H) PARAMETERS ,5E18.8/(18X,5E18.8))
909   FORMAT(/13X,4H PHI,14X,4H S E,9X,7H  LAMDA,6X,25H ANALYTIC PARTIAL
     1S USED           /5X,2E18.8,E13.3)
910   FORMAT(1H ,/7X,3HOBS,11X,4HPRED,10X,4HDIFF,8X,7HPRNT(1),7X,
     17HPRNT(2),7X,7HPRNT(3),7X,7HPRNT(4),7X,7HPRNT(5))
911   FORMAT(/13X,4H PHI,14X,4H S E,11X,7H LENGTH,6X,7H GAMMA ,6X,
     17H  LAMDA,6X,25HESTIMATED PARTIALS USED  /5X,2E18.8,3E13.3)
912   FORMAT(/13X,4H PHI,14X,4H S E,11X,7H LENGTH,6X,7H GAMMA ,6X,
     17H  LAMDA,6X,24HANALYTIC PARTIALS USED  /5X,2E18.8,3E13.3)
913   FORMAT(2X,I3,18HPARAMETER NOT USED)
914   FORMAT(2X,I3,10HNONE FOUND)
915   FORMAT(2X,I3,36X,2E18.8)
916   FORMAT(1H ,/12H PTP INVERSE)
917   FORMAT(1H ,/29H PARAMETER CORRELATION MATRIX)
918   FORMAT(2X,I3,5E18.8)
919   FORMAT(1H /1H /13X,4H STD,17X,16H ONE - PARAMETER,21X,
     114H SUPPORT PLANE,/3X,2H B,7X,6H ERROR,12X,6H LOWER,12X,
     26H UPPER,12X,6H LOWER,12X,6H UPPER)
920   FORMAT(1H /1H /30H  NONLINEAR CONFIDENCE LIMITS  / /
     116H PHI CRITICAL = ,E15.8)
921   FORMAT(1H /5H PARA,6X,8H LOWER B,8X,10H LOWER PHI,10X,
     18H UPPER B,8X,10H UPPER PHI)
923   FORMAT(1H1/90X,12HEPSILON TEST)
922   FORMAT(1H1/60X,17H GAMMA LAMDA TEST,6X,2E13.3)
924   FORMAT(1H1/90X,9HFORCE OFF)
925   FORMAT(1X,8E14.6)
926   FORMAT(40H BAD DATA, SUBSCRIPTS FOR UNUSED BS = 0 ///)
927   FORMAT(2X,I3,5E18.8)
928   FORMAT(1H ,11OA1)
930   FORMAT(7F10.0)
931   FORMAT(8F10.0)
932   FORMAT(1H1/)
933   FORMAT(4HON =,I3,5X,5H K = ,I3,5X,5H P = ,I3,5X,5H M = ,I3,5X,/
     16H FF = ,E10.3,5X,5H T = ,E10.3,5X,5H E = ,E10.3,5X,7H TAU = ,
     2E10.3/)
934   FORMAT(1H1/,80X,18HGAMMA EPSILON TEST)
935   FORMAT(3X,I5,2X,10F10.4)
936   FORMAT(27HO NEGATIVE DIAGONAL ELEMENT )
937   FORMAT(3X,I5,2X,10F10.4/(10X,10F10.4))
938   FORMAT(1H /25H CONSTRAINT RESIDUALS ... /(3X,I5,33X,E18.8))
939   FORMAT(1H /23H PTP CORRELATION MATRIX )
950   FORMAT(5I3)
      END
      SUBROUTINE SUBZ(Y,X,B,PRNT,NPRNT,N)
C  INITIALIZE CODING...OPTION TO TRANSFORM X TO DEVIATION UNITS
      DIMENSION Y(100),X(100,2),B(5),PRNT(5)
      READ(5,901) YO,OPT
      DO 5 NN=1,N
5     Y(NN)=Y(NN)-0.01*YO
      IF(OPT) 21,20,21
```

```
21      SUMX=0.0
        DO 10 I=1,N
10      SUMX=SUMX+X(I,1)
        XN=N
        XBAR=SUMX/XN
        DO 15 I=1,N
15      X(I,1)=X(I,1)-XBAR
20      NPRNT=5
        RETURN
901     FORMAT(7F10.0)
        END
        SUBROUTINE GJR(A,N,EPS,MSING)
C   GAUSS-JORDAN-RUTISHAUSER MATRIX INVERSION WITH DOUBLE PIVOTING
        INTEGER P(5),Q(5)
        DIMENSION A(10,6),B(5),C(5)
        DO 10 K=1,N
        MSING=1
C   DETERMINATION OF THE PIVOT ELEMENT
        PIVOT=0.0
        DO 20 I=K,N
        DO 20 J=K,N
        IF(ABS(A(I,J))-ABS(PIVOT)) 20,20,30
30      PIVOT=A(I,J)
        P(K)=I
        Q(K)=J
20      CONTINUE
        IF(ABS(PIVOT)-EPS) 40,40,50
C   EXCHANGE OF THE PIVOTAL ROW WITH THE KTH ROW
50      IF(P(K)-K) 60,80,60
60      DO 70 J=1,N
        L=P(K)
        Z=A(L,J)
        A(L,J)=A(K,J)
70      A(K,J)=Z
C   EXCHANGE OF THE PIVOTAL COLUMN WITH THE KTH COLUMN
80      IF(Q(K)-K) 85,90,85
85      DO 100 I=1,N
        L=Q(K)
        Z=A(I,L)
        A(I,L)=A(I,K)
100     A(I,K)=Z
90      CONTINUE
C   JORDAN STEP
        DO 110 J=1,N
        IF(J-K) 130,120,130
120     B(J)=1.0/PIVOT
        C(J)=1.0
        GO TO 140
130     B(J)=-A(K,J)/PIVOT
        C(J)=A(J,K)
140     A(K,J)=0.0
110     A(J,K)=0.0
        DO 10 I=1,N
        DO 10 J=1,N
10      A(I,J)=A(I,J)+C(I)*B(J)
C   REORDERING THE MATRIX
        DO 155 M=1,N
        K=N-M+1
        IF(P(K)-K) 160,170,160
160     DO 180 I=1,N
```

```
      L=P(K)
      Z=A(I,L)
      A(I,L)=A(I,K)
180   A(I,K)=Z
170   IF(Q(K)-K) 190,155,190
190   DO 150 J=1,N
      L=Q(K)
      Z=A(L,J)
      A(L,J)=A(K,J)
150   A(K,J)=Z
155   CONTINUE
151   RETURN
40    WRITE(6,45) P(K),Q(K),PIVOT
45    FORMAT(17HO SINGULAR MATRIX,3H I=,I3,3H J=,I3,7H PIVOT=,E16.8/)
      MSING=2
      GO TO 151
      END
      SUBROUTINE FCODE(Y,X,B,PRNT,F,I,RES,IXP,IXP2,IXP3,IXP4,IXP5)
C  TEST OF THIXOTROPIC MODEL
C  WHERE X(I,1) IS THE SHEAR RATE AND POSITIVE
C  WHERE X(I,2) IS THE MAXIMUM SHEAR RATE AND IS POSITIVE
C  CONSTANTS B(1),B(2),B(3), AND B(4) ARE POSITIVE
C  CONSTANT B(5) IS EXPONENT OF X(I,1),N, AND MUST BE GREATER THAN 0.0
C  AND LESS THAN 1.0
      DIMENSION Y(100),X(100,2),B(5),PRNT(5)
      B5=B(5)
      B6=B5+1.0
      PRNT(1)=B(2)*X(I,1)
      PRNT(2)=B(3)*X(I,1)**B5
      IF(I-IXP) 10,10,11
11    IF(I-IXP2) 20,20,12
12    IF(I-IXP3) 21,21,13
13    IF(I-IXP4) 22,22,14
14    IF(I-IXP5) 23,23,24
C  UPCURVE EQUATION - FIRST LOOP
C  F=B1+B2*X(I,1)+B3*X(I,1)**B5*EXP((-B4*X(I,1)**(B5+1))/(B5+1))
10    PRNT(3)=(B(4)*X(I,1)**B6)/B6
      PRNT(4)=EXP(-PRNT(3))
      GO TO 30
C  DOWNCURVE EQUATION - FIRST LOOP
C  F=B1+B2*X1+B3*X1**B5*EXP(-B4*((2.0*X2**(B5+1))-X1**(B5+1))/(B5+1))
20    PRNT(3)=(2.0*X(I,2)**B6)-(X(I,1)**B6)
      PRNT(4)=EXP((-B(4)*PRNT(3))/B6)
      GO TO 30
C  UPCURVE EQUATION - SECOND LOOP
C  F=B1+B2*X1+B3*X1**B5*EXP(-B4*((2.0*X2**(B5+1))+X1**(B5+1))/(B5+1))
21    PRNT(3)=(2.0*X(I,2)**B6)+(X(I,1)**B6)
      PRNT(4)=EXP((-B(4)*PRNT(3))/B6)
      GO TO 30
C  DOWNCURVE EQUATION - SECOND LOOP
C  F=B1+B2*X1+B3*X1**B5*EXP(-B4*((4.0*X2**(B5+1))-X1**(B5+1))/(B5+1))
22    PRNT(3)=(4.0*X(I,2)**B6)-(X(I,1)**B6)
      PRNT(4)=EXP((-B(4)*PRNT(3))/B6)
      GO TO 30
C  UPCURVE EQUATION - THIRD LOOP
C  F=B1+B2*X1+B3*X1**B5*EXP(-B4*((4.0*X2**(B5+1))+X1**(B5+1))/(B5+1))
23    PRNT(3)=(4.0*X(I,2)**B6)+(X(I,1)**B6)
      PRNT(4)=EXP((-B(4)*PRNT(3))/B6)
      GO TO 30
C  DOWNCURVE EQUATION - THIRD LOOP
```

```
C  F=B1+B2*X1+B3*X1**B5*EXP(-B4*((6.0*X2**(B5+1))-X1**(B5+1))/(B5+1))
24     PRNT(3)=(6.0*X(I,2)**B6)-(X(I,1)**B6)
       PRNT(4)=EXP((-B(4)*PRNT(3))/B6)
30      PRNT(5)=X(I,1)
       F=B(1)+PRNT(1)+PRNT(2)*PRNT(4)
       RES=Y(I)-F
       RETURN
       END
       SUBROUTINE PCODE(P,X,B,PRNT,F,I,IXP)
C  TEST OF THIXOTROPIC MODEL
C  WHERE X(I,1) IS THE SHEAR RATE AND POSITIVE
C  WHERE X(I,2) IS THE MAXIMUM SHEAR RATE AND IS POSITIVE
C  CONSTANTS B(1),B(2),B(3), AND B(4) ARE POSITIVE
C  CONSTANT B(5) IS EXPONENT OF X(I,1),N, AND MUST BE GREATER THAN 0.0
C  AND LESS THAN 1.0
       DIMENSION P(5),X(100,2),B(5),PRNT(5)
C  INSERT VARIOUS P(J)'S HERE....IF ANALYTICAL PARTIALS ARE TO BE USED.
       RETURN
       END
```

APPENDIX E

INFORMATION ON MATERIALS STUDIED

Viscosities are at 25°c

A. Brookfield Standard Solutions

Brookfield Engineering Laboratories, Stoughton, Massachusetts

BS103: Brookfield Standard-10; Viscosity = 10.3 cp

BSB985: Brookfield Standard-1000; Viscosity = 985 cp

BSA98000: Brookfield Standard-100,000; Viscosity = 98,000 cp

B. Silicone Fluids

General Electric, Silicone Products Dept., Waterford, New York

SF96100 = Silicone Fluid, SF-96-100; Viscosity = 96.8 cp.

SF96200 = Silicone Fluid, SF-96-200; Viscosity = 194.4 cp.

SF96500 = Silicone Fluid, SF-96-500; Viscosity = 488 cp.

SIL350 = Silicone Oil, Viscosity = 341 cp.

SIL5000 = Silicone Oil, Viscosity = 4875 cp.

C. Time-Independent Materials

STPP - STP Motor Oil Additive

GYVR - Goodyear Plasticized Vinyl Resin

CBP025 - 0.025% Carbopol, Water Soluble Resin

B. F. Goodrich Chemical Company, Cleveland, Ohio

D. Silicone Oil and Grease Mixtures

Silicone High Vacuum Grease - Dow Corning

Silicone Oil = General Electric, Silicone Products Dept., Waterford, New York

SG0541: 54.1% High Vacuum Silicone Grease
45.9% SIL350

25DCGGEO: 24.95% High Vacuum Silicone Grease
75.05% SF96200

50DCGGEO: 49.8% High Vacuum Silicone Grease
50.2% SF96200

E. Montmorillonite Clay Mixture

Georgia Kaolin Montmorillonite Mineral Colloid BP; Georgia Kaolin Company, Elizabeth, New Jersey

GKCBP72: 7.2% Montmorillonite Clay
92.8% water

F. Blood

BLDD: Blood, Leon Gesner-donor, St. Michael's Hospital, Newark, New Jersey

APPENDIX F

EQUIPMENT DATA AND INFORMATION

GBS = Gear box setting

TMS = Transducer meter setting in microns

YRS = Recorder Y-range setting in volts/division

XRS = Recorder X-range setting in volts/division

FSD = Distance in inches on recorder corresponding to full scale deflection of transducer meter

GBR = Gearbox ratio on control arm of variable speed transmission

All runs use the following cone and torsion bar, except as noted:

Cone diameter = 5cm, cone angle = 1.974167°

Torsion bar No. 8, $k_T = 876$ $(\text{dyne})(\text{cm})/\text{micron}$

* Torsion Bar No. 7, $k_T = 99.4$ $(\text{dyne})(\text{cm})/\text{micron}$

≠ Cone diameter = 7.5 cm, cone angle = 1.951667°

TABLE F-1

TABULATION OF EQUIPMENT SETTINGS

Date	Run No.	GBS	TMS (microns)	YRS (volts/div)	XRS (volts/div)	FSD (in)	Temp °C	GBR
4/22/70	BS103-1*	0.0	50	0.5	1.0	4.0	-	25:1
6/17/70	SF96100-1	0.0	20	0.2	0.5	10	22.7	"
6/17/70	SF96500-1	0.0	200	0.1	0.5	20	23.2	"
6/11/70	BSB985-11	"	"	0.2	"	10	24.7	"
6/12/70	BSA98000-5	1.5	500	0.5	0.5	4	25.3	"
6/11/70	SIL5000-1	0.0	500	0.5	0.5	4	25.2	"
"	SIL5000-2	0.5	200	"	"	"	25.6	"
"	SIL5000-3	1.0	"	0.1	"	20	25.5	"
"	SIL5000-4	1.5	20	0.5	"	4	25.4	"
"	SIL5000-5	2.0	"	0.1	"	20	25.4	"
7/11/70	BSB985-33	0.0	200	0.2	0.5	10	24.9	"
6/19/70	BSB985-23, 24, 25, 26, 27	0.0	200	0.2	0.5	10	-	"
7/10/70	CBP025-9	0.5	20	0.2	0.5	10	25.0	10:1
4/11/70	GYVR-4	2.0	50	0.5	1.0	4	27.0	"
7/11/70	STPPP-11	0.5	500	0.5	0.5	4	24.1	25:1
4/ 8/70	SG0541-26	1.5	200	0.2	1.0	10	26.5	10:1
4/ 8/70	SG0541-27	"	"	"	"	"	26.5	"
4/ 9/70	SG0541-42	1.5	200	0.2	1.0	10	26.8	"
4/ 8/70	SG0541-38	1.5	200	0.2	1.0	10	26.5	"
6/25/70	25DCGGE0-23	2.0	20	0.1	0.5	20	25.2	25:1
6/30/70	50DCGGE0-23	1.5	200	0.1	0.5	20	25.3	10:1
4/ 3/70	GKCBP72-13	0.5	50	0.2	0.2	10	26	"
4/ 3/70	GKCBP72-18	1.0	"	"	"	"	"	"
4/ 3/70	GKCBP72-21	1.5	"	"	"	"	"	"
6/ 4/70	BLDD-42**	0.8	5	0.1	0.05	17.5	25.9	"

TABLE F-2

GEAR RATIO OF RHEOGONIOMETER GEARBOX

Gear Box Setting	Ratio (Input/Output)
0.0	1.000000
0.1	1.256983
0.2	1.584507
0.3	1.991150
0.4	2.500000
0.5	3.169014
0.6	3.982301
0.7	5.005562
0.8	6.293706
0.9	7.922535
1.0	10.000000
1.1	12.56983
1.2	15.84507
1.3	19.91150
1.4	25.00000
1.5	31.69014
1.6	39.82301
1.7	50.05562
1.8	62.93706
1.9	79.22535
2.0	100.0000

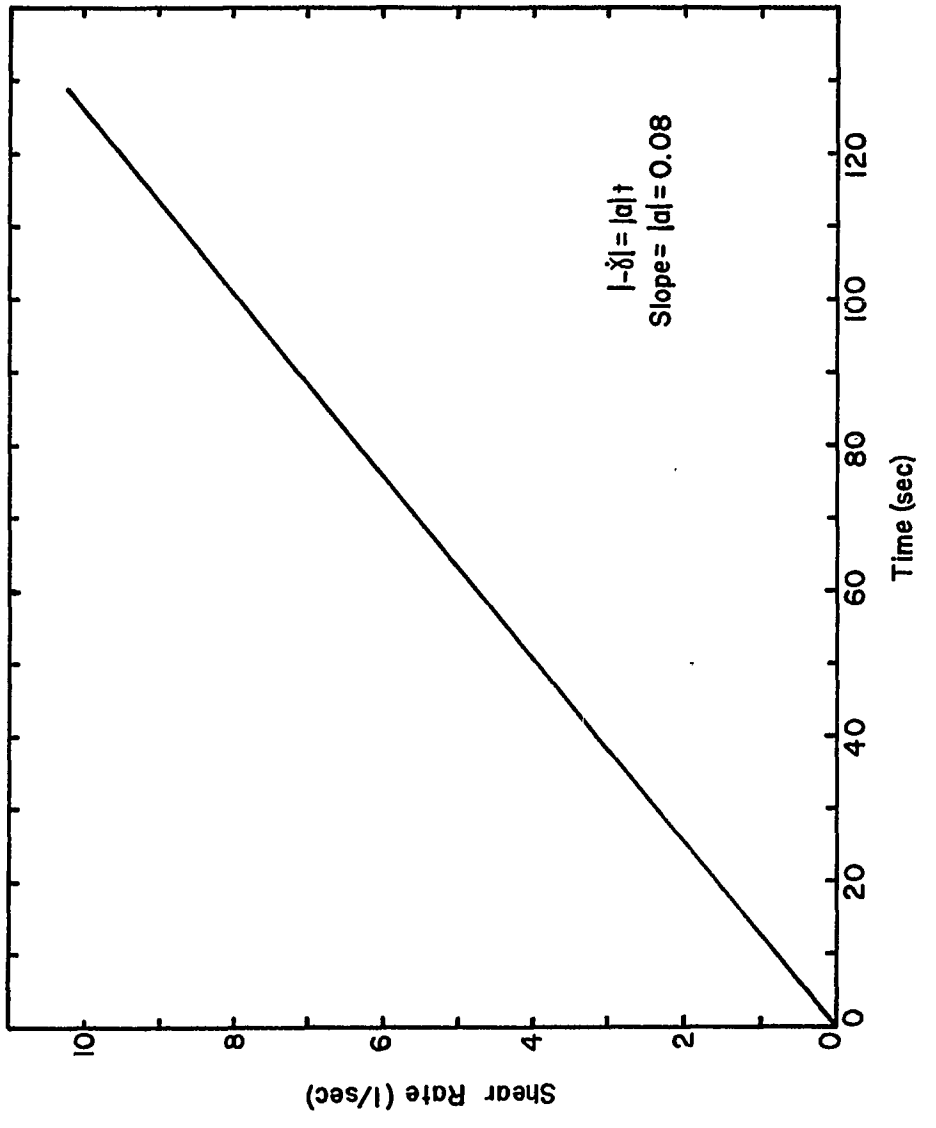

Figure F-1. Shear Rate versus Time to Reach Shear Rate

APPENDIX G

VOLTAGE-RPM CALIBRATION CURVES

Before any results from the instrument could be analyzed, a method of measuring the output signal from the tachometer-generator had to be devised. A calibration curve of output voltage versus measured or known RPM was determined. Two techniques were used to generate the voltage-RPM calibration curve using the instrument and accessories exactly as they would be used during the performance of an actual experimental run.

The first technique consisted of using the Rheogoniometer drive unit without the Graham variable-speed transmission. The tachometer-generator signal was measured at the output of the 60-step gearbox, fed into an electronic filter that was used during actual run conditions, and finally measured on the X-Y Recorder. A sample graph of the results can be seen in figure G-1. The numbers indicated in figure G-1 refer to the settings on the 60-step gearbox which in turn refer to a known RPM. This method of calibrating the tachometer-generator was performed before any experimental runs were made and again after all the experimental runs were completed, a type of double check as to the accuracy of the results. The actual measurements are given in tables G-1 and G-2. It should be noted that the plate RPM is 1/4 of the RPM at the output from the 60-step gearbox due to internal gearing of the instrument drive box.

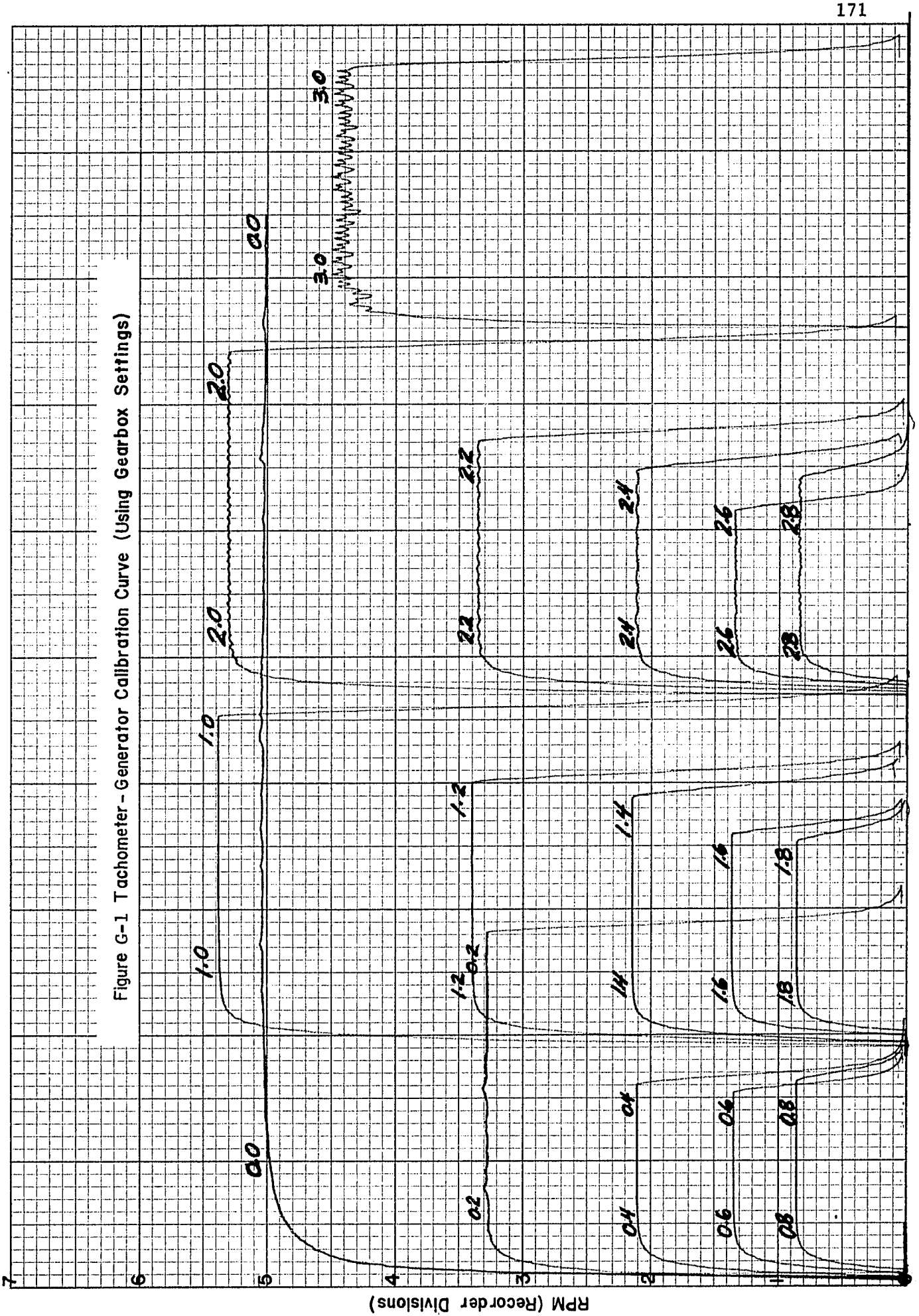

Figure G-1 Tachometer-Generator Calibration Curve (Using Gearbox Settings)

TABLE G-1

TACHOMETER-GENERATOR DATA

(USING GEARBOX SETTINGS)

Date: 3/4/70

Recorder speed: 50 sec/division

Gearbox Setting	Gearbox RPM	Plate RPM	Recorder Range (volts/div)	Recorder Reading (div)	Tachometer Voltage (volts)
0.4	720.0	180.0	2.0	2.11	4.22
0.6	452.0	113.0	2.0	1.345	2.69
0.8	286.0	71.5	2.0	0.86	1.72
1.0	180.0	45.0	0.2	5.38	1.076
1.2	113.6	28.4	0.2	3.40	0.68
1.4	72.0	18.0	0.2	2.15	0.43
1.6	45.2	11.3	0.2	1.365	0.273
1.8	28.6	7.15	0.2	0.86	0.172
2.0	18.0	4.5	0.02	5.33	0.1066
2.2	11.36	2.84	0.02	3.36	0.0672
2.4	7.2	1.8	0.02	2.12	0.0424
2.6	4.52	1.13	0.02	1.34	0.0268
2.8	2.86	0.715	0.02	0.835	0.0167

TABLE G-2

TACHOMETER-GENERATOR DATA

(USING GEARBOX SETTINGS)

Date: 9/10/70

Recorder speed: 50 sec/division

Gearbox Setting	Gearbox RPM	Plate RPM	Recorder Range (volts/div)	Recorder Reading (div)	Tachometer Voltage (volts)
0.3	904.0	226.0	2.0	2.53	5.06
0.4	720.0	180.0	2.0	2.025	4.05
0.5	568.0	142.0	1.0	3.25	3.25
0.6	452.0	113.0	0.5	5.175	2.5825
0.7	359.6	89.9	0.5	4.13	2.065
0.8	286.0	71.5	0.5	3.29	1.645
0.9	227.2	56.8	0.2	6.55	1.31
1.0	180.0	45.0	0.2	5.20	1.04
1.1	143.2	35.8	0.2	4.13	0.826
1.2	113.6	28.4	0.1	6.55	0.655
1.3	90.4	22.6	0.1	5.22	0.522
1.4	72.0	18.0	0.1	4.145	0.4145
1.5	56.8	14.2	0.1	3.28	0.328
1.6	45.2	11.3	0.05	5.19	0.2595
1.7	35.96	8.99	0.05	4.125	0.20625
1.8	28.6	7.15	0.05	3.28	0.164
1.9	22.72	5.68	0.05	2.62	0.131
2.0	18.0	4.5	0.05	2.08	0.104
2.1	14.32	3.58	0.05	1.655	0.08275
2.2	11.36	2.84	0.02	3.25	0.065
2.3	9.04	2.26	0.02	2.60	0.052
2.4	7.2	1.8	0.01	4.035	0.04035
2.5	5.68	1.42	0.01	3.21	0.0321

With the variable-speed transmission in the system, an alternate technique was used to determine a tachometer-generator voltage versus tachometer RPM calibration curve. This technique consisted of using a Smith's Hand Tachometer to physically measure the RPM at the output shaft from the variable speed transmission (actual position of tachometer-generator during run conditions). The transmission RPM was fixed at numerous values between zero and maximum with the RPM measured and voltage recorded. To insure maximum effectiveness in this analysis, the various runs were made with a variable changing in each. For example, in one run the X-Range on the recorder was decreased in sensitivity, while in another run the resistance beyond the transmission was varied to note any effect on the results. The results of this approach are given in figure G-2 and tables G-3, G-4, and G-5.

The data of tables G-1 through G-5 were plotted on log-log paper (due to the large range, magnitude of 100 to 1000), with axes representing transmission output RPM versus tachometer voltage. As can be seen from figure G-3 , all the data fell on a straight line, indicating accurate and reproducible measurement of RPM at the output from the variable-speed transmission as a function of tachometer voltage at this position. Using the data from figure G-3 resulted in the following equation:

$$(\text{RPM})_{\text{tach}} = 172.1\ (\text{Volts})_{\text{tach}} \qquad \text{(G-1)}$$

7/20/70

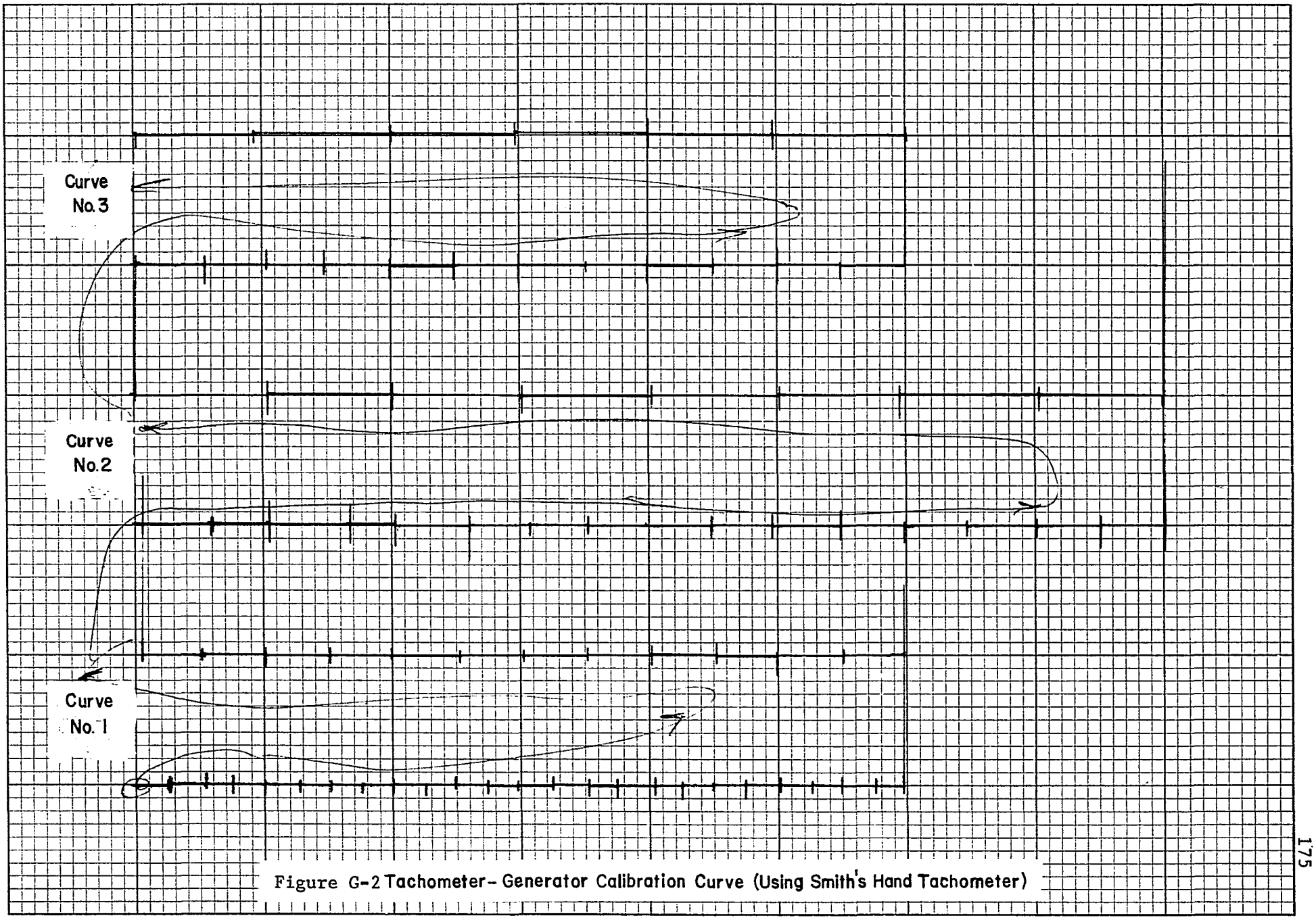

Figure G-2 Tachometer-Generator Calibration Curve (Using Smith's Hand Tachometer)

TABLE G-3

TACHOMETER-GENERATOR DATA

(USING SMITH'S HAND TACHOMETER)

Date: 7/20/70; Curve No. 1
Smith's Hand Tachometer
Recorder Setting (X-Range): 0.5 volts/div
Gearbox Setting: 1.0

Recorder Reading (div)	Tachometer Voltage (volts)	Smith's Tachometer (RPM)
0.55	0.275	45.5
0.76	0.380	62.5
1.00	0.500	83.0
1.27	0.635	107.2
1.52	0.760	127.5
1.76	0.880	148.8
2.00	1.000	169.2
2.26	1.13	191.3
2.49	1.245	212.0
2.74	1.37	235.0
2.97	1.485	253.0
3.24	1.62	278.0
3.53	1.765	301.0
3.75	1.875	320.0
4.05	2.025	346.0
4.25	2.125	364.0
4.49	2.245	386.0
4.74	2.37	407.0
5.02	2.51	430.0
5.26	2.63	452.0
5.49	2.745	472.0
5.76	2.88	495.0
5.97	2.985	514.0
5.51	2.755	474.0
4.98	2.49	428.0
4.52	2.26	387.0
4.02	2.01	343.0
3.52	1.76	300.0
3.02	1.51	257.0
2.53	1.265	214.0
2.00	1.00	168.1
1.52	0.76	126.1
1.02	0.51	83.0

TABLE G-4

TACHOMETER-GENERATOR DATA

(USING SMITH'S HAND TACHOMETER)

Date: 7/20/70; Curve No. 2
Smith's Hand Tachometer
Recorder Setting (X-Range): 0.20 volts/div
Gearbox Setting: 1.0

Recorder Reading (div)	Tachometer Voltage (volts)	Smith's Tachometer (RPM)
0.59	0.118	20.7
1.05	0.210	36.1
1.67	0.334	57.8
2.03	0.406	70.1
2.61	0.522	89.7
3.07	0.614	106.1
3.53	0.706	121.9
4.00	0.800	138.9
4.48	0.896	155.5
4.96	0.992	172.2
5.48	1.096	190.6
5.98	1.196	209.0
6.47	1.294	225.0
7.02	1.404	244.0
7.51	1.502	263.0
8.02	1.604	281.0
7.04	1.408	245.0
5.95	1.190	207.0
5.03	1.006	174.3
4.03	0.806	139.5
3.02	0.604	104.2
2.02	0.404	69.2
1.04	0.208	35.4

TABLE G-5

TACHOMETER-GENERATOR DATA

(USING SMITH'S HAND TACHOMETER)

Date: 7/20/70; Curve No. 3
Smith's Hand Tachometer
Recorder Setting (X-Range): 0.5 volts/div
Gearbox Setting: 0.0

Recorder Reading (div)	Tachometer Voltage (volts)	Smith's Tachometer (RPM)
0.56	0.28	48.5
1.04	0.52	91.3
1.48	0.74	130.4
1.99	0.995	175.2
2.49	1.245	217.0
3.00	1.500	263.0
3.52	1.76	308.0
3.99	1.995	351.0
4.51	2.255	394.0
5.00	2.50	437.0
5.49	2.745	483.0
6.00	3.00	526.0
4.97	2.485	435.0
4.01	2.005	347.0
2.97	1.485	257.0
2.01	1.005	174.5
0.94	0.47	80.5

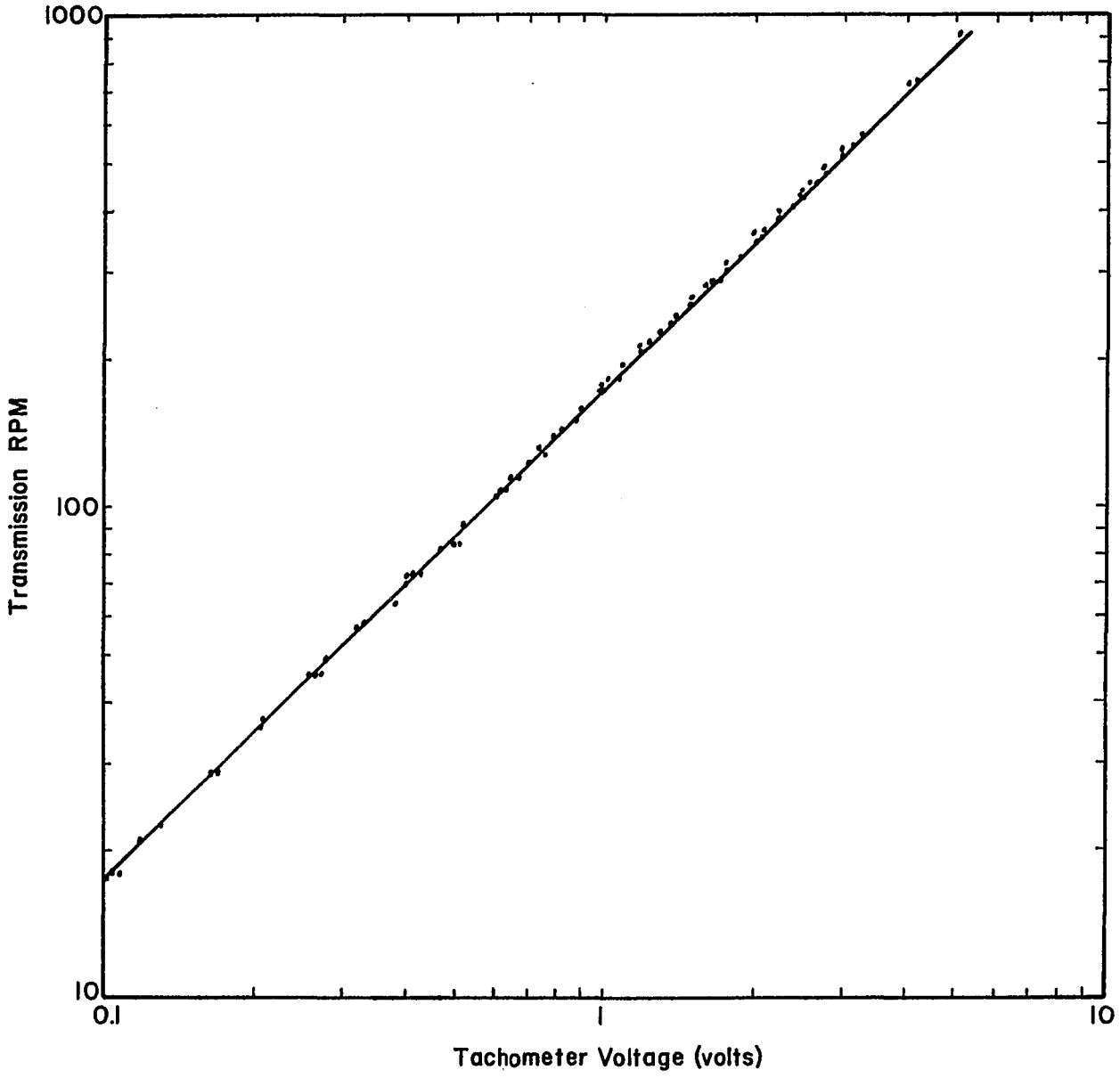

Figure G-3 Transmission RPM as a Function of Tachometer Voltage

where $(RPM)_{tach}$ is the rev/min of the tachometer which is also the RPM at the output shaft of the variable speed transmission, and $(Volts)_{tach}$ is the voltage of the tachometer as recorded on the X-Y Recorder after passing through the electronic filter.

Because of the excellent reproducibility between the three different sets of voltage-RPM readings, equation (G-1) can be used as a means of converting tachometer-generator output to tachometer RPM which is equal to the RPM at the output shaft from the variable speed transmission. By noting the setting on the 60-step gearbox, the reduction in RPM can be easily calculated to give the RPM from the 60-step gearbox which is the input RPM to the instrument. Correcting for the 4 to 1 internal gear reduction in the instrument, the lower platen RPM can be determined.

APPENDIX H

BIBLIOGRAPHY

1. Bauer, W.H., Finkelstein, A.P., Larom, C.A., and S.E.Wiberly, The Review of Scientific Instruments, 30(3), 167-9 (1959).

2. Bird, R.E., Stewart, W.E., and E.N.Lightfoot, 'Transport Phenomena', John Wiley & Sons, Inc., New York (1960).

3. Bogie, K. and J. Harris, Rheologica Acta, 7(3), 255-60 (1968).

4. Cheng, D.C. - H. and F. Evans, Brit. J. Appl. Phys., 16(11), 1599-1617 (1965).

5. Cokelet,G.R., Merrill,E.W., Gilliland,E.R., Shin, H., Britten, A., and R.E.Wells, Trans. Soc. Rheol.,7, 303 (1963).

6. Dahlgran, S. - E., Trans. Chalmers Univ. Technol., Gutherburg, No. 159, 18 pp (1955).

7. Dintenfass, L., Biorheology, 1, 91 (1963).

8. Fredrickson, A.G., A.I.Ch.E.J., 16(3), 436-441 (1970).

9. Gabrysh, W.F., Eyring, H., Lin-sen, P., and A.F.Gabrysh, J. of the Am. Ceramic Soc., 46(11), 523-9 (1963).

10. Gabrysh, A.F., Eyring, H., McKee, N., and I.Cutter, Trans. Soc. Rheol., 5, 67-84 (1961).

11. Gabrysh, A.F., Eyring, H., Ma, S. - M., and K. Liang, Rev. Sci. Instr., 33(6), 670-82 (1962).

12. Goodeve, C.F., and G.W.Whitfield, Trans. Faraday Soc., 34, 511-20 (1938).

13. Green, H., 'Industrial Rheology and Rheological Structures', John Wiley & Sons, Inc., New York (1949).

14. Green, H., Ind. Eng. Chem., Anal. Ed., 14, 576-85 (1942).

15. Green, H. and R.N.Weltmann, Ind. Eng. Chem., Anal. Ed., 15, 201-6 (1943).

16. Green, H. and R.N.Weltmann, Ind. Eng. Chem., Anal. Ed., 18, 167-72 (1946).

17. Green, H. and R.N.Weltmann, J. Appl. Phys., 15, 414-20 (1944).

18. deGroot, S.R. and P. Mazur, 'Non-Equilibrium Thermodynamics', North Holland Publ. Co., Amsterdam (1962).

19. Hagendorn, D.W., 'Prediction of Batch Heat Transfer Coefficients for Pseudoplastic Fluids in Agitated Vessels', Doc of Eng. Sci. Dissertation in Chemical Engineering, Newark College of Engineering, Newark, New Jersey (1965).

20. Hahn, S.J., Ree, T., and H.Eyring, Ind.Eng.Chem., 51, 856-7 (1959).

21. Hahn, S.J., Ree, T., and H.Eyring, N. L. G. I. Spokesman, 21(3), 12-20 (1957).

22. Hahn, S.J., Ree, T., and H.Eyring, N. L. G. I. Spokesman, 23(4), 129-36 (1959).

23. Huang, C. - R., The Chemical Engineering Journal, 3, 100-4, (1972).

24. Huang, C. - R., Trans. Soc. Rheol., 15(1), 25-30 (1971).

25. Huang, C. - R., Trans. Soc. Rheol., 15(1), 31-38 (1971).

26. King, R.G., and A.L.Copley, Biorheology, 7, 1 (1970).

27. Leonard, J.T. and R.N.Hazlett, Ind. Eng. Chem., Fundamentals, 5(2), 233-7 (1966).

28. Marquardt, D.W., J. Soc. Indust. Appl. Math. 11(2), 431 (1963).

29. Marquardt, D.W., Bennett, R.G., and E.J.Burrell, J.of Molec. Spectroscopy, 7(4), 269 (1961).

30. McKennell, R., Anal. Chem., 28, 1710-4 (1956).

31. Moore, F., Trans. Brit. Ceram. Soc., 58, 470-92 (1959).

32. Orosz, P., Siskovic, N., Huang, C.R., and R.G.Griskey, J. Physics E., Scientific Instr., 6(4), 389-91 (1973).

33. Pinder, K.L., Can. J. Chem. Eng., 42, 132-8 (1964).

34. Seno, M., Bull. Chem. Soc., Japan, 39, 1401-6 (1966).

35. Singhal, J.P. and W.U.Malik, Rheologica Acta, 3(3), 127-31 (1964).

36. Utsugi, H., Kim, K., Ree, T., and H.Eyring, N.L.G.I. Spokesman, 25, 125-31 (1961).

37. Van Wazer, J.R., Lyons, J.W., Kim, K.Y., and R.E.Colwell, 'Viscosity and Flow Measurements', Interscience Publishers, Inc., New York (1963).

38. Wells, R.E., Denton, R., and E.W.Merrill, J. Lab. Clin. Med., 57, 646 (1961).

39. Weltmann, R.N., Ind. Eng. Chem., 40(2), 272-80 (1948).

40. Weltmann, R.N., J. Appl. Phys., 14, 343-50 (1943).

41. Weltmann, R.N., N.L.G.I. Spokesman, 20(3), 34-40 (1956).

42. Wilkinson, W.L., 'Non-Newtonian Fluids', Pergamon Press, New York (1960).

VITA

NAME: Paul J. Orosz, Jr.

EDUCATION:

Newark College of Engineering B.S.Ch.E. 1965
Newark College of Engineering M.S.Ch.E. 1967

PROFESSIONAL EXPERIENCE:

1973-Present: Hooker Chemicals & Plastics Corporation; Niagara Falls, New York; Chemical Engineer in Process Development

1970-1973: Indiana Institute of Technology; Fort Wayne, Indiana; Assistant Professor in Chemical Engineering Department

1966-1970: Newark College of Engineering; Newark, New Jersey; Teaching Assistant

Summer 1969: ESSO Research and Development Co.; Linden, New Jersey; Chemical Engineer in Government Research Laboratory

Summer 1966: FMC Corporation; Princeton, New Jersey; Chemical Engineer in Physical Chemistry Section

Summer 1965: FMC Corporation, Carteret, New Jersey; Chemical Engineer in Process Development

RESEARCH LOCATION:

Newark College of Engineering
Chemical Engineering Laboratories

FINANCIAL ASSISTANCE:

ESSO Fellowship
NSF Traineeship